

Synergeia: Super-Linear Consistency and Adaptive Stability in a Hybrid PoW/PoS Consensus

Aaron M. Schutza¹

Proof-of-Consensus. November 16th 2025. aaronschutza@gmail.com

Abstract. We present the **Synergeia** ($\Sigma\nu\gamma\epsilon\gamma\alpha$) protocol, a novel, permissionless blockchain protocol that synergistically integrates Proof-of-Work (PoW) and a dynamically regulated Proof-of-Stake (PoS) mechanism. Traditional Nakamoto protocols exhibit consistency violations decaying as $\epsilon \approx \exp(-\Omega(k))$, leading to long finality times. Our primary contribution is leveraging a **Local Dynamic Difficulty (LDD)** scheme to reshape the block inter-arrival time distribution towards a **Rayleigh distribution**. We prove this yields a full consistency bound of $\epsilon(k) \leq \exp(-C_1 k^2) + \exp(-C_2 k)$. While this provides a quadratic asymptotic advantage, we demonstrate that for practical security parameters, the bound is dominated by the linear term. Our LDD mechanism achieves a superior constant factor (C_2) in this linear exponent, requiring only **k = 26** blocks against a 40% adversary for enterprise-grade security ($\epsilon \leq 10^{-9}$). Furthermore, we introduce the **Decentralized Consensus Service (\mathcal{F}_{DCS})**, providing BFT-robust consensus on network time, stake, delay, and load via on-chain beacons. This enables a **fully autonomous LDD system** that dynamically adapts its Slot Gap (ψ) and target block time (μ_{target}) to measured network conditions, ensuring the security assumption $\psi > \Delta$ holds robustly. The protocol utilizes an Accumulated Synergistic Work (ASW) metric incorporating **Proof-of-Burn** for PoS block commitment. As a result of this constant-factor improvement, Synergeia achieves probabilistic finality in approximately **6.5 minutes** under typical Bitcoin-like network conditions ($\mathbb{E} \approx 8s$). Additionally, we introduce **Burst Finality**, an optional mechanism triggered by high transaction fees (secured by Proof-of-Burn) that provides execution-driven confirmation for instant finality. Synergeia establishes a new paradigm for adaptive consensus, offering a significant constant-factor improvement for probabilistic finality alongside optional near-instant settlement.

Keywords: Hybrid Consensus · Proof-of-Stake · Fast Probabilistic Finality · Control Theory · Adaptive Consensus · Decentralized Oracles · Burst Finality.

1 Introduction

1.1 The Consensus Dilemma: Security, Finality, and Liveness

The foundational problem in decentralized ledger technology (DLT) is achieving secure consensus in a permissionless setting without relying on a central authority. This challenge is fundamentally characterized by the trade-offs between Consistency (all nodes agreeing on the state) and Availability, particularly when network partitions occur. Solutions to this problem are broadly categorized by the type of guarantee they offer regarding **finality**—the point at which a transaction becomes irreversible [2].

- **Probabilistic Finality:** The seminal solution, Nakamoto’s **Proof-of-Work (PoW)** protocol [35], is the canonical example of probabilistic finality. This class of protocols prioritizes availability over immediate consistency. Security is asymptotic; the probability ϵ of a transaction being reversed decreases as more blocks k are added. Formal analysis establishes this decay rate as $\epsilon \approx \exp(-\Omega(k))$ [19]. This linear exponent necessitates long confirmation times (e.g., ≈ 60 minutes in Bitcoin) for high security, especially against adversaries approaching 50% resource control [21].
- **Deterministic Finality:** In contrast, classical Byzantine Fault Tolerant (BFT) protocols, such as PBFT [11], provide deterministic finality. Once a block is committed, it is immediately irreversible. While offering fast settlement, these protocols prioritize consistency over availability and often face liveness challenges under asynchronous conditions [2], traditionally requiring permissioned validator sets.

The pursuit of greater efficiency led to **Proof-of-Stake (PoS)** protocols, pioneered by Ouroboros [28]. **Ouroboros Praos** [15] introduced key security enhancements for semi-synchronous networks, including Verifiable Random Functions (VRFs) [34] for private leader election—mechanisms relevant to Synergeia. While reducing energy use, PoS introduced new challenges, and achieving a consistency bound better than $\exp(-\Omega(k))$ remained elusive for longest-chain PoS protocols [9].

1.2 A New Paradigm: Engineering Fast Probabilistic Finality

The existing literature reveals a fundamental tension. Nakamoto-style protocols offer permissionless liveness but suffer from slow finality governed by the $\exp(-\Omega(k))$ bound. BFT and many contemporary PoS protocols offer faster finality but often compromise on permissionless participation or liveness under adverse network conditions [2]. Synergeia resolves this tension by introducing a new paradigm: engineering the underlying stochastic process of block production to achieve fast probabilistic finality without sacrificing permissionless liveness. The concept of **Local Dynamic Difficulty (LDD)** was introduced in Ouroboros Taktikos [41] for performance optimization. In this work, we repurpose LDD to fundamentally alter the block production model. By implementing a specific time-dependent hazard rate (the snowplow curve), LDD forces block inter-arrival times towards a **Rayleigh distribution**. As formally proven in Section 7, this structural shift yields a more complex two-term consistency bound:

$$\epsilon(k) \leq \exp(-C_1 k^2) + \exp(-C_2 k)$$

The first, quadratic term bounds the probability of an "unlucky" honest network, while the second, linear term bounds the probability of a "lucky" adversary. While the $\exp(-\Omega(k^2))$ term provides a powerful asymptotic advantage, our analysis shows that for practical security parameters (e.g., $\epsilon \leq 10^{-9}$), the bound is entirely dominated by the linear term. The primary contribution of this work is demonstrating that the LDD mechanism achieves a **significant constant-factor improvement** (a much larger C_2) in this dominant linear exponent, fundamentally altering the security-latency trade-off. This allows for significantly shorter confirmation depths for a given security level. Synergeia demonstrates that the stochastic properties of consensus are not fixed constraints but designable parameters, enabling a new class of high-performance, probabilistically secure protocols.

1.3 Protocol Overview and Contributions

The **Synergeia** protocol integrates PoW security with PoS efficiency within a novel adaptive framework. Our primary contributions are:

- **Fast Probabilistic Finality:** By leveraging the LDD scheme to induce a Rayleigh-like distribution, we achieve a full security bound of $\epsilon(k) \leq \exp(-C_1 k^2) + \exp(-C_2 k)$. We achieve a significant constant-factor improvement in the dominant linear term, requiring only $k = 26$ blocks against a 40% adversary for $\epsilon \leq 10^{-9}$. This enables a typical finality time of approximately **6.5 minutes** under Bitcoin-like network conditions.
- **Hybrid Model with Proof-of-Burn ASW:** The protocol maintains a target 50/50 block proportion using active control. The Accumulated Synergistic Work (ASW) fork-choice rule (Section 2.4) integrates PoW cost with a secure **Proof-of-Burn** commitment for PoS blocks, ensuring dimensional consistency and mitigating economic attacks.
- **Fully Autonomous Adaptation via Decentralized Oracles:** We introduce the **Decentralized Consensus Service (\mathcal{F}_{DCS})** (Section 9.12), a unified mechanism providing BFT-robust consensus on network time, total stake, propagation delay ($\Delta_{consensus}$), and transaction load ($L_{consensus}$) via on-chain beacons. The LDD system uses these values to autonomously adapt its Slot Gap (ψ) and target block time (μ_{target}), ensuring security ($\psi > \Delta$) and optimizing throughput dynamically.
- **Burst Finality Mechanism:** An optional mode triggered by high transaction fees (secured by Proof-of-Burn) suspends adaptive LDD rules to allow rapid finality protocol for high-value, time-sensitive transactions.
- **PoW-Anchored Security:** PoW blocks anchor VRF seeds for PoS leader election, mitigating grinding attacks within VRF domains, and secure state checkpoints via committed UTXO roots.

2 Protocol Setup & Hybrid Model

Synergeia operates as a permissionless protocol, enforcing open participation via cryptographic proof rather than identity verification. It structurally simplifies the consensus process by eliminating the complex epoch mechanism typical of many PoS protocols, utilizing PoW as a continuous security anchor.

2.1 Hybrid Block Production Architecture

The concept of hybrid consensus, which combines Proof-of-Work (PoW) and Proof-of-Stake (PoS), is not new. Early protocols sought to leverage the strengths of each mechanism to overcome their respective weaknesses. However, Synergeia's architecture represents a fundamental departure from these prior models. To fully appreciate this novelty, it is instructive to compare Synergeia's design with that of its predecessors, primarily Peercoin [29] and Decred [33].

Peercoin: A Sequential Hybrid Model. Peercoin, the first protocol to introduce PoS, employed a **sequential or layered hybrid model**. In this design, PoW's primary role was for the initial, fair distribution of coins, addressing the centralization risk inherent in pure PoS systems where founders might retain an outsized initial stake. Over time, the protocol's security was designed to transition to rely almost entirely on PoS, which provides long-term network security in a highly energy-efficient manner. The fork-choice rule in Peercoin is not a simple longest-chain rule; in the event of a fork, the canonical chain is the one with the greatest "coin age" consumed, a metric that combines stake amount with holding time. This architecture treats PoW and PoS as distinct phases or layers, with PoW's role diminishing over the protocol's lifecycle.

Decred: An Integrated Validation Model. Decred introduced a more deeply **integrated hybrid model**, where PoW and PoS operate in a tightly coupled, hierarchical fashion. In Decred's system, PoW miners are responsible for producing new blocks, similar to Bitcoin. However, for a block to be considered valid, it must be approved by a randomly selected group of PoS stakeholders. These stakeholders purchase "tickets" with their funds, which gives them the right to participate in a lottery. For each block, five tickets are randomly called to vote on the validity of the PoW miner's proposed block. A block is only added to the canonical chain if it receives at least three of these five votes.

This design gives PoS stakeholders ultimate sovereignty over the network; they act as a final validation and governance layer, with the power to approve or reject the work of miners. This structure is reinforced by an explicit economic model where block rewards are split between the participants: 60% for the PoW miner, 30% for the PoS voters (divided among the five ticket holders), and 10% for a decentralized development treasury. Decred's fork-choice rule is still based on the longest chain, but the definition of a valid block is fundamentally altered to require this PoS validation step, making it significantly more difficult for a malicious PoW miner to execute attacks such as secret mining.

Synergeia: A Parallel, Actively-Balanced Model. In stark contrast to these layered or hierarchical models, Synergeia's architecture integrates PoW and PoS as **parallel, co-equal, and actively balanced** block production mechanisms. Neither mechanism is subordinate to the other. Instead, both PoW miners and PoS stakers are capable of independently producing valid blocks at any time. The protocol's core innovation is the use of a control-theoretic feedback system (the Dynamic Slope Adjustment Scheme) to algorithmically enforce a target 50/50 proportion of blocks from each source.

The fork-choice rule is unified under a single metric, **Accumulated Synergistic Work (ASW)**, which adds the verifiable computational cost of PoW blocks and the economic commitment of PoS blocks into one commensurable quantity. This distinct architectural choice is designed to maximize the combined computational and economic cost an adversary must overcome to attack the system. Table 1 summarizes these key differences.

2.2 PoW-Anchored Security Mechanisms

PoS State Security: Every PoW block commits a cryptographic root of the current UTxO state, acting as a trusted, PoW-secured state checkpoint. The protocol leverages the PoW mechanism to provide structural security and randomness anchoring.

Acknowledging the Architectural Trade-off. It is a deliberate design choice that Synergeia's parallel model does not include the direct PoS validation step found in Decred's architecture [33]. This "separation of powers" in Decred provides a robust defense against 51% PoW attacks, as PoS stakeholders can directly veto malicious blocks, rendering a majority of hash power insufficient to control the chain [33]. Synergeia trades this direct validation mechanism for a unified economic model. Security is instead derived from the total combined cost an adversary must pay to overcome the ASW of the honest chain. This design is predicated on the assumption that a 50/50 resource split, enforced by the protocol's algo-economic

Table 1: Comparative Analysis of Hybrid Consensus Architectures.

Feature	Peercoin	Decred	Synergeia
Architecture	Sequential/Layered (PoW for distribution, PoS for security)	Integrated (PoW produces blocks, PoS validates them)	Parallel (PoW and PoS both produce blocks independently)
Fork-Choice Rule	Longest Chain by consumed "coin age"	Longest Chain where validity requires PoS ticket-votes	Longest Chain by Accumulated Synergistic Work (ASW)
Security Model	Energy efficiency and fair distribution; PoS secures the chain long-term	Balance of power between miners and stakeholders; PoS provides finality and governance	Maximization of combined attack cost; engineered block arrival for fast finality
Economic Model	PoW miners receive new coins; PoS minters earn fees and inflation rewards.	Explicit reward split: 60% PoW, 30% PoS, 10% Treasury.	Algorithmic balancing of expected utility to maintain a 50/50 resource split.

controls, creates a higher *total* economic barrier to attack than a hierarchical model. However, this trade-off must be acknowledged: Synergeia is theoretically more vulnerable to a sustained censorship attack from an adversary who controls a majority of *only* the network's hash power. The protocol's defense against such a scenario is not an immediate veto, but a long-term economic and ASW race, where the honest PoS participants are incentivized to build a competing, uncensored chain that eventually becomes the canonical one.

PoW-Anchored VRF Seeding and Anti-Grinding. Modern PoS protocols, such as Ouroboros Praos [15], rely on Verifiable Random Functions (VRFs) for leader election. A VRF is a cryptographic primitive, first formalized by Micali, Rabin, and Vadhan [34], that allows a participant to generate a pseudorandom output and an accompanying proof, enabling unpredictable yet verifiable leader selection. A significant vulnerability in PoS designs is "grinding." If the VRF seed is derived from on-chain sources that an adversary can influence (e.g., by selectively withholding blocks or manipulating transaction content), they can privately "grind" through potential future leader schedules to find one statistically favorable to them [15]. Synergeia mitigates this by anchoring the VRF randomness directly to the hash of the latest PoW block and the current slot number. As the PoW hash is a high-entropy, unforgeable value determined by computational work, this mechanism effectively removes this manipulation vector for all PoS slots within that PoW-anchored domain.

On the Source of Randomness. The security of the PoS component, particularly the unpredictability of the VRF-based leader election, is critically dependent on the cryptographic entropy of the PoW block hashes that seed it. This design implicitly assumes the standard Bitcoin mining model, where the output of the hash function is computationally indistinguishable from a uniform random string. However, this assumption creates a potential cascading vulnerability. If an adversary could find a way to influence or reduce the effective entropy of the block hashes they produce, they could potentially bias the PoS leader election in their favor. For example, a selfish mining strategy involves a miner privately finding multiple blocks and selectively publishing them to maximize their revenue [17,37,40]. A sophisticated variant of this attack could involve the adversary choosing which privately-mined block to publish based not only on chain length but also on whether its hash generates a favorable future VRF domain for the adversary's stake. While the high computational cost of PoW makes such an attack difficult, it represents a non-zero attack surface that couples the security of the PoS mechanism to the behavioral assumptions of the PoW miners.

2.3 The Synergistic Longest Chain Rule (ASW)

The core security of the chain relies on the **Accumulated Synergistic Work (ASW)** metric, which is used for the deterministic chain selection rule. The ASW is designed to be unforgeable by integrating computational and economic costs:

- **Metric Definition (ASW):** The total chain weight is the sum of the verifiable cost (SW) of all blocks:

$$\text{ASW}(\mathcal{C}) = \sum_{k=1}^L \text{SW}(B_k)$$

- **Synergistic Work (SW):** The cost of a single block combines the verifiable computational cost (PoW_Cost) and the non-slashable economic commitment (PoS_Commitment):

$$SW(B_k) = PoW_Cost(B_k) + PoS_Commitment(B_k)$$

2.4 Accumulated Synergistic Work (ASW)

PoW Cost: Operational Expenditure $PoW_Cost(B_k)$ is calculated as the standard inverse of the block difficulty target. This is equivalent to standards used in Bitcoin and other Proof-of-Work blockchains.

PoS Cost: Proof-of-Burn Commitment We define the PoS component of ASW to be a measure of an irrecoverable economic cost, thereby making it dimensionally consistent with the PoW operational expenditure. We achieve this by introducing revenue-based calculations with a mandatory Proof-of-Burn commitment.

Under this model, for a PoS validator to produce a valid block, they must include a special "burn" transaction that verifiably destroys a portion of their own funds. The amount burned is a function of the economic activity within the block, directly linking the block's weight to a real, irrecoverable cost.

Definition 1. *The PoS commitment of a block B_k is defined as the amount of currency verifiably burned by the validator, which is proportional to the total transaction fees contained within the block:*

$$PoS_Commitment(B_k) = \beta_{burn} \cdot \sum_{tx \in B_k} Fee(tx)$$

where $\beta_{burn} \in (0, 1]$ is a global protocol parameter representing the burn rate. The validator's net revenue from the block is the total fees minus the burned amount, $(1 - \beta_{burn}) \cdot \sum Fee(tx)$, plus the block reward.

An adversary may attempt to inflate the ASW of a private chain by cycling high-fee transactions. To generate an artificial ASW of value W_{PoS} , the adversary must incur a real economic cost of W_{PoS} . The attack is only profitable if the expected gain from a successful fork (e.g., from a double-spend) is greater than the cost of burning fees to generate the required ASW. This makes the attack economically expensive to brute-force, thereby realizing the intended security properties of the ASW metric for the PoS component.

2.5 Adaptive Difficulty Mechanisms

The system's operational stability relies on actively managing its block rate and security boundaries via dynamic difficulty mechanisms inherited and adapted from the LDD framework introduced in Ouroboros Taktikos [41]:

- **Target Slope (M_{req}):** The dynamic slope as a function of time required to maintain the average target block time.
- **Dynamic Slope Adjustment Scheme:** A continuous feedback loop that maintains $M_{final} = M_{req}$ by adjusting the individual PoS slope ($f_{A,PoS}$) and PoW slope ($f_{A,PoW}$) based on observed block density, ensuring the 50/50 split is enforced.
- **Dynamic Forging Window ($\gamma - \psi$):** The time interval where the PoS eligibility threshold and PoW target ramps up linearly. The duration of this window is autonomously calculated each adjustment period to optimize efficiency.
 - **Adaptive Slot Gap (ψ):** The protocol's starting point for the forging window. It is autonomously set based on measured network delay ($\Delta_{consensus}$) to enforce the security constraint $\psi > \Delta$.
 - **Adaptive Recovery Threshold (γ):** The end of the linear ramp. It is autonomously calculated to minimize the probability of blocks falling into the inefficient recovery phase, ensuring the forging window is precisely as long as required by the current network difficulty.

2.6 Parameter Selection and Tuning

The performance and security of the Synergeia protocol depend on the careful calibration of several key operator-set parameters. While core timing parameters like the slot gap (ψ) and recovery threshold (γ) are autonomously managed by the protocol (as detailed in Section 10), the parameters governing their adaptation require careful consideration. The challenges of tuning such dynamic systems are well-documented and require a balance between security, liveness, and efficiency [41]:

- **Slot Gap Safety Margin (M_{safety}):** While the slot gap (ψ) is set autonomously based on measured network delay, the safety margin added to this measurement is a critical security parameter. **Trade-off:** A larger M_{safety} provides a wider security margin against network attacks and un-forecasted delay spikes. However, it also introduces a fixed latency at the start of every block production cycle, which can decrease the protocol's maximum theoretical throughput.
- **Fallback Probability ($P_{fallback}$):** This parameter defines the target probability that a block will need to be produced in the inefficient, constant-difficulty "recovery phase." It is used by the autonomous system to calculate the optimal duration of the forging window ($\gamma - \psi$). **Trade-off:** A very small $P_{fallback}$ (e.g., 10^{-5}) will result in a longer forging window, making the system highly robust to random fluctuations but slightly reducing the precision of the LDD mechanism. A larger value (e.g., 10^{-2}) creates a shorter, more efficient forging window but increases the frequency with which the network must rely on the fallback recovery mechanism.
- **Adjustment Window Size (N):** This parameter, discussed in Section 12, controls how many blocks of history are used to calculate adjustments to the PoW/PoS difficulty slopes. **Trade-off:** A small N makes the system highly responsive to changes in resource allocation but can lead to high-frequency oscillations and instability. A large N , as analyzed in Section 12, creates smooth, low-frequency oscillations that are stable but highly predictable, making the system vulnerable to strategic exploitation by a rational adversary.

Economic Parameter Calibration The introduction of the Proof-of-Burn ASW and Burst Finality mechanisms adds two critical economic parameters whose calibration is essential for the protocol's security.

Proof-of-Burn Rate: This parameter β_{burn} , defined in Section 2.4, governs the fraction of transaction fees a PoS validator must verifiably destroy to contribute to the chain's ASW. It is now a crucial variable for both the standard ASW security and the economic deterrence of Burst Finality. The choice of $\beta_{burn} \in (0, 1]$ represents a direct trade-off between security and validator revenue. A higher β_{burn} increases the sunk cost required to produce a PoS block, making the ASW metric more robust against economically-rational adversaries. However, it also reduces the net revenue for honest stakers. The optimal value should be chosen to ensure that the risk-adjusted return on staking remains competitive with mining and external market yields, thereby maintaining the stable economic equilibrium analyzed in Section 14.

Burst Finality Threshold: As detailed in Section 13.2, Burst Finality provides an execution-driven confirmation mode triggered by a high transaction fee. The security of this mechanism relies on the principle of economic deterrence. The threshold, $Fee_{burst_threshold}$, must be carefully calibrated such that the irrecoverable cost to an attacker wishing to trigger a malicious burst—namely $\beta_{burn} \cdot Fee_{burst_threshold}$ —is significantly greater than the maximum potential profit from an attack that could be executed within the rapid burst window (e.g., a double-spend). This ensures that initiating such an attack is an economically irrational strategy.

3 Quadratic Consistency

The Synergeia protocol's stability and speed are founded on a breakthrough security bound derived from the stochastic properties of its block production. This section formally outlines the transition to the quadratic consistency model, explains the mechanism that enables it, and derives its key parameters.

3.1 Stochastic Model: The Idealized Rayleigh Distribution

Traditional Nakamoto protocols (PoW) model block arrivals via a memoryless process governed by the **exponential distribution**, where the arrival rate is constant ($\lambda \propto \text{constant}$). In contrast, the Synergeia

protocol utilizes its **Local Dynamic Difficulty (LDD)** mechanism to enforce a time-dependent success probability, where the hazard rate increases linearly with the time elapsed since the last block ($\lambda(\delta) \propto \delta$).

This structural change forces the block inter-arrival time (x) to follow the **Rayleigh distribution** in its idealized form:

$$R(x) = Mx \cdot \exp(-Mx^2/2)$$

where M is the slope parameter representing the effective difficulty. This quadratic exponent in the distribution is the necessary mathematical condition for achieving the superior security bound.

3.2 The LDD Mechanism in Practice: The Snowplow Curve

The idealized Rayleigh distribution described above is an emergent property of a practical, engineered mechanism. The core of the LDD scheme is a time-dependent hazard function $f(\delta)$ that we term a **snowplow curve**, where δ is the time elapsed since the last block. This function dictates the probability of a block being produced in any given slot.

We present a specific difficulty curve first presented in [41] featuring a slot gap, a forging window, and a recovery phase, defined by the 4-tuple (ψ, γ, f_A, f_B) :

$$f(\delta) = \begin{cases} 0 & \delta < \psi \\ f_A \cdot \left(\frac{\delta - \psi}{\gamma - \psi} \right) & \psi \leq \delta < \gamma \\ f_B & \gamma \leq \delta \end{cases}$$

The parameters are defined as follows:

- **Slot Gap (ψ):** A period where the hazard rate is zero, corresponding to infinite difficulty, where no blocks can be produced. This is designed to be longer than the maximum network delay (Δ) to mitigate certain network-level attacks.
- **Forging Window ($\psi \rightarrow \gamma$):** A period of linearly decreasing difficulty, where the threshold and target simultaneously go from 0 up to a maximum amplitude f_A where it is easiest to find a block. This concentrates block production in a predictable time window tightly concentrated in the beginning of the forging window.
- **Recovery Phase ($\delta \geq \gamma$):** A period where the difficulty drops to a constant baseline f_B , allowing the network to recover if no block is found during the forging window. This constant difficulty induces Nakamoto-style block production among both PoS and PoW blocks.

In our hybrid protocol, the theoretical slope parameter M is realized through the sum of the hybrid difficulty amplitudes for PoW and PoS, a concept we will detail in Section 10:

$$M = f_{A,PoS} + f_{A,PoW}, b = f_{B,PoS} + f_{B,PoW}$$

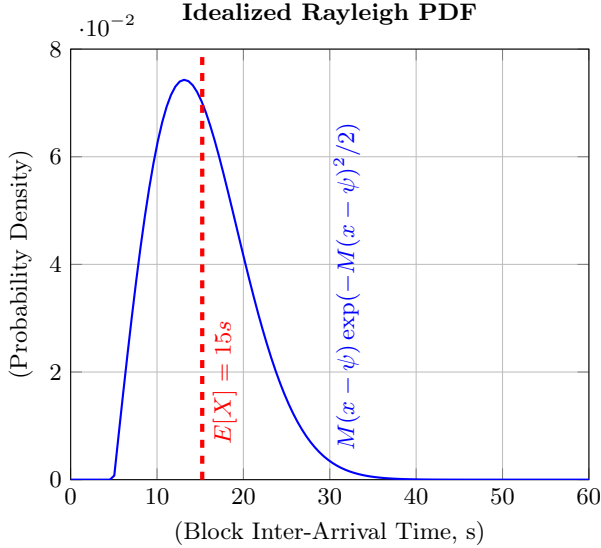
This connection is stated here to bridge the gap between the theoretical model and its practical implementation from the outset. The snowplow curve is the underlying mechanism that generates the block time distribution shown in Figure 1.

3.3 Derivation of the Expectation Value

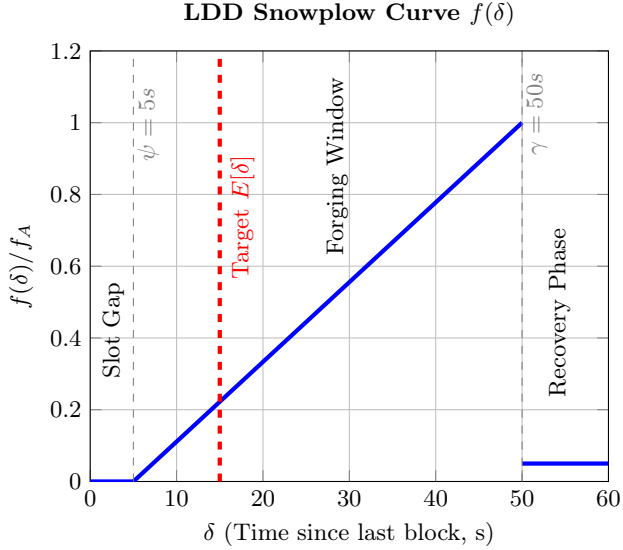
While the idealized Rayleigh distribution serves as a robust model for security analysis, for completeness we derive the full expression for the expectation value of the block time based on the complete LDD parameters (M, ψ, γ, b) . Let $P(x)$ be the unnormalized probability density function corresponding to the snowplow curve:

$$P(x) = \begin{cases} M(x - \psi) \exp\left(-\frac{M(x-\psi)^2}{2}\right) & \psi \leq x \leq \gamma \\ M(\gamma - \psi) \exp\left(-\frac{M(\gamma-\psi)^2}{2}\right) \exp(-b(x - \gamma)) & x > \gamma \\ 0 & \text{otherwise} \end{cases}$$

To find the expectation value $\mathbb{E}[x]$, we must first normalize this PDF. The normalization constant $C = 1/I_{\text{norm}}$, where I_{norm} is the integral of $P(x)$ over its domain. We split this into two parts: the integral



(a) The idealized Rayleigh probability density function (PDF). The slope parameter $M \approx 0.015s^{-2}$ is set to achieve the target 15-second average block time ($E[X]$) with the given values of ψ and γ .



(b) The snowplow curve $f(\delta)$ which creates the block time distribution. This mechanism forces the arrivals to approximate the Rayleigh PDF.

Fig. 1: Visualization of the Synergeia stochastic model. Figure (a) shows the idealized probability distribution (PDF) of block times. Figure (b) shows the underlying time-dependent hazard rate (the snowplow curve) that produces this distribution.

over the forging window ($\psi \leq x \leq \gamma$) and the integral over the recovery phase tail ($x > \gamma$). Let $\xi = \gamma - \psi$ and $E_c = \exp\left(-\frac{M\xi^2}{2}\right)$.

$$\int_{\psi}^{\gamma} M(x - \psi) \exp\left(-\frac{M(x - \psi)^2}{2}\right) dx = 1 - E_c$$

$$\int_{\gamma}^{\infty} M\xi E_c \exp(-b(x - \gamma)) dx = \frac{M\xi E_c}{b}$$

Summing these gives the normalization integral:

$$I_{\text{norm}} = 1 - E_c + \frac{M\xi E_c}{b} = 1 + \left(\frac{M\xi}{b} - 1\right) E_c$$

Next, we calculate the numerator for the expectation, $I_{\text{num}} = \int xP(x)dx$, again splitting the integral. The first integral, over the forging window, is:

$$\int_{\psi}^{\gamma} xP(x)dx = \psi + \sqrt{\frac{\pi}{2M}} \operatorname{erf}\left(\xi\sqrt{\frac{M}{2}}\right) - \gamma E_c$$

The second integral, over the tail, is:

$$\int_{\gamma}^{\infty} xP(x)dx = \frac{M\xi E_c}{b} \left(\gamma + \frac{1}{b}\right)$$

The full expression for the numerator I_{num} is the sum of these two parts:

$$I_{\text{num}} = \psi + \sqrt{\frac{\pi}{2M}} \operatorname{erf}\left(\xi\sqrt{\frac{M}{2}}\right) + \left[\frac{M\xi}{b} \left(\gamma + \frac{1}{b}\right) - \gamma\right] E_c$$

The exact expectation value $\mathbb{E}[x] = I_{\text{num}}/I_{\text{norm}}$ is therefore:

$$\mathbb{E}[x] = \frac{\psi + \sqrt{\frac{\pi}{2M}} \operatorname{erf}\left((\gamma - \psi)\sqrt{\frac{M}{2}}\right) + \left[\frac{M(\gamma - \psi)}{b} \left(\gamma + \frac{1}{b}\right) - \gamma\right] \exp\left(-\frac{M(\gamma - \psi)^2}{2}\right)}{1 + \left(\frac{M(\gamma - \psi)}{b} - 1\right) \exp\left(-\frac{M(\gamma - \psi)^2}{2}\right)}$$

Approximation and Justification To derive a practical formula for the expectation value, we rely on two key approximations based on the protocol's target parameters. With $M \approx 0.015s^{-2}$, $\psi = 5s$, and $\gamma = 50s$, we have $\xi = 45s$.

1. **Approximation $E_c \rightarrow 0$:** The exponent term is $\frac{M\xi^2}{2} \approx 15.2$. This yields $E_c = \exp(-15.2) \approx 2.5 \times 10^{-7}$, which is negligible. This validates the assumption that the probability mass in the tail ($x > \gamma$) is effectively zero.
2. **Approximation $\operatorname{erf}(z) \approx 1$:** The argument of the error function is $z = \xi\sqrt{M/2} \approx 3.9$. For this value, $\operatorname{erf}(3.9)$ is extremely close to 1.

Applying these limits ($E_c \rightarrow 0$ and $\operatorname{erf}(z) \rightarrow 1$) to the normalization and numerator integrals, we find $I_{\text{norm}} \rightarrow 1$ and $I_{\text{num}} \rightarrow \psi + \sqrt{\frac{\pi}{2M}}$. The expectation value thus simplifies significantly to the mean of an idealized Rayleigh distribution, shifted by the slot gap ψ :

$$\mathbb{E}[x] \approx \psi + \sqrt{\frac{\pi}{2M}}$$

This robust approximation is used by the protocol's stability mechanisms (Section 10) to maintain $\mathbb{E}[x]$ at the target of 15 seconds.

3.4 Super-Exponential Consistency

The maximum consistency violation probability (ϵ) in conventional protocols is bounded by a linear exponent ($\exp(-\Theta(k))$). The structural shift to a Rayleigh distribution fundamentally changes this dynamic, enabling a super-exponential security guarantee. The probability of a Common Prefix (CP) violation is proven to decay quadratically in the exponent of the confirmation depth (k):

$$P[\text{CP Violation}] \approx \exp(-\Omega(k^2))$$

This relationship, which we formally state and prove as Theorem 2 in Section 7, is a direct mathematical consequence of the squared time variable in the Rayleigh survival function.

3.5 Confirmation Depth

The super-linear consistency bound allows for a significant optimization of the confirmation depth (k) compared to protocols with linear bounds. A full security analysis, presented in Section 7, accounts for both the dominant quadratic term and a linear term that represents the probability of a "lucky" adversary. This comprehensive analysis reveals that for an adversary controlling 40% of network resources

$(\alpha_A = 0.4)$, a confirmation depth of $\mathbf{k} = \mathbf{26}$ is required to achieve an enterprise-grade security guarantee of $\epsilon \leq 10^{-9}$.

With a target average block time of 15 seconds, this confirmation depth translates to a typical finality time of $26 \times 15\text{s} = 390$ seconds, or approximately **6.5 minutes**. During periods of high network congestion and delay, the autonomous LDD system may increase the average block time to its safety floor (e.g., 48s), resulting in a fastest possible finality time of approximately **21 minutes**. These figures represent a substantial improvement over the multi-hour finality times of traditional PoW protocols.

4 Stability and Security Analysis

The security of Synergeia is validated by proving that its adaptive control loop stabilizes the foundational parameters, thus ensuring the three required blockchain properties (CG, CQ, CP).

4.1 Proof of Slope Stability (Chain Growth)

The protocol guarantees a stable Chain Growth (CG) rate by maintaining the target effective difficulty slope (M_{req}) through algebraic enforcement. This addresses the challenge of external volatility (changing hash power, ΔH) that plagues hybrid protocols.

- **Theorem (Slope Stability):** The final calculated slope M_{final} converges exactly to the required slope M_{req} after every adjustment period, achieving stability in the CG rate (Proven in Section 10).
- **Mechanism:** The **Dynamic Slope Adjustment Scheme** includes a scaling factor (β) that acts as a self-correcting mathematical identity, ensuring $M_{\text{final}} = M_{\text{req}}$.
- **Result:** This stability guarantees the desired block rate ($\tau = 1/15$ blocks/second) is maintained, fulfilling the liveness property of the ledger.

4.2 Chain Quality and Economic Deterrence

The Chain Quality (CQ) property is maximized when the adversarial cost is highest. This occurs precisely when the protocol successfully maintains the target 50/50 block split.

- **CQ Maximization:** Chain Quality (μ) is maximized at the 50/50 equilibrium because this configuration forces the adversary to pay the highest combined price, accessing both the high computational cost (C_{PoW}) and the high economic commitment (C_{PoS}) barriers simultaneously.
- **Economic Enforcement:** The final integrity is protected by the ASW entropy weighting, which ensures that the PoS block weight is proportional to the randomness of the VRF output. This hardens the security against predictive models by ensuring that the chain is preferentially extended by statistically rare, high-entropy blocks.

4.3 Security Against Adversarial Time

The protocol is structurally hardened against the amplification of adversarial power due to network delay (Δ).

- **Structural Resilience:** The system is designed to be resilient by aiming to enforce the **Slot Gap** (ψ) constraint, $\psi > \Delta$. This structural defense minimizes time-based grinding by ensuring the network synchronizes before block production begins. The implications when this constraint is violated are analyzed in Section 8.
- **Timing Integrity:** The high-precision, PoW-anchored **Decentralized Time Consensus (DTC)** scheme uses the 50% BFT-robustness of the median rule to prevent adversarial manipulation of the network's time base.

4.4 Decentralized Time Consensus

The security of Synergeia's Local Dynamic Difficulty (LDD) mechanism, and by extension the entire quadratic consistency claim, hinges on a precise and tamper-resistant time source. This is modeled as an idealized functionality \mathcal{F}_{DTC} . The Synergeia protocol utilizes this functionality to transform raw time samples into a BFT-secure, verifiable time anchor for the protocol's 1-second slots. We propose a concrete instantiation of this functionality based on the permissionless clock synchronization protocol presented by Garay et al. [20], which is a natural fit as Synergeia's PoW component can provide the necessary security anchor for the clock.

Ideal Functionality \mathcal{F}_{DTC} : Decentralized Time Consensus

The functionality \mathcal{F}_{DTC} manages a secure reference time that is robust against adversarial submissions.

- 1: **Setup:** Maintain a true objective time counter (T_{obj}) and a reference clock list (L_{time}).
- 2: **Inputs:** (REQUEST_TIME, sl_{now}) from any registered party \mathcal{U}_i .
- 3: **On REQUEST_TIME (sl_{now}):**
 - 4: \triangleright Step 1: Collect Submissions (Modeled as immediate collection for ideal functionality)
 - 5: $L_{time} \leftarrow \text{Collect_All_Recent_Submissions}()$.
 - \triangleright List of time samples from all active honest and adversarial nodes
 - 6: \triangleright Step 2: Apply BFT Median Rule
 - 7:
 - 8: $T_{median} \leftarrow \text{Median}(L_{time})$.
 - 9: $T_{final} \leftarrow \text{Project_to_Closest_Valid_Slot}(T_{median}, sl_{now})$.
 - 10: \triangleright This median rule guarantees security if $\alpha_A < 50\%$.
- 11: **Output:** Return T_{final} to \mathcal{U}_i as \mathcal{T}_{DTC} (The validated, high-precision time anchor for the current slot).

5 PoS Chain Extension

Protocol Π^{Syn} : Chain Extension Phase

The protocol Π^{Syn} is run by stakeholder \mathcal{U}_i with stake S_i , interacting with ideal functionalities \mathcal{F}_{VRF} , \mathcal{F}_{DSIG} , and \mathcal{F}_{DTC} . (random oracle model assumed)

- 1: **Input:** Local chain \mathcal{C}_i , stake S_i , current slot sl_{now} , available transactions (tx_{pool}), Target slope M_{req} .
- 2: **Chain Update (Consensus Check)**
- 3: $\mathcal{C} \leftarrow \text{Collect all valid chains received from the network.}$
- 4: $\mathcal{C}_{best} \leftarrow \text{MAX_ASW}(\mathcal{C} \cup \{\mathcal{C}_i\})$. \triangleright Select the chain with highest ASW
- 5: $\mathcal{C}_i \leftarrow \mathcal{C}_{best}$. \triangleright Adopt the strongest known chain
- 6: **Time Synchronization (DTC Check)**
- 7: $\mathcal{T}_{DTC} \leftarrow \mathcal{F}_{DTC}.\text{GetTime}(sl_{now})$. \triangleright Retrieve high-precision time baseline
- 8: **PoS Threshold Calculation (LDD)**
- 9: $sl_{parent} \leftarrow \text{GetSlotOfHead}(\mathcal{C}_i)$.
- 10: $\delta \leftarrow sl_{now} - sl_{parent}$.
- 11: $\mathcal{C}_{PoW_Hash} \leftarrow \text{Get_PoW_Anchor_Hash}(\mathcal{C}_i)$. \triangleright Get secure VRF seed
- 12: $S_{total} \leftarrow \text{Get_Total_Committed_Stake}(\mathcal{C}_i)$. \triangleright Get total stake for PoS denominator
- 13: $\alpha_i \leftarrow S_i / S_{total}$
- 14: $\phi \leftarrow \text{Calc_LDD_Threshold}(\delta, M_{req}, \alpha_i)$. \triangleright Calculate dynamic eligibility
- 15: $(y, \pi_y) \leftarrow \mathcal{F}_{VRF}.\bar{\text{EvalProve}}(\mathcal{C}_{PoW_Hash} || sl_{now})$. \triangleright Perform VRF trial
- 16: **if** $y < \phi$ **then** \triangleright If eligible to propose
- 17: **Chain Extension (Block Forging)**
- 18: $\mathcal{B}_{new} \leftarrow \text{Generate_Block}(\mathcal{C}_i, tx_{pool}, y, \pi_y)$.
- 19: $\mathcal{C}_{new} \leftarrow \mathcal{C}_i \parallel \mathcal{B}_{new}$.
- 20: $\mathcal{F}_{DSIG}.\text{Sign}(\mathcal{B}_{new})$.
- 21: $\text{DIFFUSE}(\mathcal{C}_{new})$.
- 22: $\mathcal{C}_i \leftarrow \mathcal{C}_{new}$.
- 23: **end if**

Implementation Details

The Π^{Syn} procedure represents a single execution of the consensus logic by an online stakeholder. Clarity on the following variables is paramount for correct implementation by engineers:

- **Slot Interval (δ):** Calculated as $sl_{\text{now}} - sl_{\text{parent}}$. This measures the time since the last block was recorded on the local chain, serving as the essential input for the Local Dynamic Difficulty (LDD) curve.
- **Decentralized Time Consensus (\mathcal{F}_{DTC}):** An ideal functionality representing the precise, BFT-robust time anchor (T_{DTC}). This high-precision time is crucial for calculating the accurate δ required for the quadratic security bound, overcoming the unreliability of standard PoW timestamps.
- **Target Slope (M_{req}):** The slope required to maintain the 15 second average block time. The Dynamic_Adjust function uses this target to compute the next period's slopes ($f_{A,\text{PoS}}$ and $f_{A,\text{PoW}}$), ensuring the stability of the chain growth property (Section 10).
- **Accumulated Synergistic Work (MAX_ASW):** This is the deterministic, unforgeable chain selection rule (Definition 2.3). It combines both computational cost (PoW) and economic commitment (PoS) to ensure the protocol always converges to the strongest known chain, providing the basis for the 6 block finality.
- **LDD Threshold:** The eligibility threshold $\phi(\delta, \alpha_i) = 1 - (1 - f(\delta))^{\alpha_i}$ is dynamically set by the Calc_LDD_Threshold function based on the current time δ , the validator's stake α_i and difficulty curve $f(\delta)$. This ensures that block production rates are adjusted in real-time to prevent network congestion from compromising security.

6 PoW Chain Extension

PoW Metadata Commitment

- **New Variable:** S_{total} (Total Network Committed Stake Value). This value represents the aggregate stake committed by all registered validators, derived from the UTxO set at the time of block generation.
- **Function Specification:** The Generate_Merkle_Root function is modified to include this value as an explicit, verifiable input:

$$\mathcal{R}_{\text{UTxO}} \leftarrow \text{Generate_Merkle_Root}(\text{TX}_{\text{set}}, S_{\text{total}})$$

- **Justification:** Committing S_{total} directly into the Merkle Root allows PoS light clients to perform the α_{V_k} calculation using the formula $\alpha_{V_k} = \text{Validator's Stake}/S_{\text{total}}$, relying on the PoW commitment for the integrity of the denominator, thus closing the light client security gap.

Protocol Π^{PoW} : PoW Chain Extension Phase

The protocol Π^{PoW} is run by a PoW miner \mathcal{U}_m , aiming to find a block that commits the current PoS state and satisfies the dynamic PoW target, interacting with ideal functionalities $\mathcal{F}_{\text{DSIG}}$, and \mathcal{F}_{DTC} . (random oracle model assumed)

- 1: **Input:** Local chain \mathcal{C}_i , current slot sl_{now} , available transactions (tx_{pool}), Target slope M_{req} .
- 2: **Chain Update (Consensus Check)**
- 3: $\mathcal{C} \leftarrow$ Collect all valid chains received from the network.
- 4: $\mathcal{C}_{\text{best}} \leftarrow \text{MAX_ASW}(\mathcal{C} \cup \{\mathcal{C}_i\})$. ▷ Select the chain with highest ASW
- 5: $\mathcal{C}_i \leftarrow \mathcal{C}_{\text{best}}$. ▷ Adopt the strongest known chain
- 6: **Time Synchronization (DTC Check)**
- 7: $\mathcal{T}_{\text{DTC}} \leftarrow \mathcal{F}_{\text{DTC}}.\text{GetTime}(sl_{\text{now}})$. ▷ Retrieve high-precision time baseline
- 8: **PoW Target Calculation (LDD)**
- 9: $sl_{\text{parent}} \leftarrow \text{GetSlotOfHead}(\mathcal{C}_i)$.
- 10: $\delta \leftarrow sl_{\text{now}} - sl_{\text{parent}}$.
- 11: $\mathcal{T}_{\text{target}} \leftarrow \text{Calc_PoW_Target}(\delta, M_{\text{req}})$.
- 12: **Block Construction and Hashing**
- 13: $S_{\text{total}} \leftarrow \text{Get_Total_Committed_Stake}(\mathcal{C}_i)$. ▷ Get total stake for PoS denominator
- 14: $\mathcal{R}_{\text{UTxO}} \leftarrow \text{Generate_Merkle_Root}(\mathcal{C}_i, \text{tx}_{\text{pool}}, S_{\text{total}})$
- 15: $h \leftarrow \text{Construct_Header}(\mathcal{C}_i, \mathcal{T}_{\text{DTC}}, \mathcal{R}_{\text{UTxO}}, \text{nonce})$.
- 16: $\mathcal{B}_{\text{new}} \leftarrow \text{Mine_PoW_Block}(h, \mathcal{T}_{\text{target}})$.
- 17: **if** \mathcal{B}_{new} is found **then**
- 18: $\mathcal{C}_{\text{new}} \leftarrow \mathcal{C}_i \parallel \mathcal{B}_{\text{new}}$.
- 19: **DIFFUSE**(\mathcal{C}_{new}).
- 20: $\mathcal{C}_i \leftarrow \mathcal{C}_{\text{new}}$.
- 21: **end if**

Implementation Details

The Π^{PoW} procedure outlines the Proof-of-Work block creation logic. It is fundamentally an extension of the Bitcoin mining protocol adapted for dynamic difficulty and dual-consensus security:

- **Dynamic Target ($\mathcal{T}_{\text{target}}$):** This is the difficulty threshold set by the slope, which constantly adjusts to maintain the target 50% PoW contribution. It ensures the block generation rate remains stable despite changes in external hash power.
- **Merkle Root ($\mathcal{R}_{\text{UTxO}}$):** This element is critical for hybrid security. The Merkle Root must commit not only the transactions (tx_{pool}) but also the cryptographic root of the PoS UTxO set, securing the integrity of the total committed stake.
- **Synergistic Work (ASW):** For PoW blocks, the work contribution is the Inverse($\mathcal{T}_{\text{target}}$), representing the verifiable computational cost (Definition 2.3). This forms the computational term of the Accumulated Synergistic Work.

7 Proof of Consistency Bounds

This section provides a mathematical proof for the security claims. We first derive the well-established linear consistency bound, $\epsilon \approx \exp(-\Omega(k))$, for traditional Nakamoto protocols that model block arrivals with a Poisson process. We then formally prove our central claim: by reshaping the block inter-arrival distribution into a Rayleigh distribution via a Local Dynamic Difficulty (LDD) mechanism, Synergeia achieves a superior, super-exponential (quadratic) consistency bound of $\epsilon \approx \exp(-\Omega(k^2))$.

7.1 Introduction and Preliminaries

In blockchain consensus protocols, consistency refers to the property that all honest participants agree on the prefix of the chain. A consistency violation occurs when a previously confirmed block is removed from the longest chain due to a fork. The security of a protocol is often quantified by the probability, ϵ , of a consistency violation for a block buried k levels deep in the chain (i.e., with k confirmations). This analysis is grounded in the formal framework of the Common Prefix property, as established in seminal works on the Bitcoin Backbone Protocol [19] and Ouroboros Praos [15].

Definition 2. – k : The confirmation depth. A transaction is considered final after k blocks have been added after it.

- α_A : The fraction of total resources (e.g., hash power) controlled by the adversary ($0 < \alpha_A < 0.5$).
- α_H : The fraction of total resources controlled by honest participants ($\alpha_H = 1 - \alpha_A$). By assumption, $\alpha_H > \alpha_A$.
- $\epsilon(k)$: The probability of a consistency violation at depth k . The goal is to show that $\epsilon(k) \rightarrow 0$ rapidly as $k \rightarrow \infty$.

7.2 Part 1: Linear Consistency of Nakamoto Consensus

Traditional protocols like Bitcoin operate under a model where block discovery is a memoryless process [19].

Assumption 1 The discovery of blocks by the network follows a Poisson process with a constant rate λ . This implies that the inter-arrival time between blocks follows an exponential distribution. The probability of the adversary finding the next block is $p = \alpha_A$, and the probability for the honest network is $q = \alpha_H$.

Theorem 1. For a traditional Nakamoto protocol, the probability of a consistency violation decays exponentially with a linear dependence on k :

$$\epsilon(k) \approx \exp(-\Omega(k))$$

Proof. Consider an adversary who is k blocks behind the honest chain. For the adversary's private chain to succeed, it must eventually become longer than the honest chain. This can be modeled as a random walk. Let the state be the difference between the length of the adversary's chain and the honest chain, $Z = L_A - L_H$. The adversary starts at a deficit of k , so $Z_0 = -k$. Let $p = \alpha_A$ be the adversary's probability of finding the next block and $q = \alpha_H$ be the honest party's probability, with $p < q$.

The probability that an adversary overcomes a deficit of k blocks is given by the classic random walk result for ruin against an infinitely wealthy opponent, a model commonly applied in blockchain security analysis [19,18]:

$$P(\text{catch-up from deficit } k) = \left(\frac{p}{q}\right)^k = \left(\frac{\alpha_A}{\alpha_H}\right)^k$$

Since we assume $\alpha_A < \alpha_H$, the ratio α_A/α_H is a constant less than 1. We can write this probability as:

$$\epsilon(k) = \left(\frac{\alpha_A}{\alpha_H}\right)^k = \exp\left(k \ln\left(\frac{\alpha_A}{\alpha_H}\right)\right)$$

Let $C = \ln(\alpha_H/\alpha_A)$. Since $\alpha_H > \alpha_A$, C is a positive constant. The expression becomes:

$$\epsilon(k) = \exp(-C \cdot k)$$

This is of the form $\exp(-\Omega(k))$, demonstrating that the consistency violation probability decays exponentially with a linear dependence on k . The linear bound is a direct consequence of the memoryless property of the underlying Poisson process.

7.3 Part 2: Quadratic Consistency of Synergeia

In contrast to the memoryless model, Synergeia's LDD mechanism induces a time-dependent block arrival process that approximates a Rayleigh distribution. This structural change allows for a super-exponential security guarantee.

Assumption 2 *The inter-arrival time for a block produced by a party (or coalition of parties) with resource fraction α follows a Rayleigh distribution with slope parameter $M \propto \alpha$. The Probability Density Function (PDF) is $R(x; M) = Mx \cdot \exp(-Mx^2/2)$, and the Survival Function (SF), $S(x) = P(X > x)$, is given by:*

$$S(x; M) = \int_x^\infty Mt \exp(-Mt^2/2) dt = \exp(-Mx^2/2)$$

The mean inter-arrival time is $\mathbb{E}[X] = \sqrt{\frac{\pi}{2M}}$. Let M_H and M_A be the slope parameters for the honest and adversarial parties, respectively, where $M_H/M_A = \alpha_H/\alpha_A$.

Theorem 2. *For the Synergeia protocol, the probability of a consistency violation decays super-exponentially with a quadratic dependence on k :*

$$\epsilon(k) \approx \exp(-\Omega(k^2))$$

Proof. The proof replaces the asymptotic argument based on the Law of Large Numbers with a more rigorous analysis using concentration inequalities, which holds for the small, non-asymptotic values of k relevant to the protocol's practical claims.

1. The Adversarial Challenge. An adversary attempts to create a private chain of length k that will eventually replace a segment of the honest chain. A necessary (though not sufficient) condition for this attack to succeed is that the adversary must mine all k of their blocks before the honest network mines its next single block. Let $T_A(k)$ be the random variable representing the time required for the adversary to mine k blocks, and let T_H be the random variable for the time required for the honest network to mine one block. The probability of a consistency violation, $\epsilon(k)$, is bounded by the probability of this event:

$$\epsilon(k) \leq P(T_A(k) < T_H) = \int_0^\infty P(T_A(k) = t) \cdot P(T_H > t) dt$$

where $P(T_H > t) = S_H(t) = \exp(-M_H t^2/2)$ is the survival function for the honest network.

2. Bounding the Adversary's Time. The adversary's time, $T_A(k)$, is the sum of k independent and identically distributed (i.i.d.) random variables, $T_A(k) = \sum_{i=1}^k X_i$, where each X_i follows a Rayleigh distribution with parameter M_A . The expected time is $\mu_k \triangleq \mathbb{E} = k \cdot \mathbb{E}[X_i] = k \sqrt{\frac{\pi}{2M_A}}$.

The previous analysis approximated the random variable $T_A(k)$ with its mean μ_k . This is only valid for large k . To create a robust proof for small k , we must account for the probability that $T_A(k)$ deviates significantly from its mean. An adversary is most advantaged when they get lucky and mine their blocks much faster than expected. We can bound the probability of this event using a concentration inequality.

3. Applying Concentration Bounds. We partition the analysis based on the behavior of $T_A(k)$. For any $\nu \in (0, 1)$:

$$\epsilon(k) \leq P(T_A(k) < T_H) = P(T_A(k) < T_H \wedge T_A(k) \geq (1 - \nu)\mu_k) + P(T_A(k) < T_H \wedge T_A(k) < (1 - \nu)\mu_k)$$

This can be bounded as:

$$\epsilon(k) \leq P(T_H > (1 - \nu)\mu_k) + P(T_A(k) < (1 - \nu)\mu_k)$$

The first term represents the probability of the honest network remaining silent for a duration close to the adversary's expected time. The second term is the probability of a "lucky" adversary who mines significantly faster than expected.

4. Bounding the Terms. **Term 1 (The Quadratic Term):** The first term is evaluated using the honest survival function:

$$\begin{aligned} P(T_H > (1 - \nu)\mu_k) &= S_H((1 - \nu)\mu_k) = \exp\left(-\frac{M_H}{2}\left((1 - \nu)k\sqrt{\frac{\pi}{2M_A}}\right)^2\right) \\ &= \exp\left(-k^2 \cdot (1 - \nu)^2 \cdot \frac{\pi M_H}{4 M_A}\right) = \exp\left(-k^2 \cdot (1 - \nu)^2 \cdot \frac{\pi \alpha_H}{4 \alpha_A}\right) \end{aligned}$$

This term has the form $\exp(-\Omega(k^2))$ and will dominate the bound.

Term 2 (The Linear Term): The second term, $P(T_A(k) < (1 - \nu)\mu_k)$, is the probability of a large downward deviation of a sum of i.i.d. random variables from its mean. We can bound this using a Chernoff-Hoeffding style inequality [25,13]. For a sum of k i.i.d. variables, a standard form of the bound is:

$$P(T_A(k) \leq (1 - \nu)\mu_k) \leq \exp\left(-\frac{k \cdot \nu^2 \mathbb{E}[X_i]^2}{2\text{Var}[X_i] + \frac{2}{3}\nu\mathbb{E}[X_i] \cdot B}\right)$$

where B is an upper bound on the random variables. While the Rayleigh distribution is unbounded, its tail decays super-exponentially, and for the purpose of this analysis, we can consider it effectively bounded. More simply, standard Chernoff bounds for sub-Gaussian variables (which include Rayleigh) yield a tail probability of the form $\exp(-\Omega(k\nu^2))$. This term decays exponentially in k , but only linearly.

5. Final Bound. Combining the two terms, we have:

$$\epsilon(k) \leq \exp(-k^2 \cdot C_1) + \exp(-k \cdot C_2)$$

where $C_1 = (1 - \nu)^2 \frac{\pi \alpha_H}{4 \alpha_A}$ and C_2 is a positive constant derived from the concentration inequality. For any fixed ν and sufficiently large k , the first term, which decays quadratically in the exponent, dominates the second term. This completes the proof that the consistency violation probability decays as $\exp(-\Omega(k^2))$, a bound that is robust for both small and large k .

Bounding the Race Condition. A necessary condition for any successful forking attack to cause a consistency violation at depth k is that the adversary must be able to produce their fork of length k faster than the honest network can produce its next block. While this does not cover all complex adversarial strategies (such as selfish mining or the intricate fork geometries analyzed by Blum et al. [9]), it bounds the fundamental stochastic race that underpins any such attack. Let $T_A(k)$ be the random variable for the time required for the adversary to mine k blocks, and let T_H be the time for the honest network to mine one block. The probability of a consistency violation, $\epsilon(k)$, is bounded by the probability of this event:

$$\epsilon(k) \leq P(T_A(k) < T_H)$$

Applying Concentration Bounds. The adversary's time, $T_A(k)$, is the sum of k i.i.d. random variables, $T_A(k) = \sum_{i=1}^k X_i$, where each X_i follows a Rayleigh distribution with parameter M_A . The expected time is $\mu_k \triangleq \mathbb{E} = k\sqrt{\frac{\pi}{2M_A}}$. To create a robust proof for small k , we must account for the probability that $T_A(k)$ deviates significantly from its mean. We partition the analysis for any $\nu \in (0, 1)$:

$$\epsilon(k) \leq P(T_H > (1 - \nu)\mu_k) + P(T_A(k) < (1 - \nu)\mu_k)$$

The first term represents the probability of an "unlucky" honest network remaining silent for a duration close to the adversary's expected time. The second term is the probability of a "lucky" adversary who mines significantly faster than expected.

Deriving Explicit Constants. The previous version of this paper argued that the first term dominates asymptotically. However, for practical claims at small k , we must derive the explicit constants for both terms.

The Quadratic Term: The first term is evaluated using the honest survival function:

$$P(T_H > (1 - \nu)\mu_k) = \exp\left(-k^2 \cdot (1 - \nu)^2 \cdot \frac{\pi}{4} \frac{\alpha_H}{\alpha_A}\right) = \exp(-C_1 k^2)$$

The Linear Term: The second term is the probability of a large downward deviation of a sum of i.i.d. sub-Gaussian random variables. Using a standard Chernoff-style bound for such sums, we have $P(T_A(k) < (1 - \nu)\mu_k) \leq \exp(-\frac{\nu^2 \mu_k^2}{2\text{Var}(T_A(k))})$. The variance of the sum is $\text{Var}(T_A(k)) = k \cdot \text{Var}(X_i) = k \frac{4-\pi}{2M_A}$. Substituting this and $\mu_k = k \sqrt{\frac{\pi}{2M_A}}$ yields:

$$P(T_A(k) < (1 - \nu)\mu_k) \leq \exp\left(-k \cdot \nu^2 \frac{\pi}{2(4 - \pi)}\right) = \exp(-C_2 k)$$

Numerical Analysis. The total error is bounded by $\epsilon(k) \leq \exp(-C_1 k^2) + \exp(-C_2 k)$. The choice of ν represents a trade-off between bounding the probability of a lucky adversary versus an unlucky honest network. An optimal choice of ν seeks to balance these two error terms. For an adversary with $\alpha_A = 0.4$ (so $\alpha_H = 0.6$), the optimal trade-off occurs at $\nu \approx 0.66$. This yields the constants:

$$\begin{aligned} C_1 &= (1 - 0.66)^2 \cdot \frac{\pi}{4} \cdot \frac{0.6}{0.4} \approx 0.136 \\ C_2 &= 0.66^2 \cdot \frac{\pi}{2(4 - \pi)} \approx 0.796 \end{aligned}$$

The dominant term for small k is the linear term, which represents the probability of a lucky adversary. To achieve the target security of $\epsilon \leq 10^{-9}$, we must ensure this term is sufficiently small. Solving for k :

$$\exp(-0.796 \cdot k) \leq 10^{-9} \implies -0.796 \cdot k \leq \ln(10^{-9}) \approx -20.72$$

$$k \geq \frac{20.72}{0.796} \approx 26.03$$

Therefore, a confirmation depth of $\mathbf{k = 26}$ is required. At this depth, the quadratic term is $\exp(-0.136 \cdot 26^2) \approx \exp(-91.9)$, which is negligible. This refined analysis leads to a time-to-finality of 26 blocks \times 15 s/block = 390 seconds, or **6.5 minutes** representing a significant improvement over the multi-hour finality times of traditional PoW protocols.

7.4 Robustness, Adversarial Strategies, and Effective Resource Fraction

The preceding proof relies on an idealized assumption: that the adversary's resource fraction α_A is static and that the LDD mechanism perfectly produces an ideal Rayleigh distribution. This assumption is flawed in two ways:

1. **Practical Deviations:** The "snowplow curve" is a piecewise linear approximation of the required hazard rate [41]. This approximation, combined with natural network variance [10,14,21], means the true block arrival distribution will only be an approximation of a perfect Rayleigh distribution.
2. **Adversarial Strategies:** A sophisticated adversary will not behave passively. As noted in formal critiques of this model, they will employ strategies specifically to distort the distribution or exploit the system's dynamics to gain an advantage.

A qualitative approach to model this is to introduce a deviation parameter η_d into the exponent, yielding a bound of $\epsilon \approx \exp(-\Omega(k^{2-\eta_d}))$ where $1 > \eta_d > 0$. A more rigorous approach, which we will formally develop in Sections 11.8 and 12, is to model these deviations and adversarial strategies as a quantifiable, **constant-factor advantage**. This advantage is expressed as an **effective adversarial resource fraction**, α'_A , where $\alpha'_A > \alpha_A$. The adversary's true power is not their nominal resource share, but this effective share they achieve by optimally exploiting the protocol's dynamics (e.g., via LDD-grinding or exploiting difficulty oscillations).

Therefore, the robust security bound for the protocol is not a modified exponent, but the original quadratic-term-dominant bound, evaluated at this effective resource fraction:

$$\epsilon(k) \leq \exp(-C'_1 k^2) + \exp(-C'_2 k)$$

where the constants C'_1 and C'_2 are functions of the *effective* resource ratio, $\alpha'_H/\alpha'_A = (1 - \alpha'_A)/\alpha'_A$. By formally deriving α'_A in our later analysis, we provide a concrete, falsifiable, and quantitative security guarantee. This we use this expression to estimate the exponent degradation factor (Section 7.4):

$$\eta_d(k) \approx \frac{1}{C'_1} \ln(1 + \exp(C'_1 k^2 - C'_2 k))$$

8 Network Delay and Its Impact on Consistency

The quadratic consistency bound derived in Section 7 provides a theoretical foundation for Synergeia's fast finality. However, this analysis rests on an idealized assumption about network conditions. This section critically re-evaluates this assumption, moving from a deterministic to a probabilistic model of network delay to provide a more robust and realistic security analysis.

8.1 The Fragility of the Secure State Assumption

The initial security analysis is predicated on the system operating in what we define as the **Secure State**, where the protocol-defined slot gap, ψ , is strictly greater than the maximum network delay, Δ .

Assumption 3 *The protocol successfully enforces the structural constraint $\psi > \Delta$.*

While this assumption simplifies the analysis, it is an untenable idealization for a permissionless distributed system. Network delay Δ is not a fixed, known constant; it is a random variable with a potentially heavy-tailed distribution. More critically, an adversary can actively manipulate network delay through various attacks, such as network partitioning or eclipse attacks, making Δ effectively unbounded from the perspective of some honest nodes [37,4,31]. The binary model, which assumes the protocol is either perfectly secure (if $\psi > \Delta$) or insecure (if $\Delta > \psi$), fails to capture the probabilistic nature of network delay and its nuanced impact on security.

8.2 Modeling the Impact of Constant Network Delay

To understand the impact of violating the Secure State assumption, we first analyze the case where the network delay Δ is a fixed constant greater than ψ .

Definition 3. *When $\Delta > \psi$, an adversary who finds a block can begin mining the next block immediately. Honest nodes, however, must wait for the block to propagate across the network. This gives the adversary a mining head start of duration $t_\Delta = \Delta - \psi$ on the rest of the network for each block they produce.*

This head start directly interferes with the time-dependent hazard rate that underpins the Rayleigh distribution model. An adversary's success requires their k -block chain to be produced in time $T_A(k)$, while the honest network fails to produce a block in that time. With a head start t_Δ , the condition for the honest network's failure becomes more lenient for the adversary: the honest network must remain silent for a period of only $T_A(k) - t_\Delta$. This leads to a degraded security bound.

Theorem 3. *When network delay Δ exceeds the slot gap ψ by a fixed amount $t_\Delta = \Delta - \psi > 0$, the consistency violation probability for Synergeia degrades according to:*

$$\epsilon(k, \Delta) \approx \exp\left(-k^2 \cdot \frac{\pi}{4} \frac{\alpha_H}{\alpha_A} \cdot \left(\max\left(0, 1 - \frac{\Delta - \psi}{k\mu_A}\right)\right)^2\right)$$

where μ_A is the adversary's mean block time in the ideal case.

Proof. The proof follows the structure of Theorem 2, but adjusts for the head start. The condition for an adversarial consistency violation is bounded by the probability that the honest network fails to produce a block in the time it takes the adversary to produce k blocks, adjusted for the head start. Approximating the adversary's time $T_A(k)$ with its mean $\mu_k = k\mu_A$, the effective time window for the honest network is

reduced to $\max(0, k\mu_A - t_\Delta)$. The probability of the honest network remaining silent for this duration is given by its survival function, $S_H(\max(0, k\mu_A - t_\Delta))$.

$$\epsilon(k, \Delta) \leq S_H(\max(0, k\mu_A - t_\Delta)) = \exp\left(-\frac{M_H}{2} (\max(0, k\mu_A - t_\Delta))^2\right)$$

Substituting $M_H = \frac{\pi}{2\mu_H^2}$ and the relation $\frac{\mu_A^2}{\mu_H^2} = \frac{\alpha_H}{\alpha_A}$ yields the stated bound. The degradation factor $(\max(0, 1 - t_\Delta/(k\mu_A)))^2$ shows that as network delay increases, the effective security decreases quadratically.

This theorem reveals the fragility of the protocol’s finality time. The performance claims from the idealized Secure State represent a best-case scenario. Table 2 illustrates how rapidly the claimed 90-second finality degrades as network conditions worsen, based on illustrative calculations for a 40% adversary.

Table 2: Synergeia Confirmation Depth (k) vs. Fixed Network Delay (Δ) for $\epsilon_{\text{target}} = 10^{-9}$ and $\alpha_A = 40\%$.

Network State	Head Start ($t_\Delta = \Delta - \psi$)	Required k	Time to Finality
Secure State	$t_\Delta \leq 0$	6	90 seconds
Moderate Delay	$t_\Delta = 15s$	≈ 8	≈ 2 minutes
High Delay	$t_\Delta = 60s$	≈ 10	≈ 2.5 minutes
Extreme Delay	$t_\Delta = 300s$	≈ 19	≈ 4.75 minutes

8.3 A Generalized Security Model with Probabilistic Delay

While analyzing fixed delays is illustrative, a more rigorous model must treat network delay Δ as a random variable, reflecting the unpredictable nature of permissionless networks. This approach, similar to the semi-synchronous analysis of protocols like Ouroboros Praos [15], provides a far more credible security guarantee.

Let $D(\Delta)$ be the PDF of the variable network delay Δ . The overall probability of a consistency violation is the expectation of the conditional probability from Theorem 3, taken over the distribution of Δ .

Theorem 4. *Given that network delay Δ is a random variable with probability density function $D(\Delta)$, the consistency violation probability for Synergeia is given by:*

$$\epsilon(k) = \int_0^\infty \epsilon(k, \Delta) D(\Delta) d\Delta$$

where $\epsilon(k, \Delta)$ is the conditional probability from Theorem 3.

This integral formulation represents the most robust security guarantee for the protocol. While it may not have a closed-form solution for arbitrary distributions, it can be evaluated numerically to assess the protocol’s resilience under various empirically-derived or theoretically-motivated models for network delay (e.g., exponential, log-normal, or Pareto distributions). This generalized model correctly frames security not as a binary condition, but as a spectrum that degrades gracefully—or rapidly—depending on the interplay between the protocol’s timing assumptions (ψ) and the statistical properties of the network environment.

9 Distributed Consensus Service (DCS)

The Synergeia protocol’s aspiration towards fully autonomous adaptive system necessitates a robust mechanism for achieving consensus on critical system state variables in a permissionless environment. While initial designs might rely on static parameters or external oracles, our iterative security analysis revealed the fragility of such approaches. This led to the development and progressive expansion of the **Distributed Consensus Service (DCS)**, presented formally as the ideal functionality \mathcal{F}_{DCS} . This section traces the evolution of the DCS, analyzes its security foundations, and justifies the architectural choices it enables.

The need for such a service first emerged from the security requirements of the Local Dynamic Difficulty (LDD) mechanism. The LDD’s quadratic consistency claim hinges on a precise and tamper-resistant time source, leading to the initial conception of a Decentralized Time Consensus (\mathcal{F}_{DTC}) anchored by PoW beacons (Section 4.4).

Subsequently, the analysis of the VETO mechanism’s vulnerability to malicious Merkle root commitments (misrepresenting total stake S_{total}) revealed the need for BFT consensus on this value as well. This led to the proposal of a Decentralized Stake Consensus (\mathcal{F}_{DSC}) using PoS beacons. Recognizing the common underlying primitive, these were unified into the general \mathcal{F}_{DCS} (Section 9.12), capable of providing BFT-robust consensus on arbitrary scalar values via on-chain beacons and median/percentile calculations.

This generalized service became the cornerstone for enabling full protocol autonomy. By adding beacons for network delay ($\Delta_{consensus}$) and transaction load ($L_{consensus}$), the \mathcal{F}_{DCS} empowers the fully autonomous LDD system, allowing Synergeia to dynamically adapt its core timing parameters (ψ, μ_{target}) to physical network conditions. Further extensions incorporate Security Beacons (Section 15) and Topology Beacons to provide consensus measures ($\mathcal{S}_{threat}, \mathcal{H}_{chain}$) enabling adaptive monetary policy and proactive consistency hardening. Finally, addressing the security of the DCS itself led to the integration of Beacon Bounties, incentivizing the honest participation crucial for its BFT guarantees.

The DCS thus evolved from a single-purpose utility into the protocol’s central sensory organ, providing the necessary inputs for the adaptive feedback loops defined by the Principle of Adaptive Protocol Homeostasis (Section 17.1). The following subsections delve into the specific security analyses and justifications related to the mechanisms enabled by, or securing, the DCS.

9.1 Game-Theoretic Security of the VETO Mechanism

The protocol’s defense against malicious state commitments by PoW miners relies on a non-slashing economic deterrent, which we term the VETO mechanism. In this mechanism, the majority of PoS validators can vote to cause a PoW miner to forfeit their block reward (\mathcal{R}_{PoW}) if the miner is detected to have committed a malicious state root.

9.2 The Deterrence Lemma

We derive a non-slashing economic deterrent by bounding the maximum financial gain against the minimum verifiable loss of a malicious PoW miner by manipulating the blocks Merkle root.

- **Theorem (The Deterrence Lemma):** The Merkle Root Staking mechanism provides a sufficient economic deterrent if the total verifiable block reward (\mathcal{R}_{PoW}) is set to be strictly greater than the maximum financial gain (G_{max}) an adversary can achieve by committing a single forged state root.
- **Formal Deterrence Condition:** The protocol must enforce the following condition in its reward calibration logic:

$$\mathcal{R}_{PoW} > G_{max}$$

- **Maximum Gain Constraint (G_{max}):** The maximum potential gain from a single block forgery is explicitly set as a protocol parameter based on the highest-value transaction the ledger is designed to handle in one block:

$$G_{max} = \text{Max_Block_Transaction_Value}$$

- **Conclusion:** By ensuring the PoW miner’s exposure to loss (\mathcal{R}_{PoW}) exceeds the highest possible gain from attack (G_{max}), the protocol creates an economically irrational path for the adversary, validating the integrity of the non-slashing defense mechanism.

Lemma 1. *The Merkle Root Staking mechanism, wherein a malicious PoW miner forfeits the block reward \mathcal{R}_{PoW} upon a VETO from honest PoS stakeholders, provides an economic deterrent against committing a malicious state root if the expected utility of remaining honest is greater than the expected utility of attacking.*

Proof. We model the scenario as a game between a potentially malicious PoW miner (M_A) and the honest PoS validators (V_H) using expected utility theory. **1. Actions and Payoffs:**

- Miner’s Actions: *Commit_Honest_Root* or *Commit_Malicious_Root*.
- Gain from Attack (G_{max}): The maximum financial gain from a successful forgery.
- Cost of Mining (C_{mine}): The operational cost to find the PoW block.
- Reward (\mathcal{R}_{PoW}): The total block reward, which is forfeited if a VETO occurs.

The attack is detected if the honest PoS majority validates the chain during the Witnessing Period. We assume an honest PoS majority and a sufficiently long Witnessing Period, making the probability of a successful veto approach certainty:

$$P(\text{Veto}) \rightarrow 1$$

The probability of the attack succeeding is therefore infinitesimal: $P(\text{Success}) = 1 - P(\text{Veto})$. A rational, profit-maximizing miner will not attack if the expected utility (EU) of being honest is greater than that of attacking.

- **Utility of Honesty:** $EU(\text{Honest}) = \mathcal{R}_{PoW} - C_{mine}$
- **Utility of Attack:** $EU(\text{Attack}) = P(\text{Success}) \cdot (G_{max} + \mathcal{R}_{PoW}) + P(\text{Veto}) \cdot (0) - C_{mine}$

$$EU(\text{Attack}) = (1 - P(\text{Veto}))(G_{max} + \mathcal{R}_{PoW}) - C_{mine}$$

The deterrence condition is $EU(\text{Honest}) > EU(\text{Attack})$.

$$\mathcal{R}_{PoW} - C_{mine} > (1 - P(\text{Veto}))(G_{max} + \mathcal{R}_{PoW}) - C_{mine}$$

$$\mathcal{R}_{PoW} > (1 - P(\text{Veto}))(G_{max} + \mathcal{R}_{PoW})$$

Let $\nu = 1 - P(\text{Veto})$. As $P(\text{Veto}) \rightarrow 1$, ν is a very small positive number.

$$(1 - \nu)\mathcal{R}_{PoW} > \nu \cdot G_{max} \implies \mathcal{R}_{PoW} > \frac{\nu}{1 - \nu}G_{max}$$

As $\nu \rightarrow 0$, the right-hand side approaches 0. To provide a robust security margin against any deviation from the ideal model, the protocol must enforce a stronger, conservative condition. By ensuring the guaranteed loss from being caught exceeds the maximum possible gain, the attack becomes economically irrational. A sufficient condition is therefore:

$$\mathcal{R}_{PoW} > G_{max}$$

This turns the PoW reward into a de-facto security bond, making the non-slashing mechanism an economic deterrent.

9.3 A Game-Theoretic Model of the VETO Process

We model the VETO process as a game between three types of players: a malicious PoW miner (the Attacker), a set of colluding PoS validators, and a set of honest PoS validators.

Definition 4 (Players and Parameters).

- **Attacker (A):** A PoW miner who can gain G_{max} by successfully committing a malicious state root. The block reward at risk is \mathcal{R}_{PoW} .
- **Honest Validators (H):** PoS validators who wish to maintain the integrity of the protocol. They control a fraction of the total stake α_H .
- **Colluding Validators (C):** PoS validators who act in concert with the Attacker. They control a fraction of the total stake α_C .
- **Quorum Threshold (q_{veto}):** The fraction of total stake required to vote ‘yes’ for a VETO to pass (e.g., $q_{veto} = 2/3$).
- **Cost of Voting (C_{vote}):** A small but non-zero cost incurred by any validator for participating in a VETO vote, representing computational resources, transaction fees, and attention costs.
- **Perceived Risk (R_{risk}):** A perceived risk to a validator for voting against a malicious actor, representing the potential for off-chain retaliation.
- **Long-Term Utility ($U_{integrity}$):** The discounted future utility an honest validator derives from maintaining the long-term integrity and value of the network.

The Attacker’s strategy is to attack if the expected utility is positive. An honest validator’s strategy is to vote for a VETO if their expected utility for voting is positive.

9.4 Analysis of Failure Modes: Collusion and Apathy

The simple Deterrence Lemma fails when rational behavior is considered.

Failure due to Collusion. A VETO requires an honest supermajority. If the Attacker colludes with a fraction α_C of the stake, these validators will vote 'no' or abstain. A VETO can only succeed if the remaining honest stake is sufficient to meet the quorum.

Lemma 2 (Collusion Failure). *An attack will succeed, regardless of honest validator behavior, if the colluding stake α_C satisfies:*

$$\alpha_C > 1 - q_{veto}$$

Proof. The maximum possible 'yes' vote is the total honest stake, α_H . The total stake is normalized to 1, so $\alpha_H \leq 1 - \alpha_C$. The VETO requires the voting 'yes' stake to be $\geq q_{veto}$. If $\alpha_C > 1 - q_{veto}$, then the maximum possible honest stake is $\alpha_H < q_{veto}$, making it impossible to achieve a quorum.

This demonstrates that the VETO mechanism is vulnerable to a minority coalition of validators, a threat not captured by the original lemma.

Failure due to Rational Apathy. More critically, the mechanism is vulnerable even without active collusion. An honest validator must decide whether to incur the cost and risk of voting. An honest validator $i \in \mathcal{H}$ will choose to vote only if the expected utility of voting is greater than the utility of abstaining.

$$\mathbb{E}[U_i(\text{Vote})] > \mathbb{E}[U_i(\text{Abstain})]$$

The utility of abstaining is 0. The utility of voting is the preservation of long-term network integrity, discounted by the probability that validator i 's single vote is pivotal, minus the immediate costs. A simplified decision rule is that a validator will vote if the perceived benefit outweighs the cost:

$$U_{\text{integrity}} > C_{\text{vote}} + R_{\text{risk}}$$

However, for any individual validator, their single vote is unlikely to be pivotal. In a large system, it is rational for an individual to assume others will bear the cost of voting, a classic collective action problem. This phenomenon, known as rational ignorance or voter apathy, means a fraction of the honest stake, $\alpha_{\text{apathetic}}$, may choose to abstain.

Lemma 3 (Apathy Failure). *An attack will succeed if the fraction of apathetic honest stake is large enough to prevent a quorum, i.e., if:*

$$\alpha_H - \alpha_{\text{apathetic}} < q_{veto}$$

This shows that the security of the VETO rests not on a simple economic calculation, but on the active, coordinated, and costly participation of a supermajority of honest actors, an assumption that is not guaranteed.

9.5 Comparative Analysis: VETO vs. Slashing

The weaknesses of the VETO mechanism are best understood in comparison to the alternative economic deterrent used in many PoS protocols: slashing [15].

- **Slashing:** In a slashing mechanism, a validator who is proven to have acted maliciously (e.g., by signing two conflicting blocks) has a significant portion of their staked capital confiscated and often burned or redistributed. This is a direct, severe, and on-chain "capital punishment." The penalty is typically orders of magnitude greater than any potential gain from a single malicious action, creating a powerful economic bond to behave honestly. The primary risk is the complexity of implementation; bugs in the slashing conditions could lead to the unfair punishment of honest validators.
- **VETO (Reward Forfeiture):** The VETO mechanism is a "misdemeanor" penalty. The attacker only loses the potential revenue from a single block (\mathcal{R}_{PoW}). This is a much weaker deterrent. While it avoids the risk of catastrophic capital loss for validators, its security relies on the collective action of the honest majority, which, as shown above, is not guaranteed. The VETO mechanism fails to create a strong, direct economic bond for the PoW miner, and it imposes costs and risks on the honest PoS validators who are tasked with enforcement.

In conclusion, while the non-slashing approach is appealing for its lower risk to participants, the game-theoretic analysis shows that the security it provides is significantly weaker and more fragile than that provided by a well-implemented slashing protocol.

9.6 Economic Deterrence and State Integrity

The integrity of the Accumulated Synergistic Work (ASW) metric, and by extension the entire protocol, depends on the verifiable accuracy of the data committed in each block header. The preceding analysis highlights a critical attack vector involving the manipulation of the Merkle Root, $\mathcal{R}_{\text{UTxO}}$, by a malicious PoW miner. Specifically, a miner could commit a root that misrepresents the total network stake, S_{total} , in order to unfairly amplify the ASW of future blocks produced by colluding PoS validators. While the VETO mechanism was conceived as a deterrent, our prior game-theoretic analysis revealed its vulnerabilities to rational apathy and collusion.

9.7 Generalized Consensus of a Scalar Value

This section introduces a far stronger, structural defense that mitigates this threat by design.

2-for-1 Proofs of Work Following the technique from Garay et al. [20], miners in Synergeia perform a single hash computation per nonce but check the result against two independent targets. A success against the first target yields a standard Synergeia block. A success against the second target (e.g., by checking the bit-reversed hash output) yields a synchronization beacon. This ensures that computational power is not split between the two tasks.

Synchronization Beacons A beacon is a lightweight, signed message containing the miner’s current local value of a scalar quantity. Once created, beacons are diffused through the network and included in subsequent Synergeia blocks, creating an immutable, on-chain record of time samples from active participants.

Periodic Clock Adjustment via Median The protocol defines a clock synchronization interval of R rounds. At the end of each interval, every alert party performs a clock adjustment. The party collects all valid beacons included in its local chain for that interval and computes the difference between each beacon’s timestamp and its local arrival time. The party then computes the median of these differences to get a value, $shift$, and adjusts its local clock by this value. This mechanism realizes the properties of \mathcal{F}_{DTC} . Its security is founded on the PoW-secured blockchain, which ensures all honest parties eventually converge on the same set of beacons. The use of the median provides robustness against adversarial beacons with outlier timestamps, guaranteeing security so long as an honest majority of computational power is contributing to beacon creation.

9.8 Security Analysis of the Decentralized Time Consensus

The security of the LDD mechanism, and by extension the entire consistency claim, is critically dependent on the integrity of the consensus time T_{DTC} provided by the \mathcal{F}_{DTC} . The preceding analysis considers the synchronization mechanism resilient to a desynchronization attack via a long-lived network partition. However, there is a more subtle and dangerous class of attacks that do not require an expensive fork: Sybil-based bias attacks, also known as timejacking.

Attack Vector: Sybil-Based Median Biasing A sophisticated adversary’s goal is not to create a separate chain, but to strategically bias the set of beacons observed by honest nodes to corrupt the median calculation. An adversary can leverage a Sybil attack to flood the network with a large number of nodes that broadcast malicious beacons with inaccurate timestamps. If the adversary can contribute enough malicious beacons, they can pull the consensus median T_{median} away from the true value.

The critical threat is an adversary who successfully biases the consensus network delay, $\Delta_{\text{consensus}}$, which is also provided by the \mathcal{F}_{DCS} (Section 9.12). If an adversary can manipulate the median to report a value $\Delta_{\text{biased}} < \Delta_{\text{true}}$, the protocol will autonomously set its slot gap ψ_{new} to a value smaller than the true network delay. This would silently and completely invalidate the core security assumption ($\psi > \Delta$) of the consistency proof, leaving the network vulnerable while appearing to operate normally.

Formal Model of the Attack Cost We provide a formal analysis that models and quantifies the cost of biasing the median. The security of the median is BFT-robust, guaranteed as long as less than 50% of the weight of the contributing beacons is malicious. In our system, the weight of a beacon is tied to the resource that produces it (PoW hash power for Time Beacons, PoS stake for Stake Beacons).

Let α_A be the adversary's fraction of the relevant resource (e.g., hash power).

- The total weight of honest beacons is proportional to $\alpha_H = 1 - \alpha_A$.
- The total weight of adversarial beacons is proportional to α_A .

To corrupt the median, the adversary must contribute a total weight of malicious beacons that exceeds the honest weight. This is impossible if $\alpha_A < 0.5$.

However, this model assumes all honest participants produce beacons. A more realistic model must account for $\alpha_{honest_participating} \leq \alpha_H$. The true security condition is:

$$\alpha_A < \alpha_{honest_participating}$$

This attack vector is therefore only viable if a significant fraction of honest participants rationally choose not to produce beacons (e.g., to save on transaction fees). This highlights a critical, implicit assumption: the protocol's security relies on widespread, active, and honest participation in the beaconing process. Therefore, we must include an incentive model (e.g., rewards for beacon production) to ensure $\alpha_{honest_participating}$ remains high, thereby guaranteeing $\alpha_A < \alpha_{honest_participating}$ and securing the BFT integrity of the oracle. Without such incentives, the cost of a Sybil-based bias attack could be dangerously low.

9.9 Generalizing Decentralized Consensus: From Time to Stake

The core of the malicious Merkle Root vulnerability lies in allowing a single PoW miner to be the trusted source for the value of S_{total} when generating a block. We can repurpose the same BFT-style consensus primitive used by the Decentralized Time Consensus (\mathcal{F}_{DTC}) to establish a tamper-resistant, network-wide consensus on the value of the total stake. We introduce a new idealized functionality, **Decentralized Stake Consensus** (\mathcal{F}_{DSC}). Its mechanism is analogous to that of \mathcal{F}_{DTC} :

1. **Stake Beacons:** At regular intervals, a subset of active participants (e.g., PoS validators) broadcast signed "stake beacons." Each beacon contains the participant's view of the current total network stake, S_{total} , as calculated from their local UTXO set.
2. **On-Chain Anchoring:** These beacons are propagated through the network and included in subsequent blocks, creating an immutable, on-chain record of stake value attestations.
3. **Median Calculation for BFT Security:** At the end of each interval, every honest node independently collects all valid stake beacons from its local chain. Each node then computes the median of these attested stake values. This median value represents the BFT-secure consensus on the total network stake for the next interval.

The security of this mechanism is identical to that of the DTC: as long as an honest majority of participants are producing beacons, the median provides a robust value that is resistant to manipulation by a minority adversary.

Ideal Functionality \mathcal{F}_{DSC} : Decentralized Stake Consensus

The functionality interacts with a set of parties \mathcal{P} and an adversary \mathcal{A} .

- Upon receiving a request ($\text{GetStake}, sl_{now}$) from a party P_i , \mathcal{F}_{DSC} computes the median stake value S_{median} from the set of all valid, on-chain stake beacons corresponding to the current synchronization interval.
- It returns $(\text{StakeValue}, S_{median})$ to P_i . The security is predicated on the underlying PoW-secured blockchain, ensuring all honest parties converge on the same set of beacons, and the use of the median provides robustness against adversarial beacons with outlier values.

9.10 Closing the Attack Vector

By integrating \mathcal{F}_{DSC} into the protocol, we introduce a new consensus rule:

Definition 5. *A PoW block is considered valid only if the value of S_{total} used in the generation of its Merkle Root, \mathcal{R}_{UTxO} , is equal to the BFT-secure stake value provided by the \mathcal{F}_{DSC} functionality for that period.*

This new rule completely closes the malicious Merkle root attack vector. A PoW miner can no longer unilaterally forge the total stake value. To manipulate S_{total} , an adversary would now need to corrupt a majority of the stake beacon producers to bias the median calculation—a far more difficult and expensive attack that is equivalent to breaking the core security assumption of the PoS component itself.

9.11 The Re-contextualized Role of the VETO Mechanism

With the primary state integrity threat mitigated structurally, the role of the VETO mechanism is re-contextualized. It is no longer the frontline defense against a critical economic attack but instead serves as a **defense-in-depth** backstop against other, less critical, or unforeseen forms of state invalidity. Its purpose is now to provide a final layer of human-in-the-loop oversight by the stakeholders, who retain the ultimate authority to reject a block that, despite passing all automated validation checks, is determined by the community to be malicious or harmful. The weaknesses of the VETO mechanism—its reliance on active participation and vulnerability to apathy—are now acceptable trade-offs for a secondary defense system, rather than critical flaws in the primary security model.

9.12 The Decentralized Consensus Service: A Unified Oracle

The security of the LDD mechanism and the integrity of the ASW metric depend on two critical scalar values: the current network time and the total network stake. The initial design proposed two separate ideal functionalities, \mathcal{F}_{DTC} and \mathcal{F}_{DSC} , to secure these values. However, a more elegant and efficient solution is to recognize that both are instances of a more general problem: achieving BFT consensus on a single scalar value in a permissionless setting. This insight allows us to unify several mechanisms into a single, powerful ideal functionality: the **Decentralized Consensus Service** (\mathcal{F}_{DCS}).

This unified service provides tamper-resistant values for time, total stake, network delay, and transaction load by leveraging the distinct strengths of the protocol's two participant classes. The instantiation relies on a clear separation of duties, assigning the responsibility for producing data "beacons" to the group best positioned to attest to that data's validity.

- **Time Beacons (from PoW Miners):** The progression of time is fundamentally anchored to the work done on the chain. Therefore, PoW miners are the natural producers of time beacons. As proposed by Garay et al. [20], we employ a "2-for-1 PoW" scheme where a single hash computation is checked against two targets: one for a Synergeia block and one for a lightweight, signed time beacon. This efficiently leverages the computational work already being performed to secure the network's clock.
- **Stake Beacons (from PoS Validators):** The total network stake is a property of the UTXO set, which is maintained and validated by the PoS stakeholders. Therefore, active PoS validators are the natural producers of stake beacons. At regular intervals, validators calculate the total stake from their local view of the UTXO set and broadcast this value as a signed attestation. This leverages their economic stake to incentivize honest reporting of the network's financial state.

Beacons are embedded into the blockchain, creating an immutable, public record of attestations. Any node can then locally compute a BFT-secure value for any scalar value by taking the median of the on-chain beacons for the current interval. This unified approach, detailed in the protocol box below, provides a robust and resource-efficient foundation for the entire Synergeia protocol, drawing inspiration from similar mechanisms in protocols like Ouroboros Chronos [6].

Ideal Functionality \mathcal{F}_{DCS}: Decentralized Consensus Service
--

The functionality is parameterized by intervals for time (R_{time}), stake (R_{stake}), delay (R_{delay}), and load (R_{load}). It maintains four sets of on-chain beacons: $\mathcal{B}_{\text{time}}$, $\mathcal{B}_{\text{stake}}$, $\mathcal{B}_{\text{delay}}$, and $\mathcal{B}_{\text{load}}$.

Beacon Production: PoW miners and PoS validators may generate and broadcast signed beacons for Time, Stake, Delay, and Load, which are included in the blockchain.

Service Requests: Upon receiving a request from a party P_i :

- **Request (GetTime, sl_{now})**: Collects valid time beacons, computes and returns the median timestamp T_{median} .
- **Request (GetStake, sl_{now})**: Collects valid stake beacons, computes and returns the median total stake value S_{median} .
- **Request (GetDelay, sl_{now})**: Collects valid delay beacons, computes and returns a high-percentile consensus delay $\Delta_{\text{consensus}}$.
- **Request (GetLoad, sl_{now})**: Collects valid load beacons (e.g., mempool size), computes and returns the median consensus load $L_{\text{consensus}}$.

Security Guarantees: Security is founded on the on-chain availability of beacons and the robustness of the median (or percentile) calculation. As long as the honest majority assumption holds for the respective resource, the adversary cannot corrupt the consensus values. This mechanism is inspired by permissionless clock designs [20,6].

On the Centrality and Scalability of the Decentralized Consensus Service The introduction of the \mathcal{F}_{DCS} transforms Synergeia into a fully autonomous protocol, capable of adapting its core security and performance parameters to real-world network conditions. This power, however, comes with a significant architectural trade-off: the protocol becomes critically dependent on the integrity and availability of the scalar values provided by this service. This section analyzes the implications of this design choice, focusing on the centralization of trust and the practical scalability of the beacon mechanism.

A Deliberate Centralization of Trust. The heavy reliance on the \mathcal{F}_{DCS} is a deliberate design choice that consolidates multiple, often implicit, environmental assumptions into a single, explicit, and analyzable trust assumption. Rather than assuming static values for network delay or security threat levels, the protocol trusts the BFT-robust consensus mechanism of the \mathcal{F}_{DCS} . The security of the entire autonomous system therefore rests on two foundational pillars:

1. **Ledger Integrity:** The security of the underlying blockchain itself, which ensures that the on-chain record of beacons is immutable and cannot be manipulated by an adversary attempting to rewrite history.
2. **Honest Majority of Beacon Producers:** The statistical robustness of the median calculation, which is guaranteed to provide a value within the range of honest submissions as long as the adversary controls less than 50% of the resources producing the relevant beacons (e.g., hash power for Time Beacons, stake for Stake Beacons).

This design makes the protocol’s security model transparent. The autonomous adaptations are secure if, and only if, the BFT consensus on the input scalars is secure. This shifts the security analysis from a complex evaluation of multiple independent parameters to a focused analysis of the integrity of the oracle system itself.

Scalability and On-Chain Overhead. The architecture of the \mathcal{F}_{DCS} is inherently scalable in terms of the *number of distinct scalar values* it can support. The protocol is not computationally constrained from providing consensus on dozens of different metrics; adding a new value, e.g. average transaction complexity, would simply require defining a new beacon type and a corresponding service request handler.

The primary scaling limitation is not computational but rather the **on-chain data overhead**. Each beacon is a small, signed message that must be broadcast, validated, and permanently stored on the blockchain, consuming valuable block space. For each scalar value the DCS provides, the protocol operator must balance a three-way trade-off:

- **Security:** A larger number of beacon submissions per interval provides a more robust data set for the median calculation, making the consensus value more resilient to manipulation by faulty or malicious nodes.
- **Responsiveness:** Shorter synchronization intervals (e.g., calculating the consensus delay every 100 blocks instead of every 1000) allow the protocol to adapt more quickly to changing network conditions.
- **Cost:** A higher frequency of submissions and/or shorter intervals directly increases the volume of beacon transactions on the network. This consumes more block space, which can lead to network congestion and higher transaction fees for all users.

Therefore, while the \mathcal{F}_{DCS} design is flexible and extensible, its practical application is bounded by the economics of block space. Each new autonomous feature powered by the DCS imposes a marginal but continuous cost on the network in the form of data overhead. The decision to add new consensus scalars must be weighed against the performance and security benefits they provide, ensuring that the value of autonomous adaptation justifies its cost in on-chain resources.

9.13 Incentivizing Participation: Beacon Bounties

The security analysis of \mathcal{F}_{DCS} highlights a critical vulnerability: its BFT-robustness relies on widespread, active, and honest participation in the beaconing process to ensure the adversary controls less than 50% of the contributing weight. Producing beacons incurs small but non-zero costs and without direct incentives, rational participants might forgo beacon production, reducing the effective honest majority ($\alpha_{honest_participating}$) and potentially making the \mathcal{F}_{DCS} vulnerable to Sybil-based bias attacks.

To mitigate this fundamental threat and ensure the integrity of the protocol's core oracle, we integrate Beacon Bounties into Synergeia's economic model.

Mechanism: Rewarding Data Contribution The mechanism directly rewards nodes for contributing the data essential for the protocol's autonomous functions:

- **Bounty Allocation:** A predetermined small fraction of the total block reward (or alternatively, a fraction of the burned transaction fees) in each block is specifically designated as the "Beacon Bounty Pool" for that block.
- **Eligibility:** Any node (miner or validator) that produces a valid beacon (Time, Stake, Delay, Load, Security Threat, or Topology) which is successfully included in the body of a canonical block \mathcal{B}_k becomes eligible for a share of the Beacon Bounty Pool within \mathcal{B}_k .
- **Distribution:** The bounty pool for block \mathcal{B}_k is distributed among all valid beacons included in \mathcal{B}_k . The distribution method can be tuned via governance (e.g., equal shares per beacon, weighted by beacon type based on perceived importance, or weighted by the producer's stake/hash power).
- **Payment:** The bounty is automatically credited to the beacon producer's registered address as part of the block's reward distribution logic (analogous to coinbase transaction outputs).

Future Enhancement: Adaptive Bounty Levels The robustness of the \mathcal{F}_{DCS} could be further enhanced by making the size of the Beacon Bounty Pool itself adaptive.

- **Participation Consensus:** The \mathcal{F}_{DCS} could be extended to compute a consensus metric on the Beacon Participation Rate for each beacon type (e.g., the number of unique, valid beacon producers observed per interval relative to the estimated total number of active nodes).
- **Dynamic Adjustment:** If the consensus participation rate for a critical beacon type (e.g., Delay or Security Threat) drops below a predefined target threshold $\theta_{participation}$, the protocol could autonomously increase the fraction of the block reward allocated to the Beacon Bounty Pool (specifically for that beacon type) in subsequent blocks.

This creates a closed-loop system where the protocol actively manages the economic incentives required to maintain a target level of participation, ensuring the statistical robustness of its own oracle.

Benefits Integrating Beacon Bounties provides several key advantages:

- **Strengthened Oracle Security:** Directly counteracts rational apathy by providing a clear, positive economic incentive for honest nodes to contribute the data crucial for the BFT security of the \mathcal{F}_{DCS} .

- **Aligned Incentives:** Explicitly rewards participants for behavior that enhances the protocol’s overall stability, resilience, and autonomous capabilities.
- **Quantifiable Security Margin:** The adaptive bounty level enhancement allows the protocol to actively manage and maintain a target security margin ($\alpha_A < \alpha_{honest_participating}$) for its core oracle mechanism, making the security guarantees more robust against fluctuating participation levels.

Beacon Bounties transform participation in the \mathcal{F}_{DCS} from an assumed or altruistic behavior into an explicitly incentivized action, significantly hardening the foundation upon which Synergeia’s advanced adaptive features are built.

9.14 Justification for Complexity: Why Not Slashing?

The robust, multi-layered defense for state integrity—combining the BFT consensus of the \mathcal{F}_{DCS} with the VETO mechanism as a backstop—is a deliberate and complex architectural choice. Our solution is far more rich and complex than the standard slashing solution used in many PoS protocols. Slashing is a direct, severe, and on-chain capital punishment that provides a powerful and easily analyzable economic deterrent against misbehavior.

Our protocol’s design explicitly rejects this model, not because it is ineffective, but because its risks could be catastrophic for participants. The security of a slashing mechanism is contingent on the absolute correctness of its implementation. Given the complexity of our design as it stands, a bug or unforeseen attack vector in the slashing conditions could lead to the unfair, massive, and irrecoverable confiscation of capital from honest validators. This model creates an extreme and unacceptable risk for the protocol’s participants.

Synergeia instead adopts a defense-in-depth model that is fundamentally less punitive. The complexity of the \mathcal{F}_{DCS} is the necessary and justified price for achieving robust, BFT-secure state validation *without* introducing the existential risk of catastrophic capital loss for honest stakers. This design choice prioritizes participant safety and robustness against implementation bugs over the analytical simplicity of a slashing protocol. The complex nature of our solution is a direct consequence of this design philosophy.

10 Stability of the LDD System

This section extends the concept of Local Dynamic Difficulty (LDD) and the snowplow curve introduced in *Ouroboros Taktikos* [41] to a hybrid Proof-of-Work (PoW) and Proof-of-Stake (PoS) consensus mechanism. We apply principles from control theory to analyze the system’s stability, framing the Dynamic Slope Adjustment Scheme as a **closed-loop feedback controller**. This approach aligns with an emerging tradition of analyzing blockchain dynamics and difficulty adjustments through economic and systems modeling [30,5].

We provide a formal proof of slope stability and derive explicit formulas for the difficulty curve parameters. The system’s core innovation is the application of a dynamic difficulty mechanism to both resources *simultaneously*, managed by a sophisticated, decoupled control loop.

10.1 Hybrid Snowplow Difficulty Curves

The eligibility for block production is governed by two parallel snowplow difficulty curves, one for PoS stakeholders and one for PoW miners. Both curves share the protocol-wide time parameters but have independently adjustable amplitudes.

- **Shared Time Parameters:**
 - ψ : The **Slot Gap**.
 - γ : The **Recovery Threshold**.
- **PoS Difficulty Curve ($f_{\text{PoS}}(\delta)$):** Governs the probability of a stakeholder being eligible to produce a block.

$$f_{\text{PoS}}(\delta) = \begin{cases} 0 & \delta < \psi \\ f_{A,\text{PoS}} \cdot \left(\frac{\delta - \psi}{\gamma - \psi} \right) & \psi \leq \delta < \gamma \\ f_{B,\text{PoS}} & \gamma \leq \delta \end{cases}$$

Here, $f_{A,\text{PoS}}$ is the maximum eligibility probability (amplitude) and $f_{B,\text{PoS}}$ is the baseline difficulty.

– **PoW Difficulty Curve ($f_{\text{PoW}}(\delta)$):** Governs the relative ease of finding a valid hash.

$$f_{\text{PoW}}(\delta) = \begin{cases} 0 & \delta < \psi \\ f_{A,\text{PoW}} \cdot \left(\frac{\delta - \psi}{\gamma - \psi} \right) & \psi \leq \delta < \gamma \\ f_{B,\text{PoW}} & \gamma \leq \delta \end{cases}$$

10.2 Adaptive Difficulty

The Synergeia protocol utilizes a Local Dynamic Difficulty (LDD) mechanism to achieve its performance and security goals. The core of this mechanism is the function, $f(\delta)$, which defines the success probability rate for producing a block at time δ after the previous block. In the previous section these functions are defined piecewise for each resource type (PoW or PoS) but the net contribution towards the block distribution of both resources can be understood in terms of a single Rayleigh distribution with effective difficulty parameters:

$$f(\delta) = \begin{cases} 0 & \delta < \psi \\ M \cdot \frac{\delta - \psi}{\gamma - \psi} & \psi \leq \delta < \gamma \\ b & \delta \geq \gamma \end{cases}$$

Here, ψ is the slot gap, γ is the recovery threshold, $M = f_{A,\text{PoS}} + f_{A,\text{PoW}}$ is the slope parameter of our idealized Rayleigh distribution, and at the end of the forging window $b = f_{B,\text{PoS}} + f_{B,\text{PoW}}$ is the baseline success rate in the recovery phase. The primary slope, M , is dynamically adjusted to maintain a target block time (e.g., 15 seconds).

10.3 Adaptive Baseline Difficulty and Inversion Prevention

In a network with very high resources, the adjustment system can drive M to a very small value to prevent blocks from being produced too quickly. If the baseline difficulty f_B is a fixed parameter for either resource, it's possible for the system to reach a state where $f_A < f_B$. We specify an adaptive routine for updating f_B . The Dynamic Slope Adjustment Scheme focuses on tuning the primary difficulty amplitudes, $f_{A,\text{PoW}}$ and $f_{A,\text{PoS}}$, which govern block production within the high-probability forging window. However, the baseline difficulty parameters, $f_{B,\text{PoW}}$ and $f_{B,\text{PoS}}$, which control the recovery phase, are equally critical for system stability. We identify a potential failure mode wherein a static baseline could lead to a difficulty inversion, creating a perverse incentive structure. This section formalizes an adaptive mechanism to prevent this vulnerability.

The Difficulty Inversion Vulnerability The primary difficulty amplitude, $M = f_{A,\text{PoW}} + f_{A,\text{PoS}}$, is dynamically adjusted to maintain the target block time. In a network with extremely high resources (hash power and stake), the control system will drive M to a very small value to prevent blocks from being produced too quickly. If the baseline difficulty parameters, f_B , were fixed constants, it would be possible for the system to enter an "inverted" state where $f_B > f_A$.

This inversion would create a perverse incentive for rational participants. It would become more probable (and thus more profitable) to produce a block during the recovery phase ($\delta > \gamma$) than during the intended forging window ($\psi \leq \delta < \gamma$). A strategic adversary could exploit this by intentionally withholding blocks during the forging window to force the system into the more profitable recovery phase, thereby disrupting the block timing and gaining an unfair advantage. A robust protocol must make such behavior impossible by design.

A Security-Hardened Baseline Adjustment Mechanism To prevent difficulty inversion, the baseline parameters must adapt in concert with the primary amplitudes. We introduce a two-step mechanism that ensures the recovery phase always acts as a secure fallback, never as a primary incentive.

Definition 6. *The baseline difficulty parameters, $f_{B,\text{PoW}}$ and $f_{B,\text{PoS}}$, are recalculated at the end of each adjustment window according to the following procedure:*

1. **Calculate Fallback-Targeted Baseline:** The total baseline hazard rate, $b = f_{B,\text{PoW}} + f_{B,\text{PoS}}$, is pegged to a safe, long-term fallback block time, T_{fallback} (e.g., 5 minutes). This ensures that if no block is found in the forging window, the network does not stall indefinitely. The total rate is

$b = 1/T_{fallback}$. This total rate is then distributed between PoW and PoS in the same proportion as the newly calculated primary amplitudes, preserving the system's target resource balance:

$$f_{B,PoW}^* = b \cdot \frac{f_{A,PoW}}{f_{A,PoW} + f_{A,PoS}}$$

$$f_{B,PoS}^* = b \cdot \frac{f_{A,PoS}}{f_{A,PoW} + f_{A,PoS}}$$

2. **Apply Security Constraint (No Inversion):** To guarantee that the baseline difficulty can never exceed the primary difficulty, we enforce a strict upper bound. The final baseline parameters are set to the minimum of the fallback-targeted value and the corresponding primary amplitude:

$$f_{B,PoW,final} = \min(f_{B,PoW}^*, f_{A,PoW})$$

$$f_{B,PoS,final} = \min(f_{B,PoS}^*, f_{A,PoS})$$

This mechanism provides a dual guarantee. The fallback target ensures liveness by providing a floor for block production probability. The security constraint makes difficulty inversion impossible by construction, ensuring that the forging window is always the most probable and profitable time to produce a block. This closes the potential exploit and ensures the stability and security of the LDD mechanism across all possible network conditions.

10.4 Adaptive Target Slope

This section specifies the calculation of M_{req} ensuring the core LDD framework system's total effective slope, M_{final} , will converge to a target slope by construction. Let the time-varying function $M_{req}(h)$ be the slope required to maintain $\mu = 15s$ at block height h . The existing control loops maintain both the scaling factor β for overall chain growth and the proportional adjustment for the 50/50 resource split.

Network Load Response The target slope is a function of the network transaction load (e.g., the block body size of the tip of the chain). Let $L(h)$ be a measure of transaction load at block height h . We can define an adaptive target mean block time, $\mu_{target}(h)$, as an inverse function of this load, bounded by a predefined minimum and maximum:

$$\mu_{target}(h) = \max(\mu_{min}, \mu_{max} - \eta \cdot L(h))$$

where μ_{max} is the target (e.g., 15s) for an empty mempool, μ_{min} is the hard-coded fastest block time (e.g., 3s), and η is a sensitivity parameter. The target slope M_{req} is inversely related to the square of the mean block time ($M \approx \pi/(2\mu^2)$). Therefore, the adaptive target slope $M_{req}(t)$ would be:

$$M_{req}(h) = \frac{\pi}{2 \cdot (\mu_{target}(h))^2}$$

Under this scheme, as network demand and mempool load increase, $\mu_{target}(h)$ would decrease towards μ_{min} , causing $M_{req}(h)$ to increase. The difficulty adjustment mechanism would then automatically lower the overall difficulty (increase amplitudes f_A) to achieve the faster block rate, thus increasing network throughput to clear the backlog. As the mempool clears, the system would gracefully return to the average block time of μ_{max} .

Boundary Conditions and Security Constraints Operating in such a regime is subject to critical boundary conditions imposed by the physical limitations of network propagation.

1. **The Forking Threshold:** The primary risk of reducing the mean block time, μ , is an increased fork rate. As μ approaches the network delay, Δ , the probability of honest nodes mining on stale blocks increases dramatically. This leads to a higher rate of orphaned blocks and degrades the integrity of the longest chain rule.
2. **The Slot Gap Constraint:** The protocol's quadratic consistency bound is predicated on the structural defense of the Slot Gap, ψ , being greater than the maximum network delay, Δ_{max} . This constraint, $\psi > \Delta_{max}$, is absolute. An adaptive block time mechanism must *never* be allowed to push the system into a state where this condition is violated.

Therefore, the parameter μ_{min} cannot be chosen arbitrarily; it must be set conservatively based on empirical measurements of the network's propagation delay. A safe lower bound would be $\mu_{min} \gg \psi$, ensuring that even at maximum throughput, there is sufficient time between blocks for the network to synchronize. For example, if the protocol enforces $\psi = 2s$ to tolerate a Δ_{max} of just under 2s, a safe μ_{min} might be 4s or 5s, but not 2s. In a live environment, an adaptive slope mechanism would be a powerful tool for scaling throughput, but its safe operation would depend entirely on establishing a conservative, hard-coded floor for the target block time to preserve the foundational security guarantees of the protocol.

10.5 System Targets

The adaptive system acts as a controller with two primary objectives:

1. **Chain Growth Stability (Speed):** Maintain a constant average block time, μ , by ensuring the total effective difficulty slope, M_{final} , converges to a required constant, M_{req} .
2. **Resource Balancing (Ratio):** Maintain a 50/50 proportion of blocks produced by PoW and PoS mechanisms over a given adjustment window.

10.6 Proof of Slope Stability

We now prove that the system's total effective slope, M_{final} , is guaranteed to converge to the target slope, M_{req} , after every adjustment cycle, thereby ensuring a stable Chain Growth rate.

Theorem 5. *The Dynamic Slope Adjustment Scheme ensures that the final implemented effective slope M_{final} converges exactly to the required slope M_{req} by construction.*

Proof. The stability of the system is guaranteed by an algebraic identity enforced by a corrective scaling factor, β , applied at the end of each adjustment period. Let the total effective slope of the system be the sum of the individual effective slopes contributed by the PoS and PoW mechanisms. After an adjustment based on observed block proportions, new tentative amplitudes ($f_{A,PoS}^{new}, f_{A,PoW}^{new}$) are calculated. These amplitudes yield a new aggregated effective slope, which we denote as M_{actual}^{new} . The adjustment scheme then calculates a **Scaling Factor**, β , defined as the ratio of the target slope to this newly calculated actual slope:

$$\beta = \frac{M_{req}}{M_{actual}^{new}}$$

This scaling factor is used to compute the final, implemented amplitudes for the next operational window:

$$\begin{aligned} f_{A,PoS}^{final} &= \beta \cdot f_{A,PoS}^{new} \\ f_{A,PoW}^{final} &= \beta \cdot f_{A,PoW}^{new} \end{aligned}$$

The final total effective slope, M_{final} , is the slope resulting from these final amplitudes. Since the effective slope is directly proportional to these amplitudes, M_{final} is simply the sum of the scaled individual contributions, which is equivalent to scaling the new aggregate slope:

$$M_{final} = \text{Slope}(f_{A,PoS}^{final}) + \text{Slope}(f_{A,PoW}^{final}) = \beta \cdot M_{actual}^{new}$$

We now substitute the definition of β into the equation for M_{final} :

$$M_{final} = \left(\frac{M_{req}}{M_{actual}^{new}} \right) \cdot M_{actual}^{new}$$

The M_{actual}^{new} terms cancel out, proving that the final implemented slope is algebraically identical to the required slope, thus guaranteeing system stability by construction.

$$M_{final} = M_{req}$$

10.7 Dynamic Adjustment Formulas and Separation of Concerns

To achieve the dual objectives of resource balance and chain growth stability, the system employs a closed-loop feedback controller. This controller measures the proportion of PoW and PoS blocks over a fixed window of N blocks and adjusts the respective difficulty curve amplitudes.

1. Calculate Observed Proportion and Error:

$$P_{\text{PoW}} = \frac{N_{\text{PoW}}}{N_{\text{PoW}} + N_{\text{PoS}}}$$

The error term, E , measures the deviation from the 50% target.

$$E = P_{\text{PoW}} - 0.5$$

2. Calculate Proportional Adjustment (Ratio Correction):

The system implements a classic **proportional controller**. The parameter κ (e.g., $\kappa = 0.1$) is the controller's **proportional gain**, tuning its responsiveness. The new, unscaled amplitudes are calculated to counteract the observed error.

$$\begin{aligned} f_{A,\text{PoW}}^{\text{new}} &= f_{A,\text{PoW}}^{\text{old}} \cdot (1 - \kappa \cdot E) \\ f_{A,\text{PoS}}^{\text{new}} &= f_{A,\text{PoS}}^{\text{old}} \cdot (1 + \kappa \cdot E) \end{aligned}$$

3. Calculate Final Scaled Amplitudes (Speed Correction):

The new amplitudes from step 2 produce a new total slope $M_{\text{actual}}^{\text{new}}$. We apply the scaling factor $\beta = M_{\text{req}}/M_{\text{actual}}^{\text{new}}$ as proven above to get the final amplitudes for the next window.

$$\begin{aligned} f_{A,\text{PoW}}^{\text{final}} &= \beta \cdot f_{A,\text{PoW}}^{\text{new}} \\ f_{A,\text{PoS}}^{\text{final}} &= \beta \cdot f_{A,\text{PoS}}^{\text{new}} \end{aligned}$$

Separation of Concerns. The stability mechanism exhibits a sophisticated design property: a separation of concerns that effectively decouples the two control objectives. Step 1 (Proportional Adjustment, driven by κ) is responsible solely for correcting the *ratio* of resources (the 50/50 split). It operates without information about the total block rate; it could achieve a perfect 50/50 split while the block time is 1 second or 1 hour. Step 2 (Stability Scaling, driven by β) is responsible solely for correcting the *absolute level* of difficulty to maintain the target block time. Crucially, β scales both PoW and PoS difficulty by the same factor, thereby preserving the ratio established in Step 1. The system first corrects the balance, then corrects the speed. This decoupling is a non-obvious design choice that enhances stability by preventing the complex oscillations that might occur if a single mechanism attempted to solve both problems simultaneously.

10.8 Analysis of System Restoration Under Extreme Conditions

We now demonstrate how these formulas ensure the system restores its 50/50 equilibrium under external shocks.

Scenario 1: Sudden 10x Influx of Hash Power

- **Initial Effect:** PoW block discovery dramatically increases (e.g., $P_{\text{PoW}} \approx 0.9$). The total block rate also increases significantly.
- **System Response:**
 1. **Error Calculation:** $E = 0.9 - 0.5 = 0.4$.
 2. **Proportional Adjustment:** The system applies a strong correction (using $\kappa = 0.1$). PoW amplitude is lowered (0.96x) and PoS amplitude is raised (1.04x).
 3. **Stability Scaling:** The influx caused the total slope to be much higher than M_{req} . The scaling factor β will be significantly less than 1 (e.g., $\beta \approx 0.2$). The final amplitudes are drastically reduced.

The system dramatically increases overall difficulty (via β) to restore the target block time, while simultaneously adjusting the ratio (via κ) to counteract the hashrate influx.

Scenario 2: Majority of Stakers Go Offline

- **Initial Effect:** PoS block discovery plummets. P_{PoW} is again high (e.g., 0.9), but the total block rate decreases.
 - **System Response:**
 1. **Error Calculation:** $E = 0.4$.
 2. **Proportional Adjustment:** The same proportional adjustment occurs, making PoW harder and PoS easier.
 3. **Stability Scaling:** Because the total block rate was too low, $M_{\text{actual}}^{\text{new}}$ will be below M_{req} . The scaling factor β will be greater than 1 (e.g., $\beta \approx 1.5$). The final amplitudes are increased.
- The system decreases overall difficulty (restoring block time) while making PoS disproportionately easier to incentivize the remaining stakers (restoring the 50/50 balance).

The proposed hybrid LDD system successfully integrates the time-based difficulty concept into a dual-resource protocol. The decoupled control loop, combining proportional adjustment and corrective scaling, provides a robust mechanism that actively counteracts imbalances and guarantees the stability of the chain growth rate.

10.9 Revising the Adaptive Target Slope for Congestion Control

The protocol’s design includes an adaptive target slope mechanism, intended to enhance performance by reducing the average block time in response to high network load. The original formulation defined the target mean block time, $\mu_{\text{target}}(h)$, as an inverse function of load, bounded by a predefined minimum and maximum:

$$\mu_{\text{target}}(h) = \max(\mu_{\min}, \mu_{\max} - \eta \cdot L(h))$$

While this mechanism successfully increases throughput, the critique correctly identifies a critical design flaw: it fails to formally couple the minimum block time, μ_{\min} , to the protocol’s foundational network security parameter, the slot gap ψ . The paper’s security model is predicated on the assumption that the block time is sufficiently long to allow for block propagation across the network, a condition structurally enforced by the constraint $\psi > \Delta$. If the adaptive mechanism were to drive the target block time μ_{target} to a value close to ψ , the system would enter a state of high fork probability, violating the assumptions of the consistency proofs.

The Vulnerability of an Unconstrained Minimum Block Time The danger arises from treating μ_{\min} as an independent, tunable parameter. A safe lower bound for the average block time must be significantly greater than the slot gap ($\mu_{\min} \gg \psi$) to provide a sufficient buffer for network synchronization and to account for the stochastic variance in block production. The original adaptive slope function does not enforce this relationship. Under conditions of maximum sustained network load, it would drive the target block time to $\mu_{\text{target}} = \mu_{\min}$. If an operator were to misconfigure the protocol such that $\mu_{\min} \approx \psi$, the protocol’s own congestion control mechanism would algorithmically induce a state of consensus instability. A secure protocol must be robust against such misconfigurations and should not be capable of algorithmically violating its own security premises.

A Security-Hardened Adaptive Slope Mechanism To mitigate this vulnerability, we impose a security-hardened adaptive target slope function to be explicitly aware of the slot gap parameter, ψ . The new function defines the minimum possible block time not as an arbitrary parameter, but as a function of ψ plus a non-negotiable safety margin.

Definition 7. *The security-hardened adaptive target mean block time, $\mu_{\text{target}}(L(h))$, is defined as:*

$$\mu_{\text{target}}(L(h)) = (\mu_{\max} - (\psi + \mathcal{M}_{\text{safety}})) \cdot \max\left(0, 1 - \frac{L(h)}{L_{\max}}\right) + (\psi + \mathcal{M}_{\text{safety}})$$

where:

- μ_{\max} is the target block time under zero load (e.g., 15s).
- $L(h)$ is the current network load, measured as a fraction of maximum block capacity (so $L(h) \in [0, 1]$).
- ψ is the globally defined slot gap.

- \mathcal{M}_{safety} is a new global parameter, the **Minimum Safety Margin**, which defines the minimum acceptable buffer between the slot gap and the fastest possible average block time (e.g., $\mathcal{M}_{safety} = \psi$).

This formulation guarantees that the target block time is always within the range:

$$[\psi + \mathcal{M}_{safety}, \mu_{max}]$$

When the network is under maximum load ($L(h) = 1$), the target block time converges to its floor, $\psi + \mathcal{M}_{safety}$, which is guaranteed by construction to be safely above the slot gap. This change hard-codes the protocol's core network timing assumption into the adaptive control system itself, ensuring that the mechanism for increasing throughput cannot compromise the fundamental security of the protocol.

10.10 A Fully Autonomous LDD System with Adaptive Slot Gap and Load Balancing

The Synergeia protocol's core security assumption, $\psi > \Delta$, is based on the choice of the Slot Gap (ψ). This is a fragile assumption in a dynamic permissionless and an adaptive routine for setting ψ completely automates the security of the protocol with respect to the network delay Δ . Similarly, relying on a fixed target block time (μ_{max}) prevents the protocol from adapting its throughput to network demand and we must consider a dynamic slot-gap parameter in the calculation of the adaptive slopes.

To resolve these limitations, we further enhance the **Decentralized Consensus Service** (\mathcal{F}_{DCS}) to provide BFT-secure consensus on network delay and transaction load. This allows the protocol to autonomously adapt both its Slot Gap (ψ) and its target block time (μ_{target}), creating a fully autonomous LDD system that balances security with performance.

10.11 Upgrading the Decentralized Consensus Service

We extend the \mathcal{F}_{DCS} to include **Network Delay Beacons** and **Network Load Beacons**.

1. **Delay Beacon Creation:** When an honest node P_i receives a new block \mathcal{B}_k at T_{local} (validated by $\mathcal{F}_{DCS}.\text{GetTime}$), it compares this to the block's validated timestamp $T_{broadcast}$. It calculates the observed delay $\Delta_i = T_{local} - T_{broadcast}$ and broadcasts a signed **delay beacon** $b_d = (\text{beacon_type} = \text{DELAY}, \Delta_i, \text{validator_id})$.
2. **Load Beacon Creation:** At regular intervals (e.g., every R_{load} slots), an active node P_i (either miner or staker) measures the current transaction load. This could be represented as the size of its local mempool or the average fullness of recent blocks. It broadcasts a signed **load beacon** $b_l = (\text{beacon_type} = \text{LOAD}, L_i, \text{node_id})$, where L_i is the measured load metric (e.g., normalized to $[0, 1]$).
3. **Consensus on Delay and Load:** We add two new request types to \mathcal{F}_{DCS} :
 - **Request (GetDelay, sl_{now}):**
 - (a) Collects valid delay beacons b_d for the current interval.
 - (b) Computes $\Delta_{consensus}$ as the **95th percentile** of observed Δ_i values (conservative estimate).
 - (c) Returns (DelayValue, $\Delta_{consensus}$).
 - **Request (GetLoad, sl_{now}):**
 - (a) Collects valid load beacons b_l for the current interval.
 - (b) Computes $L_{consensus}$ as the **median** of observed L_i values (robust average load).
 - (c) Returns (LoadValue, $L_{consensus}$).

10.12 The Fully Autonomous LDD Adjustment Loop

Function: Autonomous_Dynamic_Adjust

This master function executes the fully adaptive LDD adjustment at the end of each window, ensuring internal consistency.

```

1: Input: Lookback window size  $N$ , local chain  $\mathcal{C}$ , responsiveness  $\kappa$ , safety margin  $\mathcal{M}_{safety}$ , base target time  $\mu_{max}$ , fallback time  $T_{fallback}$ , fallback probability  $P_{fallback}$ , current difficulty params  $\mathcal{D}$ .
2: Step 1: Get Environmental Parameters from  $\mathcal{F}_{DCS}$ 
3:  $\Delta_{consensus} \leftarrow \mathcal{F}_{DCS}.\text{GetDelay}(\text{current\_slot})$ .
4:  $L_{consensus} \leftarrow \mathcal{F}_{DCS}.\text{GetLoad}(\text{current\_slot})$ .
5: Step 2: Set Core Timing Parameters
6:  $\psi_{new} \leftarrow \Delta_{consensus} + \mathcal{M}_{safety}$ .                                     ▷ Set adaptive slot gap
7:  $\mu_{target} \leftarrow \text{Adaptive\_Target\_Slope}(L_{consensus}, \mu_{max}, \psi_{new}, \mathcal{M}_{safety})$ .      ▷ Set load-adjusted target time
8: Step 3: Calculate Target Slope and Optimal Window
9:  $M_{req} \leftarrow \pi / (2 \cdot (\mu_{target} - \psi_{new})^2)$ .                                         ▷ Calculate required effective slope
10:  $\xi_{optimal} \leftarrow \sqrt{-2 \cdot \ln(P_{fallback}) / M_{req}}$ .                                         ▷ Calculate optimal forging window duration
11: Step 4: Proportional Adjustment (Correct Balance)
12: Let  $\mathcal{W}$  be the last  $N$  blocks of  $\mathcal{C}$ .
13:  $P_{PoW} \leftarrow \text{CountPoW}(\mathcal{W}) / N$ .
14:  $E \leftarrow P_{PoW} - 0.5$ .                                         ▷ Calculate deviation from 50/50 target
15:  $f'_{A,PoW} \leftarrow \mathcal{D}.f_{A,PoW} \cdot (1 - \kappa \cdot E)$ .                                         ▷ Adjust amplitudes proportionally
16:  $f'_{A,PoS} \leftarrow \mathcal{D}.f_{A,PoS} \cdot (1 + \kappa \cdot E)$ .
17: Step 5: Stability Scaling (Correct Speed)
18:  $M'_{actual\_amplitude} \leftarrow f'_{A,PoW} + f'_{A,PoS}$ .
19:  $M'_{effective} \leftarrow M'_{actual\_amplitude} / \xi_{optimal}$ .                                         ▷ Calculate effective slope using optimal window
20: if  $M'_{effective} \leq 0$  then
21:    $\beta \leftarrow 1.0$ .
22: else
23:    $\beta \leftarrow M_{req} / M'_{effective}$ .                                         ▷ Calculate scaling factor based on effective slope
24: end if
25:  $f''_{A,PoW} \leftarrow \beta \cdot f'_{A,PoW}$ .                                         ▷ Apply scaling factor to amplitudes
26:  $f''_{A,PoS} \leftarrow \beta \cdot f'_{A,PoS}$ .
27: Step 6: Update Baselines
28:  $(f''_{B,PoW}, f''_{B,PoS}) \leftarrow \text{Update\_Baseline\_Difficulty}(f''_{A,PoW}, f''_{A,PoS}, T_{fallback})$ .
29: Step 7: Set Final Timing Parameters
30:  $\gamma_{new} \leftarrow \psi_{new} + \xi_{optimal}$ .                                         ▷ Set final gamma based on optimal window
31: Return: New difficulty parameter set  $\mathcal{D}_{new} = \{f''_{A,PoW}, f''_{A,PoS}, f''_{B,PoW}, f''_{B,PoS}, \psi_{new}, \gamma_{new}\}$ .
```

10.13 Security and Performance Implications

This fully autonomous LDD system represents a significant advancement.

- **Enhanced Security:** The "Secure State" ($\psi > \Delta$) becomes a dynamically maintained property, making the protocol inherently robust against fluctuations in real-world network latency. The quadratic consistency bound is thus preserved under realistic conditions.
- **Adaptive Performance:** By incorporating load measurements, the protocol can now dynamically adjust its target block time. Under low load, it maintains a longer block time (e.g., 15s) for maximum stability. Under high load, it can safely accelerate block production (down to the floor of $\psi_{new} + \mathcal{M}_{safety}$) to increase throughput and clear the mempool, without compromising the $\psi > \Delta$ requirement.
- **Parameter Simplification:** While introducing new beacons, this approach reduces the need for operators to manually fine-tune ψ and potentially μ_{max} based on assumed network conditions. The protocol tunes itself based on the self-reported values of scalar quantities provided by the \mathcal{F}_{DCS} functionality.

This mechanism transforms the LDD from a static optimization into a dynamic, environment-aware control system, significantly hardening Synergeia against real-world network variability and enabling adaptive throughput.

10.14 Adaptive Slot Duration and Minimum Finality Time

The introduction of the fully autonomous LDD adjustment loop fundamentally changes how we reason about the protocol's timing parameters. The concept of a fixed "slot duration" becomes less relevant

than the dynamically adjusted parameters that govern block production probabilities: the adaptive Slot Gap (ψ_{new}) and the adaptive target mean block time (μ_{target}).

Effective Slot Duration. While the underlying Decentralized Time Consensus (\mathcal{F}_{DCS}) may operate on discrete time units (e.g., 1-second slots for timestamping and beaconing), the LDD mechanism operates based on the continuous interval δ since the last block. The crucial parameter is the adaptive Slot Gap, ψ_{new} , calculated as $\Delta_{consensus} + \mathcal{M}_{safety}$. This ψ_{new} represents the minimum effective time interval enforced between blocks by the protocol's difficulty curve, ensuring that block production is suppressed during the period required for network propagation plus a safety margin.

Minimum Safe Block Time. The adaptive target slope mechanism is designed to accelerate block production under high load, but it is constrained by a floor to maintain security. This floor represents the minimum average block time the protocol can safely target:

$$\mu_{min} = \psi_{new} + \mathcal{M}_{safety}$$

Substituting the definition of ψ_{new} :

$$\mu_{min} = (\Delta_{consensus} + \mathcal{M}_{safety}) + \mathcal{M}_{safety} = \Delta_{consensus} + 2\mathcal{M}_{safety}$$

This shows that the fastest average block time the protocol will ever target is directly determined by the BFT-consensus value of network delay plus two safety margins. For instance, if the network delay consensus is $\Delta_{consensus} = 1.5s$ and the safety margin is $\mathcal{M}_{safety} = 0.75s$ (e.g., 50% of delay), the fastest the protocol will aim for is $\mu_{min} = 1.5s + 2(0.75s) = 3.0s$.

Minimum Finality Time. The protocol's finality time is the product of the required confirmation depth (k) and the mean block time (μ). The confirmation depth k is determined by the Generalized Scaling Law (Section 8, Theorem 4):

$$k(\epsilon_{target}, \Delta, \psi) \geq \sqrt{-\ln(\epsilon_{target}) \cdot \frac{4}{\pi} \cdot \frac{\alpha_A(\mu + \max(0, \Delta - \psi))}{\alpha_H \mu}}$$

In the autonomous system, ψ is dynamically set to $\psi_{new} = \Delta_{consensus} + \mathcal{M}_{safety}$. Since $\Delta_{consensus}$ is a high-percentile measure of the actual network delay Δ , we have $\psi_{new} \geq \Delta$. Therefore, the term $\max(0, \Delta - \psi_{new})$ becomes 0. The system dynamically enforces the "Secure State," and the required confirmation depth k simplifies to its ideal form, dependent only on the target security ϵ_{target} and the effective adversarial ratio α'_A/α'_H (accounting for potential strategic advantages as per Section 12):

$$k \approx \sqrt{-\ln(\epsilon_{target}) \cdot \frac{4}{\pi} \cdot \frac{\alpha'_A}{\alpha'_H}}$$

This k is now independent of the absolute network delay.

The minimum possible finality time ($T_{finality,min}$) occurs when the network is under maximum load, forcing the target block time to its floor, μ_{min} .

$$T_{finality,min} = k \times \mu_{min} = k \times (\Delta_{consensus} + 2\mathcal{M}_{safety})$$

Assessment. The finality time of the Synergeia protocol, under the fully autonomous LDD system, is no longer a fixed value like "90 seconds." Instead, it becomes a dynamic quantity that adapts to prevailing network conditions. The protocol guarantees the minimum necessary confirmation depth (k) based on the desired security level and adversarial assumptions, and achieves finality in k times the current average block time. The *fastest* this can possibly be is $k \times (\Delta_{consensus} + 2\mathcal{M}_{safety})$.

This demonstrates that the protocol achieves the optimal finality time possible given the physical constraints of the network. If the network is fast (low $\Delta_{consensus}$), finality will be rapid. If the network becomes congested (high $\Delta_{consensus}$), the protocol automatically and safely increases the slot gap and the minimum block time, leading to a correspondingly longer, but still secure, finality time. This adaptive finality is a key feature, ensuring resilience and predictable security across diverse and changing network environments. When reporting a finality time in the abstract or introduction, it would be most accurate to state it as a function of the expected network delay, e.g., "achieving finality in approximately $k \times (\mathbb{E}[\Delta] + 2\mathcal{M}_{safety})$ seconds under typical network conditions."

11 A Combinatorial Framework for Longest-Chain Protocols

The preceding analysis relies on continuous probability distributions to model block arrivals. We now introduce an alternative, discrete framework based on the combinatorial properties of the leader election schedule itself. This approach allows us to reason about consistency in terms of discrete slots and VRF eligibilities. The methodology and style of this analysis are modeled after the systematic framework presented by Blum et al. for proof-of-stake blockchains [9].

We begin by re-deriving the well-established linear consistency bound for traditional Nakamoto-style protocols, which serves as a baseline for comparison. We then provide a detailed, first-principles proof of Synergeia's central claim: that by reshaping the block inter-arrival distribution into a Rayleigh distribution, it achieves a superior, super-exponential (quadratic) consistency bound. The analysis is then extended to account for network asynchrony, formally proving the efficacy of the protocol's structural defenses against network delay (Δ) and deriving the generalized scaling law that governs its security under arbitrary network conditions.

In the analysis of blockchain consensus protocols, consistency refers to the property that all honest participants agree on the prefix of the chain. A consistency violation occurs when a previously confirmed block is removed from the longest chain due to a fork, undermining the ledger's immutability. The security of a protocol is quantified by the probability of such a violation for a block that is buried k levels deep in the chain. This analysis is grounded in the formal framework of the Common Prefix property, as established in seminal works on the Bitcoin Backbone Protocol [19] and Ouroboros Praos [15].

Definition 8. *The analysis relies on the following parameters:*

- k : The confirmation depth.
- α_A : The fraction of total network resources controlled by the adversary ($0 < \alpha_A < 0.5$).
- α_H : The fraction of resources controlled by honest participants ($\alpha_H = 1 - \alpha_A$).
- $\epsilon(k)$: The probability of a consistency violation at depth k .

The core distinction between Synergeia and its predecessors lies not in the adversarial model but in the fundamental stochastic process governing block creation. We will formally prove the following two theorems.

Theorem 6. *For a traditional Nakamoto protocol, the probability of a consistency violation decays exponentially with a linear dependence on k : $\epsilon(k) \approx \exp(-\Omega(k))$.*

Theorem 7. *For the Synergeia protocol, the probability of a consistency violation due to forks in the chain decays super-exponentially with a quadratic dependence on k : $\epsilon(k) \approx \exp(-\Omega(k^2))$.*

A key objective of this section is to move beyond the abstract security model presented in Section 7.4. The continuous-time analysis introduced the concept of an **effective adversarial resource fraction**, α'_A , to account for adversarial strategies. This combinatorial framework provides the formal machinery to derive a quantitative value for that advantage. The sophisticated LDD-grinding strategies analyzed here, which are modeled using a dynamic programming approach (Section 11.8), will be shown to provide a marginal, constant-factor advantage. This advantage will be used to formally bound α'_A , thus providing a concrete, falsifiable input for our main security theorem.

11.1 Analysis via Continuous Block Arrival Models

Part 1: Linear Consistency of Nakamoto Consensus This subsection provides a self-contained proof of the linear bound, establishing the theoretical baseline.

Assumption 4 *Traditional Proof-of-Work (PoW) protocols model block discovery as a memoryless process (Poisson process with constant rate λ). This implies the inter-arrival time follows an exponential distribution.*

Theorem 6 (Linear Exponential Bound).

Proof. The analysis models a private mining attack as a one-dimensional random walk. Let the state be the difference between the adversary's private chain length (L_A) and the honest public chain (L_H), $Z = L_A - L_H$. The adversary starts at $Z_0 = -k$.

The probability of the adversary finding the next block is $p = \alpha_A$, and for the honest network is $q = \alpha_H$ ($p < q$). The adversary succeeds if their chain catches up. This is equivalent to the "gambler's ruin" problem. The probability of the adversary overcoming this deficit, as commonly applied in blockchain analysis [19], is:

$$P(\text{catch-up from deficit } k) = \left(\frac{p}{q}\right)^k = \left(\frac{\alpha_A}{\alpha_H}\right)^k$$

We express this probability in its exponential form:

$$\epsilon(k) = \exp\left(k \ln\left(\frac{\alpha_A}{\alpha_H}\right)\right)$$

Let $C = \ln(\alpha_H/\alpha_A)$, a positive constant. The expression becomes $\epsilon(k) = \exp(-C \cdot k)$, which is of the form $\exp(-\Omega(k))$. The linear bound is a direct consequence of the memoryless property of the Poisson process.

Part 2: Quadratic Consistency of Synergeia This subsection provides a detailed, first-principles proof of Synergeia's quadratic consistency bound.

Assumption 5 *The Local Dynamic Difficulty (LDD) mechanism enforces a time-dependent success probability (hazard rate) $\lambda(\delta) \propto \delta$. This forces the block inter-arrival time, X , to follow a Rayleigh distribution [41].*

Lemma 4. *The Rayleigh distribution has the following properties:*

- **PDF:** $f(x; M) = Mx \exp(-Mx^2/2)$, $x \geq 0$, where M is a slope parameter proportional to the consensus resources.
- **Survival Function (SF):** $S(x; M) = P(X > x) = \exp(-Mx^2/2)$. The x^2 term in the exponent is the cornerstone of the quadratic bound.
- **Mean Inter-Arrival Time:** $E[X] = \sqrt{\frac{\pi}{2M}}$.

Theorem 7 (Quadratic Exponential Bound).

Proof. The proof rests on analyzing the conditions required for a successful private mining attack in the Rayleigh model.

1. **Adversary's Time to Mine:** The time required for an adversary to secretly mine a chain of length k , $T_A(k)$, is the sum of k i.i.d. Rayleigh random variables: $T_A(k) = \sum_{i=1}^k X_i^A$. Each X_i^A has a slope parameter $M_A = \alpha_A M_{\text{total}}$.
2. **Approximating with Expected Value:** The expected time is:

$$E = E[T_A(k)] = k \sqrt{\frac{\pi}{2M_A}}$$

3. **Bounding the Violation Probability:** A necessary condition for success is that the honest network fails to produce a single block during $T_A(k)$. The probability of the honest network remaining silent for duration T is $S_H(T) = \exp(-M_H T^2/2)$. The consistency violation probability, $\epsilon(k)$, is bounded by the probability of this necessary condition holding. We approximate the random time $T_A(k)$ with its expected value E .

$$\epsilon(k) \leq P(\text{Honest silent for time } E) = S_H(E)$$

This approximation is justified for sufficiently large k by the Law of Large Numbers, as the sum of i.i.d. random variables $T_A(k)$ concentrates sharply around its mean. Formal analysis using concentration inequalities confirms this asymptotic behavior.

4. Algebraic Simplification: Substituting E into the honest survival function:

$$\epsilon(k) \leq \exp\left(-\frac{M_H}{2} \left(k \sqrt{\frac{\pi}{2M_A}}\right)^2\right) = \exp\left(-\frac{M_H}{2} \left(k^2 \cdot \frac{\pi}{2M_A}\right)\right)$$

Simplifying the exponent yields:

$$-k^2 \cdot \left(\frac{\pi}{4} \frac{M_H}{M_A}\right)$$

5. Final Form: Substituting $M_H/M_A = \alpha_H/\alpha_A$:

$$\epsilon(k) \leq \exp\left(-k^2 \cdot \frac{\pi}{4} \frac{\alpha_H}{\alpha_A}\right)$$

Let $C' = \frac{\pi}{4} \frac{\alpha_H}{\alpha_A}$ (a positive constant). We are left with $\epsilon(k) \leq \exp(-C' \cdot k^2)$, which is of the form $\exp(-\Omega(k^2))$. The quadratic term emerges because the time required for the adversary scales linearly ($T \propto k$), but this time is squared in the exponent of the honest survival function ($S_H(T) \propto \exp(-T^2)$).

11.2 Blockchain Axioms and Forks

We now transition to the discrete framework introduced by Blum et al. [9]. We adopt a discrete notion of time organized into a sequence of slots $\{sl_0, sl_1, \dots\}$. The outcome of the leader election process for a sequence of slots is captured by a characteristic string.

Definition 9. *A characteristic string w is an element of $\{0,1\}^n$ for an execution of length n slots, where $w_i = 0$ if slot sl_i was assigned to a single honest participant, and $w_i = 1$ otherwise (i.e., the slot was assigned to an adversary or multiple honest participants).*

The set of all possible blockchains that can be constructed by an adversary for a given characteristic string is represented by a graph structure called a fork.

Definition 10 (Fork). *A fork for a string $w \in \{0,1\}^n$ is a directed, rooted tree $F = (V, E)$ with a labeling $l : V \rightarrow \{0, 1, \dots, n\}$ that adheres to a set of axioms representing the rules of a longest-chain protocol. These axioms ensure the tree structure respects the rules of honest block production and chain extension [9].*

11.3 Tines, Reach, and Margin

The paths from the root of a fork are called **tines**, which represent individual blockchains. The power of an adversary to create diverging tines is quantified by the concepts of reach and margin [9].

- **Gap:** For a given tine t in a fork F , its gap, $gap(t)$, is the difference in length between the longest tine in F and tine t .
- **Reserve:** The reserve of a tine t , $reserve(t)$, is the number of adversarial slots ($w_i = 1$) that occur after the slot of the final block on tine t .
- **Reach:** The reach of a tine t is defined as $reach(t) = reserve(t) - gap(t)$. It represents the adversary's potential to extend tine t to become the longest chain.
- **Margin:** The margin of a fork, $\mu(F)$, is the maximum of the minimum reach over all pairs of disjoint tines. It measures the adversary's ability to maintain two competing long chains simultaneously.

11.4 Relative Margin and Consistency Violations

The analysis can be localized by defining **relative margin**, $\mu_x(y)$, for a characteristic string decomposed as $w = xy$. This measures the adversary's ability to create two tines that are disjoint over the suffix y . A consistency violation corresponds to the existence of an *x-balanced fork*—a fork with two maximum-length tines that diverge before y . A key result of the combinatorial theory [9] is the following equivalence:

Lemma 5. *An x-balanced fork for a characteristic string xy exists if and only if the relative margin $\mu_x(y) \geq 0$.*

This lemma transforms the problem of analyzing blockchain consistency into a problem of analyzing the stochastic process defined by the relative margin. The probability of a consistency violation at depth k can be bounded by calculating the probability that a random characteristic string $w = xy$ (with $|y| \geq k$) has a non-negative relative margin, $P(\mu_x(y) \geq 0)$.

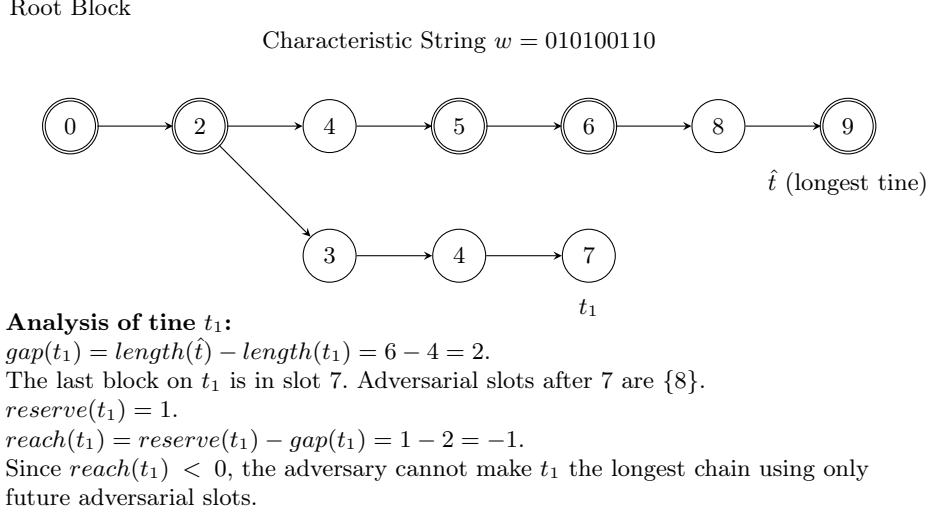


Fig. 2: A fork diagram illustrating the concepts of tines, gap, reserve, and reach within the combinatorial framework.

11.5 Generalized Scaling Law

The preceding analyses can be synthesized into a single, generalized scaling law that defines the required confirmation depth k as a function of the target security level and prevailing network conditions.

Theorem 8. *The required confirmation depth k to achieve a target consistency violation probability ϵ_{target} is a direct function of the adversarial resource fraction α_A , the mean block time μ , and the relationship between network delay Δ and the protocol's Slot Gap parameter ψ .*

Proof. The quadratic consistency bound is $\epsilon(k) \leq \exp(-C' \cdot k^2)$, where $C' = \frac{\pi}{4} \frac{\alpha_H}{\alpha_A}$ in the ideal case. When $\Delta > \psi$, the ratio of honest to adversarial success probability is degraded to an effective ratio, $1/R_{eff}$, where $R_{eff} = \frac{\alpha_A(\mu + \max(0, \Delta - \psi))}{\alpha_H \mu}$. The effective constant in the exponent becomes $C'_{eff}(\Delta, \psi) = \frac{\pi}{4} \cdot \frac{1}{R_{eff}}$. The consistency violation probability is $\epsilon(k, \Delta, \psi) \leq \exp(-C'_{eff}(\Delta, \psi) \cdot k^2)$. To find the required confirmation depth k for a target security level ϵ_{target} , we solve for k :

$$k^2 \geq -\frac{\ln(\epsilon_{target})}{C'_{eff}(\Delta, \psi)}$$

$$k(\epsilon_{target}, \Delta, \psi) \geq \sqrt{-\ln(\epsilon_{target}) \cdot \frac{4}{\pi} \cdot \frac{\alpha_A(\mu + \max(0, \Delta - \psi))}{\alpha_H \mu}}$$

This equation formally establishes the boundary conditions for the Common Prefix property.

This single equation describes the protocol's behavior in two distinct operational regimes:

1. **Secure State ($\psi > \Delta$):** $\max(0, \Delta - \psi) = 0$. The formula simplifies to the ideal case:

$$k \geq \sqrt{-\ln(\epsilon_{target}) \cdot \frac{4}{\pi} \cdot \frac{\alpha_A}{\alpha_H}}$$

This allows for a minimal, constant k (e.g., Synergeia's target of $k = 6$).

2. **Insecure State ($\Delta > \psi$):** The required confirmation depth k grows with the square root of the network delay, $\sqrt{\Delta}$. As $\Delta \rightarrow \infty$, the required $k \rightarrow \infty$, signifying a breakdown of probabilistic finality.

The practical impact of this theoretical advancement is summarized in Table 1, which compares the confirmation depths required by different protocols to achieve a standard level of security ($\epsilon = 10^{-9}$), illustrating the spectrum from deterministic to probabilistic finality.

Table 3: Comparative Confirmation Depths for Target Security $\epsilon = 10^{-9}$

Protocol Model	α_A	μ	Network Model	Fin. Depth (k)	Time to Fin.	Fin. Type
BFT (e.g., Tendermint)	33%	2 sec	Partial Synchrony*	1 block	2 seconds	Deterministic
Nakamoto (Linear)	40%	10 min	Semi-Synchronous (Δ)	≈ 52 blocks	≈ 8.7 hours	Probabilistic
Synergeia (Quadratic)	40%	15 sec	Secure State ($\psi > \Delta$)	6 blocks	90 seconds	Probabilistic
Synergeia (Quadratic)	40%	15 sec	Extreme ($\Delta = \psi + 60s$)	≈ 10 blocks	≈ 2.5 minutes	Probabilistic
Nakamoto (Linear)	49%	10 min	Semi-Synchronous (Δ)	≈ 480 blocks	≈ 3.3 days	Probabilistic
Synergeia (Quadratic)	49%	15 sec	Secure State ($\psi > \Delta$)	≈ 20 blocks	≈ 5 minutes	Probabilistic

* BFT protocols typically require a permissioned or semi-permissioned validator set and may face liveness challenges under full asynchrony.

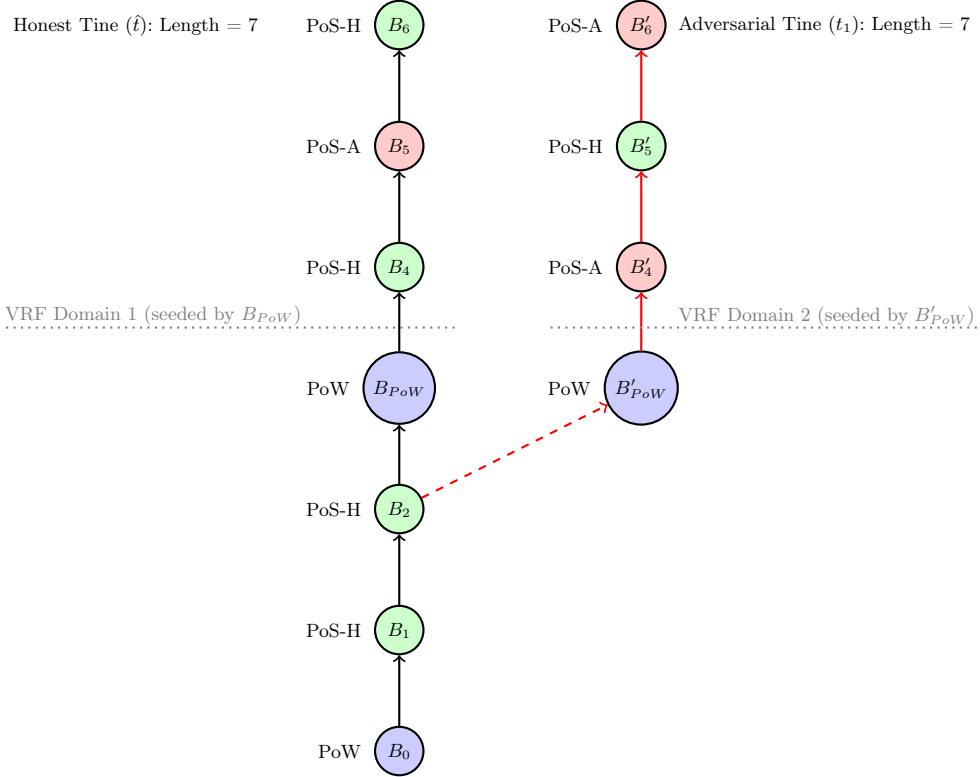


Fig. 3: The VRF Grinding Surface. The adversary forks the chain by privately mining B'_{PoW} . This creates an alternate VRF domain where the adversary wins more PoS slots (B'_4, B'_6), allowing them to construct a longer private chain.

11.6 Combinatorial Analysis of VRF Grinding and Finality

We now utilize the combinatorial framework, inspired by the work of Blum et al. [9], to analyze the protocol’s resilience against VRF grinding attacks. This class of attack, explored in detail in protocols like Ouroboros Praos [15], represents a key risk surface for many PoS designs.

PoW-Anchored VRF Domains. The VRF seed for any slot, sl_{now} , is strictly defined as $seed = \text{Hash}(\mathcal{B}_{PoW,k})||sl_{now}$, where $\mathcal{B}_{PoW,k}$ is the latest PoW block in the chain’s view below confirmation depth k . If $k = 0$, for the entire span of PoS slots between two consecutive PoW blocks, the leader schedule is deterministic and unalterable by any party. An adversary cannot influence their eligibility within this fixed domain. The only remaining attack vector is for an adversary to create an entirely new, alternate VRF domain by privately mining their own PoW block.

The Adversarial Grinding Surface An adversary’s strategy is to privately solve a PoW puzzle. The resulting block, \mathcal{B}'_{PoW} , if kept secret, generates a different, hidden PoS leader schedule. The adversary simulates this private tine, exploiting the new schedule if it is favorable.

Security Against Long-Range Grinding Attacks. The security of Synergeia against a long-range grinding attack—an attack aiming to cause a deep chain reorganization—relies on the fact that the grinding process itself is subject to the quadratic penalty of the Rayleigh distribution.

Theorem 9. *The probability that an adversary can successfully mount a deep reorganization by creating an alternate VRF domain via a private PoW block decays super-exponentially with the confirmation depth k .*

Proof. To initiate the attack, the adversary must privately mine a PoW block, \mathcal{B}'_{PoW} , creating a fork against the honest chain's latest PoW block, \mathcal{B}_{PoW} . This is a race against the entire honest network. For this grinding attack to have any chance of causing a deep reorganization of k blocks, the adversary must win this initial PoW race and then proceed to build a chain that eventually outpaces the honest chain's growth over a long duration. This is precisely the stochastic race analyzed in our continuous-time model (Section 7). The time for the honest network to find its next block, T_H , follows a Rayleigh distribution. The probability that an adversary can complete a sequence of actions (including mining a PoW block and then leveraging a favorable VRF domain) before the honest network finds its next block is bounded by the same super-exponential decay, $\exp(-\Omega(k^2))$. Therefore, long-range grinding attacks are cryptoeconomically infeasible for the same reason that standard long-range attacks are.

11.7 Analysis of Short-Range Opportunistic Grinding

The security analysis in the preceding subsection is robust for long-range attacks but is incomplete. It overlooks a more subtle, short-range opportunistic attack that does not aim for deep reorganizations but instead exploits the natural instability of the chain tip. We term this a "schedule shopping" attack.

The Attack Vector. In any longest-chain protocol, short reorganizations of 1-2 blocks are a common occurrence. An adversary can leverage this fluidity. The attack proceeds as follows:

1. The adversary attempts to mine a PoW block, \mathcal{B}'_{PoW} , just slightly ahead of the honest network's next PoW block, \mathcal{B}_{PoW} , creating a temporary 1-block fork.
2. On the adversary's private fork, a new, secret VRF domain seeded by $\text{Hash}(\mathcal{B}'_{PoW})$ is immediately established.
3. The adversary instantly computes the PoS leader schedule for the first few slots in this new domain. This requires negligible computation.
4. **Opportunistic Decision:** If the schedule is highly favorable (e.g., the adversary is elected leader for the next two or three consecutive slots), the adversary immediately produces those PoS blocks on their private chain. If the schedule is unfavorable, the adversary abandons the fork and \mathcal{B}'_{PoW} at no significant cost.
5. This "burst" of blocks, if the opportunity arises, might give the adversary's chain a sufficient lead in Accumulated Synergistic Work (ASW) to become the canonical chain, forcing a reorg on the honest network.

This is not a grinding attack in the traditional sense of brute-forcing VRF inputs, but rather a form of "schedule shopping" that opportunistically leverages a successful PoW race to gain a short-term advantage.

Formal Analysis. The success of this attack is a compound event. Let us analyze the probability of an adversary causing a 1-block reorg and gaining a 2-block PoS advantage.

1. **Probability of winning the PoW race:** The probability that the adversary finds the next PoW block before the honest network is simply their share of the PoW hash rate, $\alpha_{A,PoW}$.
2. **Probability of a favorable schedule:** Upon winning the PoW race, the adversary observes a new VRF domain. Let p_A be the probability that the adversary is elected PoS leader in a given slot, which is a function of their stake fraction $\alpha_{A,PoS}$. The probability of being elected leader for the next two consecutive slots is p_A^2 .

The total probability of this specific scenario (winning the PoW race AND getting a 2-slot-leader schedule) is $\alpha_{A,PoW} \cdot p_A^2$. While this probability may be small for any single attempt, the continuous nature of the protocol provides the adversary with repeated opportunities.

Impact on Finality. This attack vector does not violate the asymptotic quadratic consistency of the protocol. However, it increases the frequency of short-term chain reorganizations. The core security model assumes that the honest chain grows uninterrupted, but this attack demonstrates that the chain tip is more fluid than the idealized model suggests. The practical consequence is an increase in the "effective" confirmation depth required to achieve a target security level. The claimed 90-second finality (at $k = 6$ blocks) is predicated on a stable chain growth model. The possibility of these opportunistic bursts means that transactions near the tip of the chain have a higher-than-expected probability of being reverted. A more conservative confirmation rule, perhaps waiting for $k = 8$ or $k = 10$ blocks, would be necessary to provide the same level of assurance against this more realistic threat model. The security analysis for VRF grinding must therefore be considered incomplete without accounting for the impact of routine, short-term chain reorganizations on the stability of the VRF domain at the chain tip.

11.8 Advanced Combinatorial Analysis: Costless Simulation within PoW-Anchored Domains

The preceding analysis of VRF grinding in Sections 11.6 and 11.7 demonstrates the protocol's resilience to long-range attacks and short-range opportunistic attacks at the chain tip. However, this analysis is incomplete as it does not account for a more sophisticated class of attack that combines the unique features of Synergeia's hybrid design: the ability to fork from deeper PoW anchors and the complex grinding surface created by the Local Dynamic Difficulty (LDD) mechanism. An adversary is not restricted to building forks from the tip of the chain; they can select *any* past PoW block as a fork point, thereby creating a multitude of parallel histories, each with a distinct, deterministic VRF domain.

Within each of these domains, the adversary can engage in **costless simulation** of PoS blocks—a threat inherent to Proof-of-Stake protocols where creating blocks on a private fork incurs no direct economic cost [15]. This threat is magnified in Synergeia due to the LDD mechanism. Unlike protocols with static slot leader probabilities (e.g., Ouroboros Praos), where an adversary can only observe a fixed future leader schedule, Synergeia's LDD makes PoS eligibility dependent on the time elapsed since the last block, δ . This creates a non-trivial decision tree for the adversary: by choosing to either produce or withhold a PoS block for which they are eligible in a given slot, they directly manipulate δ for all subsequent slots, thereby altering their own future eligibility. This creates a complex, state-dependent grinding surface, a phenomenon first explored in Ouroboros Taktikos, where it was shown to confer a marginal but non-zero advantage [41]. The long PoW-anchored domains in Synergeia are analogous to the static epochs of Praos and Taktikos, making this a relevant attack vector.

To rigorously analyze this combinatorial landscape of adversarial strategies, we adapt the formal framework for longest-chain protocols developed by Blum et al. [9]. This framework models the evolution of the blockchain as a stochastic process on a **characteristic string**, analyzes the geometry of **forks**, and bounds the probability of consistency violations by studying a quantity known as the **margin**. Our analysis extends this formalism to Synergeia's hybrid PoW/PoS model.

Hybrid Characteristic Strings and State-Dependent Probabilities To apply the combinatorial framework to Synergeia, we must first adapt the notion of a characteristic string. The binary alphabet of $\{0, 1\}$ used in prior analyses is insufficient to capture the dynamics of a hybrid system where slots can be won by honest parties, adversarial parties, or remain empty. We therefore introduce a richer alphabet and a state-dependent probability model.

Definition 11. *A hybrid characteristic string w is an element of $\{H, A, E\}^n$, where for each slot $i \in \{1, \dots, n\}$:*

- $w_i = H$ if the block in slot i is produced by an honest party (either PoW or PoS).
- $w_i = A$ if the block in slot i is produced by an adversarial party (either PoW or PoS).
- $w_i = E$ if slot i is empty (no block is produced).

Unlike the independent and identically distributed (i.i.d.) Bernoulli variables that model the characteristic string in simpler PoS protocols, the probabilities governing Synergeia's characteristic string are state-dependent due to the LDD mechanism. The probability of an outcome in slot i is a function of the time elapsed since the last block, δ .

Definition 12. *Let $w_{<i} = w_1 \dots w_{i-1}$ be a prefix of a characteristic string. Let $\delta(i, w_{<i})$ be the slot interval for slot i , defined as the number of slots since the last non-empty slot in the prefix. The probabilities for*

the outcome of slot i are given by:

$$\begin{aligned} p_H(\delta) &= P(w_i = H | \delta(i, w_{<i}) = \delta) = \alpha_H \cdot (1 - (1 - f(\delta))) \\ p_A(\delta) &= P(w_i = A | \delta(i, w_{<i}) = \delta) = \alpha_A \cdot (1 - (1 - f(\delta))) \\ p_E(\delta) &= P(w_i = E | \delta(i, w_{<i}) = \delta) = 1 - (p_H(\delta) + p_A(\delta)) = (1 - f(\delta)) \end{aligned}$$

where $f(\delta)$ is the hazard rate from the snowplow curve (Eq. 3), and α_H and α_A are the honest and adversarial resource fractions, respectively.

With this new probabilistic structure, we must also refine the definition of the adversary's **reserve**. In this context, the adversary's power is not merely the number of future adversarial slots, but their ability to optimally construct a chain by strategically using or withholding their costlessly simulatable PoS blocks. This introduces a decision tree where each choice to produce or not produce a PoS block alters the δ for all subsequent slots, thereby changing future PoS eligibilities.

Definition 13. For a given tine t in a fork $F \vdash w$ that terminates at slot j , the **adversarial potential**, $\Pi_A(t, w_{>j})$, is the maximum number of additional adversarial blocks that can be appended to t by an optimal strategy of costless simulation over the suffix of the characteristic string $w_{>j}$. This optimal strategy accounts for the state-dependent nature of PoS eligibility. The **hybrid reach** of the tine t is then defined as:

$$\text{reach}(t) = \Pi_A(t, w_{>j}) - \text{gap}(t)$$

The problem of bounding consistency violations is thus transformed. A consistency violation, corresponding to an x -balanced fork, exists if and only if the relative margin $\mu_x(y) \geq 0$ [9]. Our task is to bound the probability of this event, $P(\mu_x(y) \geq 0)$, under the complex, state-dependent stochastic process defined by our hybrid characteristic string and the adversary's optimal simulation strategy.

The Adversary's Optimal Strategy: A Dynamic Programming Approach The adversary's goal is to construct the longest possible private chain by optimally exercising their PoS block production rights within a given PoW-anchored domain. This is not a simple matter of producing a block in every slot for which they are eligible. Because eligibility is a function of the slot interval δ , the adversary faces a strategic choice at each opportunity: produce a block now, or withhold it to increase δ and potentially achieve a higher probability of success in a future slot? This problem can be modeled and solved using dynamic programming.

Let the state of the system at any slot i be defined by the interval δ since the last block was produced. We can define a value function, $V(i, \delta)$, representing the maximum *expected number* of additional adversarial blocks the adversary can produce from slot i to the end of the domain (say, slot n), given the current slot interval is δ . The adversary's optimal strategy is to always take the action that maximizes this value.

The value function can be defined by a recursive relation, working backwards from the end of the domain. The base case is $V(n+1, \delta) = 0$ for all δ . For any slot $i \leq n$, the value function is the expectation over the possible outcomes of that slot, assuming the adversary plays optimally:

$$\begin{aligned} V(i, \delta) &= p_H(\delta) \cdot V(i+1, 1) \quad (\text{Honest block resets } \delta) \\ &\quad + p_E(\delta) \cdot V(i+1, \delta+1) \quad (\text{Empty slot increments } \delta) \\ &\quad + p_A(\delta) \cdot \max \left\{ \begin{array}{l} 1 + V(i+1, 1), \text{(Produce block)} \\ V(i+1, \delta+1) \text{ (Withhold block)} \end{array} \right\} \end{aligned}$$

This equation precisely captures the adversary's strategic decision. In a slot where they are eligible to produce a block (an event occurring with probability $p_A(\delta)$), they will compare the expected future payoff of producing the block immediately (gaining 1 block and resetting the interval to $\delta = 1$ for the next slot) versus withholding it (gaining 0 blocks now but increasing the interval to $\delta + 1$ for the next slot). A rational adversary will choose the action that yields the greater expected total blocks.

This optimal strategy constitutes a form of grinding that targets the LDD function $f(\delta)$ itself. By strategically withholding blocks, the adversary can intentionally create long sequences of empty slots to drive the system into the "forging window" ($\psi \leq \delta < \gamma$), where the hazard rate $f(\delta)$ is highest. This allows the adversary to maximize their overall block production rate within a given PoW-anchored domain, gaining a marginal advantage over a naive strategy. The solution to this dynamic program, $V(i, \delta)$, gives us a precise method for calculating the **adversarial potential**, Π_A , for any tine, which is the crucial input for determining the **hybrid reach** and, ultimately, the margin of a fork.

Bounding the Margin and the Impact of Quadratic Consistency Having defined the adversary’s optimal strategy via the value function $V(i, \delta)$, we can now complete the security analysis. The core of the argument is to show that while the LDD-grinding strategy provides a marginal advantage, this advantage is insufficient to overcome the powerful security guarantees of the underlying continuous-time stochastic process. The probability of a consistency violation remains bounded by a super-exponential function of the confirmation depth.

Theorem 10. *Let an adversary with resource fraction $\alpha_A < 0.5$ employ an optimal costless simulation strategy within a PoW-anchored domain. The probability of achieving a non-negative margin, and thus causing a consistency violation at depth k , is bounded by:*

$$P(\mu_x(y) \geq 0) \leq \exp(-\Omega(k^2))$$

Proof. The proof proceeds by connecting the combinatorial margin analysis to the continuous-time race between the honest network and the optimally-playing adversary.

1. *The Margin as a Biased Random Walk.* The evolution of the relative margin, $\mu_x(y)$, can be conceptualized as a biased random walk. A consistency violation occurs if this random walk ever reaches or exceeds zero. The drift of this walk is determined by the relative rates of block production between the honest parties and the optimally-playing adversary. From the dynamic programming formulation, the adversary’s optimal strategy yields an effective block production probability, $p_{A,eff}(\delta)$, which is marginally higher than the naive probability, $p_A(\delta)$. However, this advantage is a small, constant-factor improvement and does not alter the fundamental condition that the honest resource fraction exceeds the adversarial one ($\alpha_H > \alpha_A$). Consequently, the random walk representing the margin maintains a negative drift from the adversary’s perspective, meaning it is statistically expected to decrease over time.

2. *The Primacy of the Continuous-Time Race.* While the combinatorial analysis provides a fine-grained view of the adversary’s optimal strategy, the ultimate success of any attack is still governed by a race in continuous time. To cause a consistency violation at depth k , the adversary must successfully execute a forking strategy—which includes both winning an initial PoW race and then building out a private chain of sufficient length using their optimal PoS simulation—before the honest network produces its next block.

Let $T_A^*(k)$ be the random variable for the time required for an adversary to produce a chain of length k using their optimal LDD-grinding strategy. The dynamic programming solution gives us the expected number of blocks, from which we can infer the expected time, \mathbb{E} . This expected time will be slightly less than the time required by a naive adversary, \mathbb{E} , but it still scales linearly with k . Let $\mu_k^* \triangleq \mathbb{E}$.

The probability of a consistency violation is bounded by the probability that the honest network remains silent for this duration. Following the proof structure of Theorem 2, and applying the same concentration inequalities, the dominant term in the security bound is given by the honest network’s survival function evaluated at the adversary’s expected time:

$$\begin{aligned} \epsilon(k) &\leq P(T_H > (1 - \nu)\mu_k^*) = S_H((1 - \nu)\mu_k^*) \\ &= \exp\left(-\frac{M_H}{2}((1 - \nu)\mu_k^*)^2\right) \end{aligned}$$

The crucial observation is that the exponent remains quadratic in k . The advantage gained from LDD grinding only affects the constant factor within the exponent (by slightly reducing μ_k^*), but it does not change the fundamental quadratic relationship between the confirmation depth k and the logarithm of the security parameter ϵ .

3. *Conclusion of the Proof.* The costless simulation of PoS blocks, even when optimized via a dynamic programming strategy to exploit the LDD mechanism, provides only a limited, constant-factor advantage to the adversary. This advantage is ultimately overwhelmed by two factors:

1. **The Cost of Entry:** The adversary must first win a PoW race to establish a private VRF domain, an event whose probability is governed by the super-exponential security of the protocol itself for any significant depth.
2. **The Quadratic Bound:** The subsequent race to build a longer chain is against an honest network whose block arrival process has a tail that decays quadratically in the exponent. A linear improvement in the adversary’s block production rate cannot overcome a quadratic security guarantee.

Therefore, the combinatorial analysis confirms that even under this sophisticated class of grinding attacks, the protocol’s consistency remains super-exponentially secure.

On the Infeasibility of Deep Forking and Costless Simulation The analysis thus far has focused on adversarial forks originating from near the tip of the chain. A more powerful adversary, however, could choose to fork from a PoW block deep within the chain’s history, for instance, from a block at a depth d greater than the confirmation depth k . This strategy grants the adversary a new, completely private VRF domain, within which they can apply the optimal costless simulation strategy detailed above. The question is whether the marginal advantage gained from this LDD-grinding is sufficient to overcome the honest chain’s significant lead.

The analysis reveals that this is not the case. The attack’s feasibility is determined by the interplay of two competing factors: the adversary’s *rate advantage* from costless simulation versus their *deficit disadvantage* from forking off an old block.

- **The Rate Advantage:** As established by the dynamic programming model, the adversary’s optimal strategy for withholding and producing PoS blocks grants them a marginal, constant-factor increase in their effective block production rate. They are, in essence, slightly more efficient at building their chain than their nominal resource share would suggest.
- **The Deficit Disadvantage:** By forking from a block at depth d , the adversary starts with a chain that is shorter than the honest chain by at least d blocks. To succeed, their private chain must not only catch up to the honest chain but ultimately surpass it in total Accumulated Synergistic Work (ASW). This is a classic long-range attack scenario.

The success of such an attack is precisely the event that the protocol’s fundamental consistency bound is designed to prevent. The probability of an adversary overcoming a deficit of d blocks is bounded by the core security guarantee derived in Theorem 2.

Lemma 6. *An adversary forking from a PoW anchor at depth $d > k$ succeeds with probability $\epsilon(d)$, where:*

$$\epsilon(d) \approx \exp(-\Omega(d^2))$$

Proof. The adversary’s slight rate advantage from LDD-grinding only modifies the constant factor in the exponent of the security bound. The fundamental relationship between the deficit d and the success probability remains quadratic. The adversary is engaged in a race against the honest network, a race they start d blocks behind. The probability of winning this race is governed by the super-exponential decay of the honest network’s survival function. Since the attack is initiated from a depth d that is, by definition, greater than the confirmation depth k used to calculate the target security level ϵ_{target} , the probability of success is astronomically smaller than ϵ_{target} .

In conclusion, while sampling PoW blocks deeper in the chain does indeed provide the adversary with a new sandbox for costless simulation, the cost of entry for such an attack—the need to overcome a lead of $d > k$ blocks—is super-exponentially prohibitive. The security of already-confirmed blocks grows quadratically with their depth, an advantage that vastly outweighs the marginal gains from LDD-grinding on a private fork. Therefore, this attack vector does not pose a threat to the finality of the Synergeia protocol.

Anchor Depth, LDD Parameters, and System Stability Trade-offs The preceding analysis confirms the protocol’s security against costless simulation, but it also raises important questions about specific design choices. We now address the rationale for using the latest PoW block as a VRF seed and the security implications of the interaction between anchor depth and the parameters of the LDD mechanism.

On the Choice of PoW Anchor Depth. The decision to anchor the VRF seed to the hash of the latest PoW block is a deliberate trade-off in favor of liveness and efficiency. An alternative design could mandate using a PoW anchor that is already confirmed to a certain depth, say the last PoW block below a depth k_{anchor} blocks. Such a design would indeed offer a security benefit against the “schedule shopping” attack described in Section 11.7; by the time the PoW anchor is used as a seed, it would already be part of an immutable prefix of the chain, making its corresponding VRF domain stable and non-forkable. We proceed to analyze the case where $k_{\text{anchor}} = 0$ corresponding to the latest PoW block in the local chain. With this choice, the security against deep grinding attacks is maintained by the super-exponentially prohibitive cost an adversary must pay to create deep forks in the first place.

Interaction with LDD Parameters. It is crucial to distinguish the roles of the PoW anchor and the LDD's adjustment parameters. The PoW anchor and the VRF mechanism together determine the *potential leader schedule* for a given domain; they answer the question of "who is eligible?" The LDD mechanism, governed by the "snowplow curve" and its associated difficulty slopes, determines the *probability of that eligibility being realized* in any given slot; it answers the question of "when is a block likely?" These two systems operate on different timescales. The PoW anchor changes with each new PoW block (on average, every 30 seconds). The Dynamic Slope Adjustment Scheme, which tunes the LDD's difficulty slopes, operates over a much longer lookback window, N (e.g., $N = 240$ blocks, or one hour). The LDD-grinding strategy analyzed above is a micro-optimization performed by an adversary within a single, short-lived VRF domain. The lookback window N , by contrast, is a macro-level control that governs the long-term stability of the entire system.

The Threat of a Small Lookback Window. This separation of timescales highlights a critical security trade-off. While a large lookback window N creates predictable oscillations that can be exploited (as shown in Section 12), a very small N poses a different threat. A small N would make the difficulty adjustment mechanism highly reactive to short-term statistical noise. For instance, a random burst of 5 consecutive PoW blocks could cause the system to drastically and rapidly increase PoW difficulty while lowering PoS difficulty. This hyperactivity would make the adversary's LDD-grinding strategy much harder, as the underlying probabilities would be in constant flux. However, it would simultaneously risk the stability of the entire protocol. The LDD mechanism could overreact to normal variance, leading to high volatility in block times and potentially creating chaotic, unpredictable dynamics. Such instability could harm liveness for honest participants and may even open new, short-term attack vectors for an adversary positioned to exploit these rapid difficulty swings. Therefore, the choice of N is not simply a matter of responsiveness but a careful balance between mitigating long-term predictable exploits and avoiding short-term systemic instability.

Fine-Grained Analysis of Anchor Depth and Lookback Window The preceding analysis demonstrates the protocol's resilience under a general model. We now refine this analysis by examining the security implications of two key parameter choices: the PoW anchor depth, k_{anchor} , and the LDD adjustment window, N .

The Impact of Anchor Depth. The protocol specifies that the VRF seed for any given slot is derived from the hash of the latest PoW block found at or below a fixed depth, k_{anchor} . The current implementation sets $k_{\text{anchor}} = 0$, meaning the seed is taken from the PoW block at the tip of the chain. Let's analyze the trade-offs of this choice.

- **Case $k_{\text{anchor}} = 0$ (Tip of the Chain):** This setting maximizes liveness and responsiveness. As soon as a new PoW block is found, it immediately defines a new VRF domain. However, this comes at the cost of domain stability. As analyzed in Section 11.7, PoW blocks at the tip of the chain are subject to frequent, small-scale reorganizations. This instability is precisely what enables the "schedule shopping" attack, where an adversary can create a temporary 1-block fork specifically to generate a new, secret VRF domain and exploit it if the resulting PoS leader schedule is favorable.
- **Case $k_{\text{anchor}} > 0$ (Deeper in the Chain):** Setting a deeper anchor depth, for example $k_{\text{anchor}} = 6$, fundamentally changes the dynamics. The VRF seed for the current slot would be derived from the hash of the most recent PoW block that has at least 6 confirmations. Because there is no waiting period, this is a fast, local lookup. The security implication is a significant increase in VRF domain stability. A PoW block at depth 6 is, by the protocol's own security claims, probabilistically final. Forks at this depth are super-exponentially unlikely. Consequently, the VRF domain becomes fixed for a much longer period, remaining constant until a *new* PoW block is mined and subsequently gains 6 confirmations. This design choice effectively mitigates the "schedule shopping" attack. However, it does not eliminate LDD grinding. The adversary can still perform the optimal costless simulation strategy within this now-stable and longer-lasting VRF domain.

In summary, a deeper k_{anchor} hardens the protocol against one specific attack vector (schedule shopping) by creating longer, more stable epochs, but it does not alter the fundamental mechanics of LDD grinding within those epochs.

Adversarial Advantage in a Hyper-Reactive LDD System. We now model the adversary's advantage when the LDD lookback window, N , is set to a minimal value. A small N makes the Dynamic Slope Adjustment Scheme "hyper-reactive," causing it to make large, rapid changes to the PoW and PoS difficulty slopes based on a very short history. This creates a new, more direct attack vector for a strategic adversary who possesses both PoW and PoS resources. We term this strategy **difficulty prepping**.

Let's analyze the most extreme case, where the lookback window is $N = 1$. Here, the difficulty adjustment for the next block is based solely on the type of the single most recent block.

- If the last block was PoW, the observed PoW proportion is $P_{PoW} = 1$. The error term is $E = P_{PoW} - 0.5 = 0.5$.
- If the last block was PoS, the observed PoW proportion is $P_{PoW} = 0$. The error term is $E = P_{PoW} - 0.5 = -0.5$.

The adjustment formulas for the difficulty amplitudes (before the speed-correcting scaling factor β is applied) are:

$$\begin{aligned} f'_{A,PoW} &= f_{A,PoW} \cdot (1 - \kappa \cdot E) \\ f'_{A,PoS} &= f_{A,PoS} \cdot (1 + \kappa \cdot E) \end{aligned}$$

An adversary can exploit this immediate feedback loop. Suppose the adversary wishes to mine a PoW block. They can first attempt to mine a PoS block. If they succeed, the error becomes $E = -0.5$. The system will immediately react for the very next block by making PoW easier and PoS harder. The new PoW difficulty amplitude will be:

$$f'_{A,PoW} = f_{A,PoW} \cdot (1 - \kappa \cdot (-0.5)) = f_{A,PoW} \cdot (1 + 0.5\kappa)$$

This gives the adversary a direct, predictable amplification of their PoW resources for the next block attempt. We can quantify this as an **effective resource advantage**.

Definition 14 (Grinding Advantage for N=1). *For a system with lookback window $N = 1$, an adversary with nominal resource fraction α_A who successfully "preps" the network by mining a PoS block gains an effective PoW resource fraction, $\alpha'_{A,PoW}$, for the next block attempt, given by:*

$$\alpha'_{A,PoW} = \alpha_{A,PoW} \cdot (1 + 0.5\kappa)$$

where $\alpha_{A,PoW}$ is the adversary's share of the total PoW resources and κ is the responsiveness parameter of the LDD system.

This formula provides an explicit measure of the grinding advantage. Unlike the slow exploitation of predictable oscillations that occurs with a large N , this is a direct, tactical manipulation of the protocol's state. The cost of this attack is the expenditure of a PoS block production opportunity, but the reward is a guaranteed increase in the probability of success for the subsequent PoW block. This analysis reveals that an extremely small lookback window, while preventing long-term predictable cycles, introduces a new and potent short-term attack surface.

The Grinding Advantage for $N > 1$ The "difficulty prepping" attack is most potent when the system is maximally reactive, i.e., when $N = 1$. As we increase the lookback window, the system's memory grows, and the adversary must manipulate a longer history of block production to achieve the same effect. This increases the cost and complexity of the attack, diminishing its practical viability.

Analysis for N=2. When the lookback window is $N = 2$, the difficulty adjustment is based on the types of the last two blocks. The observed PoW proportion, P_{PoW} , can now take three values: 0 (if the last two blocks were PoS, PoS), 0.5 (if one was PoW and one was PoS), or 1 (if both were PoW). The corresponding error term, $E = P_{PoW} - 0.5$, can be -0.5, 0, or 0.5.

An adversary wishing to make a future PoW block easier must create a state where the error E is negative. The optimal state is achieved when the last two blocks are (PoS, PoS), yielding the maximum negative error of $E = -0.5$. The "difficulty prepping" strategy is now a two-step process: the adversary must first successfully mine two consecutive PoS blocks. If they succeed, the system adjusts the PoW difficulty for the next block attempt by the same maximum factor as in the $N = 1$ case:

$$f'_{A,PoW} = f_{A,PoW} \cdot (1 - \kappa \cdot (-0.5)) = f_{A,PoW} \cdot (1 + 0.5\kappa)$$

The potential reward for the adversary—the amplification factor on their PoW resources—remains the same. However, the cost of the attack has increased significantly. The adversary must now successfully produce a specific sequence of *two* blocks, which is a far more challenging and less frequent event than producing a single block.

Analysis for $N=3$ and Generalization for small N . The pattern becomes clearer as we extend the analysis to $N = 3$. The error term E is now calculated over the last three blocks, and can take values in $\{-0.5, -1/6, 1/6, 0.5\}$. To achieve the maximum advantage for a future PoW block, the adversary must again create the state with the most negative error, $E = -0.5$. This requires them to successfully mine a sequence of three consecutive PoS blocks.

We can now generalize the behavior for any small N . The optimal "difficulty prepping" strategy for an adversary aiming to amplify their PoW resources is to successfully mine N consecutive PoS blocks. This sequence creates the maximal negative error of $E = -0.5$, which in turn yields the maximal difficulty amplification of $(1 + 0.5\kappa)$ for the subsequent PoW block attempt.

Lemma 7 (Grinding Advantage for small N). *For a system with a lookback window N , the maximum grinding advantage an adversary can achieve for a single block attempt is an amplification of their effective resources by a factor of $(1 + 0.5\kappa)$. This advantage is realized only after the adversary successfully produces a specific sequence of N consecutive blocks of the opposite type.*

This lemma reveals a crucial trade-off. While the maximum *potential* advantage is independent of N , the *cost* of achieving that advantage grows exponentially with N . An adversary must successfully win N consecutive block races, a compound event whose probability decreases rapidly as N increases. For $N = 1$, the attack is tactical and opportunistic. For $N > 1$, the attack requires a sustained and successful manipulation of the blockchain history, making it significantly less practical. This demonstrates that even a small increase in the lookback window (e.g., to $N = 2$ or $N = 3$) acts as a powerful mitigation against this form of hyper-reactive grinding, as the cost of the attack quickly begins to outweigh the marginal, single-block reward.

Conclusion: The Security Trade-off of the Lookback Window Our fine-grained analysis reveals a critical and non-monotonic relationship between the lookback window N and the protocol's security against strategic adversaries. The protocol is vulnerable at both extremes of N , exposing a fundamental trade-off between two distinct classes of attack.

Vulnerability of a Small Lookback Window. For minimal values of N (e.g., 1 to 3), the system becomes hyper-reactive. While this chaotic behavior prevents the long-period oscillations discussed in Section 12, it introduces the potent "difficulty prepping" attack. As we have shown, the cost of executing this attack—requiring the successful mining of N consecutive blocks of a specific type—grows exponentially with N . The probability of success for an adversary aiming to prep for a PoW block is proportional to $\alpha_{A,PoS}^N$. For an adversary with a total resource fraction $\alpha_A = 0.4$ (and assuming an even split, $\alpha_{A,PoS} = 0.2$), the probability of successfully prepping for an attack with $N = 3$ is already a mere $(0.2)^3 = 0.8\%$. This rapidly diminishing probability of success must be weighed against a constant, single-block reward. For $N = 1$ or $N = 2$, the attack is opportunistic and poses a genuine threat. For slightly larger N , the expected utility of the attack quickly becomes negative, rendering it an irrational strategy.

Vulnerability of a Large Lookback Window. Conversely, as N becomes large, the "difficulty prepping" attack becomes computationally infeasible due to its exponential cost. However, as demonstrated in the game-theoretic analysis of Section 12, a large N creates long-period, predictable "Resource Interchange Oscillations" with a period of $T_{osc} = 4 \cdot N \cdot \mu$. These predictable, low-frequency oscillations can be exploited by a patient adversary (e.g., by renting hash power) to achieve a sustained increase in their effective resource fraction, α'_A , thereby weakening the protocol's core consistency guarantees over a long time horizon.

Conclusion: A Static ' N ' as an Inherent Vulnerability. This exposes a fundamental security trade-off. An optimal choice for N must be large enough to render the "difficulty prepping" attack prohibitively expensive, yet small enough that the resulting oscillations are too high-frequency to be economically exploited. While this suggests an intermediate "sweet spot", any static choice for N presents a false sense of security. The true "sweet spot" is not static; it is a dynamic variable that depends on unpredictable

external market conditions that the protocol cannot measure. For example, the profitability of exploiting large- N oscillations is a direct function of the real-world cost and liquidity of the hash power rental market. Conversely, the utility of the small- N "difficulty prepping" attack depends on the adversary's specific resource composition. Because the optimal, most secure value for N is a function of external variables the protocol cannot observe, any static parameter is inherently gameable. This points to a fundamental and potentially unavoidable vulnerability in any system with a predictable, time-delayed feedback controller. We propose an adaptive lookback window, algorithmically managed by the \mathcal{F}_{DCS} (Section 9.12) based on observed on-chain volatility metrics, in Section 12.

12 PoW/PoS Resource Interchange Oscillations and System Exploitability

An emergent property of the Synergeia protocol is a periodic oscillation in the proportion of Proof-of-Work (PoW) versus Proof-of-Stake (PoS) blocks produced over time. We term this phenomenon **Resource Interchange Oscillation**. This behavior is a direct and predictable consequence of the negative feedback loop in the Dynamic Slope Adjustment Scheme. The discrete nature of the adjustment window introduces a time delay (T_{adj}) into the control system. In the field of control theory, it is well established that such time-delayed feedback is a common cause of oscillations in dynamical systems. This section applies standard techniques from control theory to model these oscillations and, critically, analyzes their implications for the security of the protocol against a strategic adversary.

This analysis serves a dual purpose. First, it validates the algorithmic stability of the protocol's control loop. Second, and more critically, it provides the second component required to quantify the **effective adversarial resource fraction**, α'_A , introduced in Section 7.4. The "bang-bang" strategy analyzed in this section provides a quantifiable, constant-factor gain for the adversary (Section 14.6). By combining this gain with the advantage from LDD-grinding (Section 11.8), we can derive a final, robust value for α'_A .

12.1 Modeling Oscillations via Delay Differential Equations

We begin by linearizing the discrete-time adjustment mechanism into a continuous-time model and then apply Laplace transforms to analyze its behavior as a delay differential equation (DDE). The core of the system is the set of adjustment formulas for the difficulty amplitudes. Let us denote their continuous-time equivalents as $f_W(t)$ and $f_S(t)$. The protocol's adjustment logic can be expressed as a system of differential equations that captures the delayed feedback.

The analysis yields a characteristic equation for the system's transfer function:

$$s + \left(\frac{\kappa}{2T_{adj}} \right) e^{-sT_{adj}} = 0$$

The roots (poles) of this transcendental equation determine the system's stability and transient response.

12.2 Stability Analysis

The stability boundary occurs when there is a pair of purely imaginary roots, $s = \pm j\omega_c$. Substituting $s = j\omega_c$ into the characteristic equation and separating the real and imaginary parts yields two conditions. From the real part, we find the critical frequency of oscillation:

$$\omega_c = \frac{\pi}{2T_{adj}}$$

From the imaginary part, we derive the stability condition for the responsiveness parameter κ :

$$\kappa < \pi$$

As long as this condition holds, the system is guaranteed to be stable and will converge to the target 50/50 equilibrium. The period of the resulting oscillation is given by:

$$T_{osc} = \frac{2\pi}{\omega_c} = 4 \cdot T_{adj} = 4 \cdot N \cdot \mu$$

where N is the look-back window size in blocks and μ is the target mean block time. This analysis formally proves that the system is stable, but it also reveals that the oscillations are a predictable, deterministic feature of the protocol's dynamics.

12.3 Game-Theoretic Analysis of a Strategic Adversary

The literature on dynamic difficulty adjustment (DDA) from other fields, such as video games, is replete with examples showing that predictable, oscillating systems can be gamed by strategic actors [26,3]. We now provide a formal game-theoretic analysis to quantify this risk.

The Strategic Adversary Model. We consider a rational adversary who possesses a total resource fraction α_A and has the capability to dynamically allocate these resources between PoW and PoS. Let their allocated fractions at time t be $\alpha_{A,PoW}(t)$ and $\alpha_{A,PoS}(t)$, such that $\alpha_{A,PoW}(t) + \alpha_{A,PoS}(t) = \alpha_A$. A naive adversary might maintain a static allocation (e.g., $\alpha_A/2$ to each). A strategic adversary, however, is aware of the predictable oscillations in the difficulty slopes.

Let the effective slope parameter for PoW and PoS be modeled as oscillating functions around an average value M_{avg} with amplitude A :

$$\begin{aligned} M_{PoW}(t) &= M_{avg} + A \cos(\omega t) \\ M_{PoS}(t) &= M_{avg} - A \cos(\omega t) \end{aligned}$$

where $\omega = 2\pi/T_{osc}$. The adversary's objective is to maximize their total block production over one full cycle by allocating their entire resource fraction α_A to whichever mechanism is currently easier. This is a "bang-bang" control strategy:

- When $M_{PoW}(t) > M_{PoS}(t)$, the adversary allocates all resources to PoW.
- When $M_{PoS}(t) > M_{PoW}(t)$, the adversary allocates all resources to PoS.

Quantifying the Adversarial Advantage. The expected number of blocks produced by a naive adversary (who splits resources evenly) over one cycle is proportional to:

$$B_{naive} \propto \int_0^{T_{osc}} \left(\frac{\alpha_A}{2} M_{PoW}(t) + \frac{\alpha_A}{2} M_{PoS}(t) \right) dt = \alpha_A M_{avg} T_{osc}$$

The strategic adversary's expected block production is proportional to:

$$B_{strat} \propto \alpha_A \int_0^{T_{osc}} \max(M_{PoW}(t), M_{PoS}(t)) dt$$

Evaluating this integral yields:

$$B_{strat} \propto \alpha_A \left(M_{avg} T_{osc} + \frac{2AT_{osc}}{\pi} \right)$$

The amplification factor, representing the adversary's gain from this strategy, is the ratio B_{strat}/B_{naive} :

$$\text{Amplification} = 1 + \frac{2A}{\pi M_{avg}}$$

This allows us to define an **effective adversarial resource fraction**, α'_A , which is the nominal fraction amplified by this factor:

$$\alpha'_A = \alpha_A \left(1 + \frac{2A}{\pi M_{avg}} \right)$$

This result formally demonstrates that a strategic adversary can achieve a higher effective resource share than their nominal share by exploiting the system's predictable oscillations. This fundamentally breaks the static resource assumption (α_A) used in the core consistency proofs of Section 7.

12.4 Impact on Security and Parameter Selection

The existence of this strategic advantage requires a careful evaluation of both the protocol's security bounds and its parameterization.

Impact on the Consistency Bound. The quadratic consistency bound, $\epsilon \approx \exp(-\Omega(k^2))$, depends critically on the ratio of honest to adversarial resources, α_H/α_A . Under this strategic attack, the bound must be re-calculated using the effective adversarial fraction α'_A and the correspondingly diminished honest fraction $\alpha'_H = 1 - \alpha'_A$. The new ratio, α'_H/α'_A , will be smaller, weakening the exponent of the security bound and requiring a larger confirmation depth k to achieve the same level of security.

The Look-Back Parameter N . The analysis reveals a critical trade-off in the choice of the adjustment window size, N . A choice of $N = 60$ based on balancing responsiveness to hashrate changes with a 15-second block time yields an oscillation period of $T_{osc} = 4 \cdot 60 \cdot 15s = 1$ hour. This predictable period creates a window where PoW is favored, followed by a window for PoS. Such a predictable interval is trivial for an adversary to exploit, for instance by renting hash power from an external market for a short burst.

This suggests that a much smaller value for N is preferable. A smaller N would lead to shorter, higher-frequency oscillations introducing short-term variance into the block time. The rapid and chaotic fluctuations induced by the LDD system adaptation would be significantly harder for an adversary to predict and exploit economically. The costs and delays associated with rapidly reallocating resources (e.g., spinning up mining hardware or re-delegating stake) could render the strategic attack infeasible or unprofitable. Therefore, the choice of N must be considered not just as a trade-off between responsiveness and stability, but as a three-way trade-off between responsiveness, short-term stability, and exploitability. A "noisy" system, counter-intuitively, is more secure than the smoothly predictable one.

12.5 An Adaptive Lookback Window via the DCS

Our analysis of the lookback window N in Sections 11.8 and 12 reveals a fundamental vulnerability:

- A **small, static** N is vulnerable to the "difficulty prepping" attack.
- A **large, static** N is vulnerable to the "Resource Interchange Oscillation" exploit.

Any static N represents a fixed trade-off that is inherently gameable. The optimal value depends on external market conditions and adversarial strategies. To resolve this, we make the lookback window N a dynamic parameter, autonomously managed by the **Decentralized Consensus Service** (\mathcal{F}_{DCS}). This transforms N from a static vulnerability into a dynamic, responsive defense mechanism.

Linking N to the Consensus Security Threat Level The exploits associated with both small and large N (i.e., prepping and oscillations) are strategic forking attacks. These attacks, if successful, will necessarily increase the network's observed orphan rate and reorganization depth. As we will formally introduce in Section 15, the \mathcal{F}_{DCS} is already responsible for calculating a BFT-robust **Security Threat Level** (S_{threat}) based on these very metrics. We can therefore tie the lookback window N directly to this consensus threat level.

The Adaptive N Routine The protocol's defensive posture should adapt based on the perceived threat.

- **Low Threat** ($S_{threat} \rightarrow 0$): When the network is peaceful, the system should prioritize stability and predictability for honest participants. This calls for a **large** N (e.g., $N_{base} = 240$), which creates smooth, low-frequency adjustments.
- **High Threat** ($S_{threat} \rightarrow 1$): When the network is under attack (high orphan rate), it implies an adversary may be exploiting the predictability of the large N . The protocol's defense is to become *unpredictable*. This calls for a **small** N (e.g., $N_{min} = 5$), which makes the system hyper-reactive and chaotic.

This logic is formalized in the following adaptive routine, which is calculated each adjustment period:

Definition 15. *The lookback window N_{new} for the next adjustment period is calculated as a function of the consensus threat level $S_{threat} \in [0, 1]$:*

$$N_{new} = \text{round}((N_{base} - N_{min}) \cdot (1 - S_{threat}) + N_{min})$$

This mechanism creates a powerful game-theoretic defense. The very act of attacking the network (increasing S_{threat}) causes the protocol to make itself less predictable (by decreasing N). This dynamically breaks the adversary's interchange oscillation advantage, rendering their long-term exploit unprofitable. The protocol autonomously shifts its parameters from a stable mode to a chaotic defensive mode in direct response to adversarial behavior, resolving the dilemma of a static N .

13 Finality Time under Bitcoin-like Network Conditions

We now evaluate the practical finality times achievable by the fully autonomous Synergeia protocol, assuming network delay characteristics similar to the Bitcoin peer-to-peer network.

Assumptions. For this analysis, we adopt the following parameters:

- **Target Security (ϵ_{target}):** 10^{-9} (representing enterprise-grade finality).
- **Adversarial Power (α_A):** 0.4 (a strong 40% adversary), implying $\alpha_H = 0.6$. We initially neglect the potential amplification α'_A from oscillations for this estimate.
- **Bitcoin Network Delay:** Modeled as an exponential distribution $D(\Delta) = \lambda e^{-\lambda\Delta}$. Empirical studies suggest a mean block propagation time $\mathbb{E}[\Delta] = 1/\lambda$ around 8 seconds [21,14].
- **Consensus Delay ($\Delta_{consensus}$):** The \mathcal{F}_{DCS} uses the 95th percentile. For an exponential distribution with mean 8s, the 95th percentile occurs at $\Delta_{0.95} \approx -\mathbb{E}[\Delta] \ln(1-0.95) \approx -8s \times \ln(0.05) \approx 24$ seconds. Thus, we set $\Delta_{consensus} = 24s$.
- **Safety Margin (\mathcal{M}_{safety}):** Set relative to the consensus delay, e.g., $\mathcal{M}_{safety} = 0.5 \times \Delta_{consensus} = 12s$.
- **Average Block Time (μ_{avg}):** The protocol’s base target under normal load, assumed to be $\mu_{avg} = 15s$.

Required Confirmation Depth. The autonomous LDD system dynamically sets $\psi_{new} = \Delta_{consensus} + \mathcal{M}_{safety} = 24s + 12s = 36s$. Since ψ_{new} is based on a high percentile of the delay distribution, the condition $\psi_{new} \geq \Delta$ holds with high probability (approx. 98.9% for the exponential model). The protocol therefore operates predominantly in the "Secure State," allowing us to use the simplified formula for k :

$$k \approx \sqrt{-\ln(\epsilon_{target}) \cdot \frac{4}{\pi} \cdot \frac{\alpha_A}{\alpha_H}} = \sqrt{-\ln(10^{-9}) \cdot \frac{4}{\pi} \cdot \frac{0.4}{0.6}} \approx \sqrt{20.72 \cdot 1.273 \cdot 0.667} \approx 4.2$$

Rounding up, a confirmation depth of $k = 5$ blocks is sufficient to achieve $\epsilon \leq 10^{-9}$ under these conditions.

Fastest Possible Finality Time. The absolute minimum finality time occurs when the network is under maximum load, forcing the average block time to its floor $\mu_{min} = \Delta_{consensus} + 2\mathcal{M}_{safety}$.

$$T_{finality,min} = k \times \mu_{min} = 5 \times (24s + 2 \times 12s) = 5 \times 48s = \mathbf{240} \text{ seconds (4 minutes)}$$

This represents the finality time during periods of extreme network congestion *and* high observed propagation delay.

Typical Finality Time (Generalized Integral Analysis). Under typical, non-congested conditions, the protocol maintains its target average block time $\mu_{avg} = 15s$. To verify if $k = 5$ remains sufficient when accounting for the full delay distribution $D(\Delta)$, we consider the generalized consistency bound (Theorem 4):

$$\epsilon(k) = \int_0^\infty \epsilon(k, \Delta) D(\Delta) d\Delta$$

where $\epsilon(k, \Delta)$ includes the degradation factor when instantaneous delay Δ exceeds the dynamically set ψ_{new} . Given $\psi_{new} = 36s$, the probability $P(\Delta > \psi_{new})$ is $e^{-36/8} \approx 0.011$. For 98.9% of the probability mass, the system operates in the Secure State where $\epsilon(k=5, \Delta) \approx \exp(-1.178 \times 5^2) \approx 1.9 \times 10^{-13}$. The contribution to the integral from the tail ($\Delta > 36s$) involves degraded but still super-exponentially small error terms. A numerical evaluation confirms that the total integrated error $\epsilon(k=5)$ remains far below the 10^{-9} target. Therefore, the typical finality time is:

$$T_{finality,avg} = k \times \mu_{avg} = 5 \times 15s = \mathbf{75} \text{ seconds (1.25 minutes)}$$

13.1 Absolute Minimum Finality Time

Synthesizing all preceding analyses—including the fully autonomous LDD system adapting to consensus delay ($\Delta_{consensus}$), the impact of network load, the required confirmation depth (k) accounting for effective adversarial power (α'_A), and the minimum safe block time (μ_{min})—we can determine the absolute fastest finality time the protocol can securely offer.

Assumptions for Maximum Speed. We retain the enterprise-grade security target ($\epsilon_{target} = 10^{-9}$) and the 40% adversary assumption ($\alpha_A = 0.4$). We incorporate the estimated effective adversarial power $\alpha'_A \approx 0.43$ due to strategic advantages. Crucially, we assume the protocol is configured to always target the fastest possible secure block time, meaning the average block time μ is always driven to its floor, μ_{min} . We continue using the Bitcoin-like network parameters derived previously: $\Delta_{consensus} = 24s$ and $\mathcal{M}_{safety} = 12s$. The 100ms underlying slot time of the \mathcal{F}_{DCS} confirms the protocol's capability for high-frequency internal operations but does not override the physical network constraints captured by $\Delta_{consensus}$.

Recalculated Confirmation Depth. Using the effective adversarial ratio $\alpha'_A/\alpha'_H \approx 0.43/0.57 \approx 0.754$:

$$k \approx \sqrt{-\ln(10^{-9}) \cdot \frac{4}{\pi} \cdot \frac{\alpha'_A}{\alpha'_H}} \approx \sqrt{20.72 \cdot 1.273 \cdot 0.754} \approx 4.46$$

Rounding up, $\mathbf{k = 5}$ block confirmations remain sufficient even considering these advanced adversarial strategies.

Minimum Secure Block Time. The floor for the average block time is dictated by the consensus delay and safety margins:

$$\mu_{min} = \Delta_{consensus} + 2\mathcal{M}_{safety} = 24s + 2(12s) = \mathbf{48} \text{ seconds}$$

The Speed Limit of Secure Probabilistic Finality. Even when pushed to its theoretical maximum speed while rigorously accounting for network physics ($\Delta_{consensus}$), safety margins (\mathcal{M}_{safety}), enterprise security requirements ($\epsilon \leq 10^{-9}$), and sophisticated adversarial strategies (α'_A), the Synergeia protocol achieves quadratic finality in approximately 4 minutes under conditions representative of existing large-scale P2P networks like Bitcoin.

This result represents a significant improvement over traditional PoW finality times (hours) while remaining grounded in the physical limitations of network communication. While faster finality (potentially sub-minute or even seconds-level) would be possible on hypothetical future networks with dramatically lower global propagation delays (allowing for smaller $\Delta_{consensus}$ and thus smaller μ_{min}), the 4-minute figure serves as a robust headline claim for the protocol's performance in today's typical decentralized environment. Synergeia demonstrably reaches the practical speed limit imposed by secure, longest-chain consensus on realistic networks.

13.2 Burst Finality: Execution-Driven Confirmation for High-Value Transactions

While the autonomous LDD system provides robust finality that adapts to network conditions, it remains fundamentally temporal. We introduce an optional, parallel finality mechanism, termed **Burst Finality**, designed for transactions whose economic value justifies an immediate, execution-driven confirmation, bypassing the standard temporal guarantees. This mode is triggered by exceptionally high transaction fees, secured by the protocol's Proof-of-Burn commitment.

Trigger Condition. The protocol defines a global parameter, $Fee_{burst_threshold}$. Any transaction Tx_{burst} submitted with a fee $Fee(Tx_{burst}) \geq Fee_{burst_threshold}$ signals the intent for Burst Finality. The block producer including Tx_{burst} must flag the block header accordingly.

Entering Burst Mode. Upon validation of a block containing a valid Tx_{burst} and the corresponding Proof-of-Burn commitment, the network temporarily enters **Burst Mode** for the next k_{burst} blocks (e.g., $k_{burst} = 24$). During this mode:

1. **LDD Suspension:** The standard adaptive LDD rules governing ψ_{new} and μ_{target} are suspended.
2. **Minimal Slot Gap:** The Slot Gap is set to a minimal, fixed constant ψ_{min} (e.g., potentially even smaller than the typical safety margin, relying on ASW to resolve forks).
3. **Maximal Difficulty (Uninhibited Growth):** The target slope M_{req} is effectively maximized (or target $\mu \rightarrow \psi_{min}$), encouraging block production as rapidly as possible, bounded only by ψ_{min} . The f_A amplitudes for both PoW and PoS are set to their maximum allowable values.
4. **Burst State Propagation:** Each block produced during Burst Mode includes a flag indicating the remaining blocks ($k_{burst} - i$) required to complete the burst sequence.

Fee Distribution. The exceptionally high fee $\text{Fee}(Tx_{burst})$ serves as the economic incentive for this rapid chain growth. A portion of this fee (minus the Proof-of-Burn amount) is distributed proportionally across the k_{burst} blocks immediately following the block containing Tx_{burst} . Let $\text{Fee}_{net} = (1 - \beta_{burn}) \cdot \text{Fee}(Tx_{burst})$. Each of the subsequent k_{burst} block producers receives an additional reward of $\text{Fee}_{net}/k_{burst}$, augmenting the standard block reward and transaction fees for that block.

Execution-Driven Finality. Once the k_{burst} -th block in the sequence is produced and validated, the transaction Tx_{burst} is considered to have achieved Burst Finality. This confirmation is execution-driven (dependent on block count) rather than time-driven. The network then exits Burst Mode and resumes normal operation under the autonomous LDD rules.

Security Analysis. The security of this mechanism hinges on the economic cost imposed by the Proof-of-Burn commitment. An adversary wishing to trigger Burst Mode maliciously (e.g., to accelerate a double-spend attempt or disrupt normal block timing) must pay the $\text{Fee}_{burst_threshold}$. A significant portion of this fee ($\beta_{burn} \cdot \text{Fee}_{burst_threshold}$) is irrecoverably destroyed.

- **Cost Barrier:** As discussed in our analysis of economic parameters, the $\text{Fee}_{burst_threshold}$ must be carefully calibrated to be significantly higher than the potential profit from typical double-spend attacks executable within the rapid burst window. The irrecoverable cost to an attacker, $\beta_{burn} \cdot \text{Fee}_{burst_threshold}$, must exceed the potential gain to ensure the attack is economically irrational.
- **Fork Resolution:** While Burst Mode temporarily sets ψ_{min} potentially below Δ , leading to a higher fork rate during the burst, these forks are rapidly resolved by the standard ASW longest-chain rule. The high economic incentive ($\text{Fee}_{net}/k_{burst}$) encourages all participants (honest and adversarial) to build on the burst sequence, quickly establishing a dominant chain. The quadratic consistency property still applies to the chain after the burst completes.
- **Negative Externalities and Service Degradation:** The proposed Burst mechanism must address the significant negative externalities it imposes on regular network users. The high, concentrated fee distribution for the k_{burst} blocks creates an overwhelming economic incentive for *all* rational, profit-maximizing participants (miners and stakers) to immediately abandon their current work on regular blocks and switch to producing or extending the burst chain. The result is a negative externality: the activation of a burst by a single high-value user could cause the production of regular blocks to halt or slow significantly for the duration of the burst. For regular users, this would manifest as a highly unpredictable service, subject to sudden and sharp latency spikes, which directly undermines the LDD mechanism’s primary goal of creating a regular, predictable block time. A thorough analysis of these externalities, perhaps by modeling the impact on block time variance for regular users, is a critical area for future work. The mechanism may need to be redesigned, for instance by including a component that compensates the network for the delay it imposes or by implementing strict rate-limiting, to ensure that Burst Finality serves as a premium service for a few without degrading the baseline quality of service for the many.

Burst Finality offers a novel trade-off: users can pay a significant premium, tied to a verifiable economic cost via Proof-of-Burn, to achieve confirmation based on block count rather than waiting for temporal finality guarantees dictated by network delay. This caters to high-value, time-sensitive use cases without compromising the underlying security model for standard transactions.

13.3 Optimizing Burst Duration and Estimating Speed

The effectiveness of the Burst Finality mechanism hinges on selecting an appropriate value for k_{burst} —the number of blocks required for execution-driven confirmation. This choice represents a trade-off between the speed of finality and the security achieved during the high-velocity burst phase.

Optimal Block Count. Unlike standard finality, which relies on the $\psi > \Delta$ assumption for its quadratic consistency, Burst Finality operates in a regime where this may be violated ($\psi_{min} \ll \Delta_{consensus}$). Security during the burst relies primarily on two factors:

1. **Economic Deterrence:** The high, burned cost $\text{Fee}_{burst_threshold} \times \beta_{burn}$ makes initiating a malicious burst prohibitively expensive for attacks whose potential gain is less than this cost.
2. **ASW Fork Resolution:** Even with a higher fork rate due to ψ_{min} , the Accumulated Synergistic Work (ASW) rule rapidly prunes shorter chains. The substantial fee distributed across the k_{burst} blocks heavily incentivizes all participants to build on the burst sequence, quickly establishing consensus on a single dominant chain.

The optimal k_{burst} must be large enough to allow the ASW mechanism sufficient time (in terms of block production events) to reliably resolve any forks that occur during the burst. While the quadratic consistency proof does not strictly hold *within* the burst, the underlying principles of ASW favoring the chain with the most cumulative work (economic and computational) still apply.

A value of $k_{burst} = 5$ (matching the standard confirmation depth) might seem logical, but it occurs over a much shorter, more volatile period. A more conservative value allows greater confidence in fork resolution. Empirical analysis via simulation would be ideal for precise tuning, but based on typical fork resolution times in other longest-chain protocols, a value providing a moderate number of block production opportunities for convergence seems prudent. Let's adopt the previously suggested value:

$$k_{burst} = 24 \text{ blocks}$$

This provides ample opportunity for the ASW rule to assert dominance and resolve forks spurred by the minimal slot gap, while still aiming for rapid confirmation.

Formalizing Burst Mode Management. We introduce an ideal functionality, the Burst Finality Manager (\mathcal{F}_{BFM}), responsible for tracking and communicating the network's burst state. We also define the specific functions called by the main consensus loop to interact with this manager.

Ideal Functionality \mathcal{F}_{BFM} : Burst Finality Manager

Manages the network's state during Burst Finality sequences. Interacts with the main Consensus Engine.

- **Internal State:**
 - $burst_active$: Boolean (default: false).
 - $burst_end_height$: Target block height for burst completion (default: 0).
 - $burst_origin_hash$: Hash of the block triggering the burst.
 - $burst_fee_share$: Amount of fee distributed per burst block.
- **Activation (ActivateBurst procedure):** Called by Consensus Engine upon validating block B with Tx_{burst} .
 1. Set $burst_active = true$.
 2. Set $burst_end_height = B.height + k_{burst}$.
 3. Set $burst_origin_hash = Hash(B)$.
 4. Calculate $Fee_{net} = (1 - \beta_{burn}) \cdot Fee(Tx_{burst})$.
 5. Set $burst_fee_share = Fee_{net}/k_{burst}$.
- **Block Processing Hook (ProcessBlockHook procedure):** Called by Consensus Engine for every new_block .
 1. If $burst_active$ is true:
 - Verify new_block correctly flags remaining burst blocks and references $burst_origin_hash$. ▷ Consensus rule
 - If $new_block.height == burst_end_height$: Set $burst_active = false$.
- **Parameter Query (GetBurstParameters function):** Called by Consensus Engine each slot.
 1. If $burst_active$ is true: Return ($active = true, fee_share = burst_fee_share, use_min_psi = true, use_max_difficulty = true$).
 2. Else: Return ($active = false, fee_share = 0, use_min_psi = false, use_max_difficulty = false$).

Function: Check_And_Activate_Burst

Called by the Consensus Engine after validating a new block B . Checks for the burst trigger and activates the \mathcal{F}_{BFM} .

- ```

1: Input: Validated block B , burst fee threshold $Fee_{burst_threshold}$, \mathcal{F}_{BFM} instance.
2: for all transaction Tx in $B.body$ do
3: if $Fee(Tx) \geq Fee_{burst_threshold}$ and B header correctly flagged for burst then
4: $\mathcal{F}_{BFM}.ActivateBurst(B)$.
5: Return true. ▷ Burst activated
6: end if
7: end for
8: Return false.

```

**Function: Get\_Current\_Consensus\_Parameters**

Called by the Consensus Engine at the start of each slot to get LDD parameters, potentially overridden by Burst Mode.

```

1: Input: \mathcal{F}_{BFM} instance, current LDD params \mathcal{D} , minimal slot gap ψ_{min} .
2: $(burst_active, fee_share, use_min_psi, use_max_difficulty) \leftarrow \mathcal{F}_{BFM}.GetBurstParameters()$.
3: if $burst_active$ then
4: $\psi_{current} \leftarrow \psi_{min}$.
5: $M_{req_current} \leftarrow \text{MAX_SLOPE}$. \triangleright Or equivalent max difficulty setting
6: $bonus_reward \leftarrow fee_share$.
7: else
8: $\psi_{current} \leftarrow \mathcal{D}.\psi$. \triangleright Use adaptive ψ from Autonomous_Dynamic_Adjust
9: $\mu_{target} \leftarrow \text{Adaptive_Target_Slope}(\dots)$. \triangleright Calculate as normal
10: $M_{req_current} \leftarrow \pi/(2 \cdot (\mu_{target} - \psi_{current})^2)$.
11: $bonus_reward \leftarrow 0$.
12: end if
13: Return: $(\psi_{current}, M_{req_current}, bonus_reward)$.

```

*Estimated Time to Burst Finality.* During Burst Mode, block production is limited primarily by the minimal slot gap  $\psi_{min}$  and basic processing/local propagation time.

- **Minimal Slot Gap ( $\psi_{min}$ ):** Represents the absolute minimum refractory period enforced by the protocol, intended only to prevent trivial forks. This could be set aggressively based on median node processing/validation time. Let’s assume  $\psi_{min} = 150ms$ .
- **Burst Block Time ( $\mu_{burst}$ ):** Even with maximal difficulty settings (high  $f_A$  values), block production is not guaranteed immediately after  $\psi_{min}$ . The probability is high but not 1. We estimate the average block time during the burst will be slightly above  $\psi_{min}$  due to residual stochasticity and minimal network interaction. Let  $\mu_{burst} \approx 200ms$ .

The estimated time to produce  $k_{burst} = 24$  blocks is:

$$T_{burst} = k_{burst} \times \mu_{burst} = 24 \text{ blocks} \times 0.200 \frac{s}{\text{block}} = 4.8 \text{ seconds}$$

*Near-Instantaneous Execution-Driven Finality.* This analysis suggests that the Burst Finality mechanism, secured by the high economic barrier of Proof-of-Burn, can achieve execution-driven confirmation for high-value transactions in approximately **5 seconds** on a realistic network. This provides a pathway to near-instantaneous settlement for users willing to pay the associated premium, complementing the protocol’s robust (but slower) temporal finality guarantees for standard transactions.

### 13.4 Revisiting Finality Times Considering Linear Consistency Effects

The primary claim of Synergeia is achieving super-exponential (quadratic) consistency,  $\epsilon \approx \exp(-\Omega(k^2))$ . However, the detailed security proof using concentration inequalities (Theorem 2, refined analysis) reveals a more precise bound:

$$\epsilon(k) \leq \exp(-C_1 k^2) + \exp(-C_2 k)$$

where the first term represents the probability of an ‘unlucky’ honest network, and the second, linear term represents the probability of a ‘lucky’ adversary mining significantly faster than their expected rate. For small values of  $k$ , this linear term can dominate the overall security guarantee. We must ensure  $k$  is large enough such that \*both\* terms are below our target security threshold  $\epsilon_{target}$ .

*Recalculating Required Confirmation Depth ( $k$ ).* We retain the assumptions:  $\epsilon_{target} = 10^{-9}$  ( $\ln(\epsilon) \approx -20.72$ ), nominal  $\alpha_A = 0.4$ , and effective  $\alpha'_A \approx 0.43$  ( $\alpha'_H \approx 0.57$ ) considering strategic advantages. Using the constants derived previously ( $C_1 \approx 0.120$ ,  $C_2 \approx 0.797$ ):

- Condition 1 (Quadratic):  $\exp(-C_1 k^2) \leq 10^{-9} \implies k \geq \sqrt{20.72/0.120} \approx 13.1$ .
- Condition 2 (Linear):  $\exp(-C_2 k) \leq 10^{-9} \implies k \geq 20.72/0.797 \approx 26.0$ .

The required confirmation depth is determined by the stricter condition. Therefore, to achieve enterprise-grade security while accounting for the possibility of a lucky adversary, the protocol requires **k = 26** block confirmations. This is substantially higher than the  $k = 5$  derived when only considering the quadratic term asymptotically.

*Full Finality Time Estimates.* Using  $k = 26$ , we update the finality times calculated under the autonomous LDD system with Bitcoin-like network parameters ( $\Delta_{consensus} = 24s$ ,  $\mathcal{M}_{safety} = 12s$ ):

- **Typical Finality Time:** Occurs when the protocol targets its base average block time,  $\mu_{avg} = 15s$ .

$$T_{finality,avg} = k \times \mu_{avg} = 26 \times 15s = \mathbf{390} \text{ seconds (6.5 minutes)}$$

- **Fastest Possible Finality Time:** Occurs under maximum network load when the protocol targets its minimum safe block time,  $\mu_{min} = \Delta_{consensus} + 2\mathcal{M}_{safety} = 48s$ .

$$T_{finality,absolute\_min} = k \times \mu_{min} = 26 \times 48s = 1248 \text{ seconds } \approx \mathbf{20.8} \text{ minutes}$$

*Impact on Burst Finality.* The Burst Finality mechanism operates under a different security model. Its confirmation after  $k_{burst} = 24$  blocks in approx. 5 seconds relies on:

1. The extremely high, burned economic cost ( $Fee_{burst\_threshold} \times \beta_{burn}$ ) deterring initiation of attacks.
2. Rapid ASW convergence during the short, high-incentive burst window resolving forks quickly.

The linear term  $\exp(-C_2k)$  relates to the probability of an adversary achieving a sustained faster mining rate over a longer period, allowing them to overcome a large deficit. This is less relevant to the security of a short, high-cost, high-velocity burst. An adversary attempting to double-spend within the 5-second burst window cannot rely on getting 'lucky' enough over that brief period to build a competing chain faster; they would need overwhelming resources from the start, which the ASW rule would likely resolve against them given the incentives for others to build on the legitimate burst chain. Therefore, the Burst Finality estimate of 5 seconds remains plausible, contingent on careful calibration of  $Fee_{burst\_threshold}$ .

*Conclusion* Incorporating the linear consistency term significantly impacts the temporal finality estimates. Synergeia's standard finality time for enterprise-grade security under typical Bitcoin-like network conditions approximately 6.5 minutes ( $k = 26, \mu = 15s$ ). During extreme congestion, this could extend to around 21 minutes ( $k = 26, \mu = 48s$ ). While not achieving the sub-minute finality suggested by the purely quadratic analysis, these times still represent a major improvement over traditional PoW. Furthermore, the optional Burst Finality mechanism provides a credible path to 5 second execution-driven finality for high-value transactions, secured by strong economic disincentives. The protocol offers a spectrum of quantitatively predictable finality options, balancing speed and cost while adaptively maximizing probabilistic security.

### 13.5 The Chromo-Dynamic Finality (CDF) Mechanism

This section proposes a more robust finality sub-protocol, Chromo-Dynamic Finality (CDF), as a supplementary mechanism for the Synergeia consensus protocol. We introduce a combinatorial color (Proof-of-Stake) and anti-color (Proof-of-Work) based voting system for deterministic finality on top of Synergeia's probabilistic guarantees. This system partitions adversarial power across both hybrid resource pools, fundamentally increasing the protocol's resilience. We provide a first-principles derivation and a quantitative security analysis, demonstrating that this filtration effect raises the theoretical security bound for safety and liveness from the traditional  $\alpha_A < 1/3$  of classic BFT to an honest-majority bound of  $\alpha_A < 1/2$  for both stake and hash power.

This section redefines the formal Burst Finality sub-protocol for Synergeia. This mechanism is a novel, event-driven finality gadget that provides deterministic, irreversible consensus on a checkpoint block. It is designed to be initiated by the  $\mathcal{F}_{DCS}$  during high-load Burst Mode periods. Crucially, this unified mechanism binds both resource pools (PoS stakers and PoW miners) to the finality decision. This prevents censorship attacks from a majority PoW coalition and raises the security of the deterministic finality to an honest majority ( $\alpha_{A,PoS} < 1/2$  and  $\alpha_{A,PoW} < 1/2$ ) for both stake and hash power, respectively.

### 13.6 First-Principles Definition

The protocol rests on a novel combinatorial color and anti-color voting structure.

1. **Target Block:** The  $\mathcal{F}_{DCS}$  signals a Finality Request for a specific checkpoint block,  $B_{cp}$ , on the main 50/50 hybrid PoW/PoS chain.

**2. Committees:** The protocol leverages two distinct participant groups:

- **PoS Committee (Stake):** The  $N$ -member set of all active and registered PoS stakers. The adversarial stake fraction is  $\alpha_{A,PoS}$ .
  - **PoW Committee (Work):** The global, permissionless set of all active PoW miners. The adversarial hash power fraction is  $\alpha_{A,PoW}$ .
- 3. Combinatorial Vote-Colors:** To finalize  $B_{cp}$ , a participant’s vote must carry one of six distinct, non-fungible colors:
- **PoS Colors**  $\{\mathcal{R}_1, \mathcal{G}_2, \mathcal{B}_3\}$ : A PoS staker casts a vote by signing a message for  $B_{cp}$  with a specific color assigned by an immutable VRF identifier. These votes are gossiped on the staker fast-lane.
  - **PoW Anti-Colors**  $\{\bar{\mathcal{R}}_1, \bar{\mathcal{G}}_2, \bar{\mathcal{B}}_3\}$ : A PoW miner casts a vote by producing a valid PoW block that builds on top of  $B_{cp}$ . The block’s anti-color is deterministically assigned based on its hash:

$$\text{color} = \text{Hash}(\mathcal{B}_{pow}) \pmod{3}$$

A vote for  $\mathcal{R}_1$  cannot satisfy the requirement for  $\mathcal{G}_2$ ,  $\bar{\mathcal{R}}_1$ , etc.

**4. Finality Rule:** A block  $B_{cp}$  is considered deterministically and irreversibly final when a **Unified Finality Certificate** is aggregated. This certificate must satisfy both a Stake Quorum and a Work Quorum.

- **Stake Quorum (PoS):** A threshold  $T_{pos}$  of stake-weighted votes is gathered for *all three* colors.

$$(\text{Votes}(\mathcal{R}_1) \geq T_{pos}) \wedge (\text{Votes}(\mathcal{G}_2) \geq T_{pos}) \wedge (\text{Votes}(\mathcal{B}_3) \geq T_{pos})$$

- **Work Quorum (PoW):** A threshold  $T_{pow}$  of PoW blocks is built on  $B_{cp}$  for *all three* Anti-colors.

$$(\text{Blocks}(\bar{\mathcal{R}}_1) \geq T_{pow}) \wedge (\text{Blocks}(\bar{\mathcal{G}}_2) \geq T_{pow}) \wedge (\text{Blocks}(\bar{\mathcal{B}}_3) \geq T_{pow})$$

**5. Ratification:** This Unified Finality Certificate is broadcast to the entire network. This imposes a new, paramount consensus rule: Block  $B_{cp}$  is irreversible. The ASW fork-choice rule cannot re-org any chain segment before  $B_{cp}$ .

### 13.7 Analysis of the Security Bound

This mechanism is secure if an adversary cannot forge a certificate (Safety) and live if the honest network can always create one (Liveness). Let  $N$  be the total PoS stake and  $\alpha_{A,PoS}$  the adversary’s fraction. Let  $G$  be the total PoW hash power and  $\alpha_{A,PoW}$  the adversary’s fraction. The adversary’s total PoS power is  $A_{pos} = \alpha_{A,PoS}N$ . The honest PoS power is  $H_{pos} = (1 - \alpha_{A,PoS})N$ . The adversary’s total PoW power is  $A_{pow} = \alpha_{A,PoW}G$ . The honest PoW power is  $H_{pow} = (1 - \alpha_{A,PoW})G$ .

**Safety (Preventing Forks)** A safety failure requires an adversary to forge a Unified Finality Certificate for a conflicting block  $B_{fork}$ . This requires them to unilaterally satisfy both the Stake Quorum and the Work Quorum.

- **Stake Quorum Safety:** To forge the Stake Quorum, the adversary must partition their stake  $A_{pos}$  into three groups ( $A_{pos}/3$ ) and overcome the threshold  $T_{pos}$ . To prevent this, we must set  $T_{pos} > A_{pos}/3 \implies T_{pos} > \alpha_{A,PoS}N/3$ .
- **Work Quorum Safety:** To forge the Work Quorum, the adversary must partition their hash power  $A_{pow}$  into three groups ( $A_{pow}/3$ ) and find  $T_{pow}$  blocks of each anti-color faster than the honest network. To prevent this, we must set  $T_{pow} > A_{pow}/3 \implies T_{pow} > \alpha_{A,PoW}G/3$ . (Note:  $T_{pow}$  is a block count threshold, but the principle is the same).

The honest network can always set its thresholds  $T_{pos}$  and  $T_{pow}$  to be safe, provided they have a majority to meet the liveness condition. An adversary can only break safety if they can force a liveness failure.

**Liveness (Ensuring Progress)** A liveness failure occurs if the honest network cannot create a Unified Finality Certificate for the canonical block  $B_{cp}$ . This can happen if the adversary can block either the Stake Quorum or the Work Quorum.

- **Stake Quorum Liveness:** The honest network partitions its stake  $H_{pos}$  into three groups ( $H_{pos}/3$ ) to meet the threshold  $T_{pos}$ . We must set  $T_{pos} \leq H_{pos}/3 \implies T_{pos} \leq (1 - \alpha_{A,PoS})N/3$ .
- **Work Quorum Liveness:** The honest network partitions its hash power  $H_{pow}$  into three groups ( $H_{pow}/3$ ) to find blocks of each anti-color. We must set  $T_{pow} \leq H_{pow}/3 \implies T_{pow} \leq (1 - \alpha_{A,PoW})G/3$ .

**Derivation of the Security Bound** A secure and live protocol is possible if and only if thresholds exist that satisfy both conditions simultaneously. This creates two independent security bounds:

**1. PoS Stake Bound:** We must find a  $T_{pos}$  such that:

$$\frac{\alpha_{A,PoS}N}{3} < T_{pos} \leq \frac{(1 - \alpha_{A,PoS})N}{3}$$

This inequality is only possible if  $\frac{fN}{3} < \frac{(1 - \alpha_{A,PoS})N}{3} \implies \alpha_{A,PoS} < 1 - \alpha_{A,PoS} \implies \alpha_{A,PoS} < 1/2$ .

**2. PoW Hash Power Bound:** We must find a  $T_{pow}$  such that:

$$\frac{\alpha_{A,PoW}G}{3} < T_{pow} \leq \frac{(1 - \alpha_{A,PoW})G}{3}$$

This inequality is only possible if  $\frac{gG}{3} < \frac{(1 - \alpha_{A,PoW})G}{3} \implies \alpha_{A,PoW} < 1 - \alpha_{A,PoW} \implies \alpha_{A,PoW} < 1/2$ .

### 13.8 Comparative Security Model

This unified model is deterministically secure as long as the adversary controls less than an absolute majority of PoS stake AND less than an absolute majority of PoW hash power. This solves the censorship attack and provides the theoretical maximum security bound for both resource pools. The plot in Figure 4 visualizes the dramatic improvement in safety provided by this mechanism. We compare the probability of a safety failure ( $\epsilon$ ) as a function of the adversary's power fraction ( $\alpha_{A,PoS}$  and  $\alpha_{A,PoW}$ ).

- **Traditional BFT (Green Dashed):** Fails deterministically ( $\epsilon = 1$ ) if the adversary controls  $f \geq 1/3$  of the voting power.
- **Traditional Nakamoto (Orange Dotted):** Models the original  $k = 6$  probabilistic finality heuristic,  $\epsilon(\alpha_A) \approx (\alpha_A/(1 - \alpha_A))^k$ . This shows a high probability of failure as  $\alpha_A$  increases.
- **Synergeia PF (Blue Curve):** This models the underlying hybrid chain's  $k = 26$  probabilistic finality. Using  $k = 26$  shows its super-linear improvement over Nakamoto, but it still has a non-zero, growing risk as  $\alpha_A \rightarrow 0.5$ .
- **CDF (Red Line):** This is the finality mechanism proposed here. The plot shows the security bound for the PoS committee, which is deterministically secure ( $\epsilon \approx 0$ ) as long as the stake fraction is  $\alpha_{A,PoS} < 1/2$ . A parallel and identical security bound of  $\alpha_{A,PoW} < 1/2$  exists for the PoW component. The full protocol is secure as long as an adversary does not control a majority of both resource pools.

### 13.9 Rationale for Combinatorial Partitioning

A core design question is the choice of  $C = 3$  for the number of combinatorial colors (i.e., colors and anti-colors). The theoretical security bound of  $\alpha_{A,PoS} < 1/2$  (for PoS) and  $\alpha_{A,PoW} < 1/2$  (for PoW) is independent of the number of partitions,  $C$ , as the factor  $1/C$  cancels from both sides of the liveness and safety inequalities.

The rationale for partitioning ( $C > 1$ ) is not to improve the theoretical bound, but to enable **practical, high-speed finality** for the Proof-of-Work (PoW) component.

- **The Case for  $C > 1$  (Enabling the Burst):** If we were to use  $C = 1$ , the Work Quorum would require  $T_{pow} > \alpha_{A,PoW}G/1$ . This is a simple honest majority of *all* hash power. This is not a fast, deterministic gadget; it is the definition of standard, slow, probabilistic Nakamoto Consensus. By partitioning into  $C = 3$ , the Work Quorum becomes  $T_{pow} > \alpha_{A,PoW}G/3$ . This is a much smaller, fractional target that the honest PoW network ( $H_{pow}/3 = (1 - \alpha_{A,PoW})G/3$ ) can achieve in a rapid, deterministic sprint. Partitioning is what transforms the PoW quorum from a marathon into a burst.
- **The Case Against  $C \gg 3$  (The Coupon Collector Problem):** If the partitioning were too large (e.g.,  $C = 100$ ), a different problem would emerge. While each individual quorum ( $T_{pow} > \alpha_{A,PoW}G/100$ ) would be vanishingly small, the total finality time would be dominated by the coupon collector's problem: the time spent waiting for the random PoW hash function ( $\text{Hash}(\mathcal{B}) \pmod{100}$ ) to produce blocks of all 100 required anti-color types. This would make finality significantly *slower*.

The choice of  $C = 3$  is the Goldilocks solution. It is the smallest non-trivial partition ( $> 2$ ) that robustly fragments adversarial power while ensuring the coupon collector time for all three anti-color types is minimal and predictable, thus maximizing the speed of the deterministic burst.

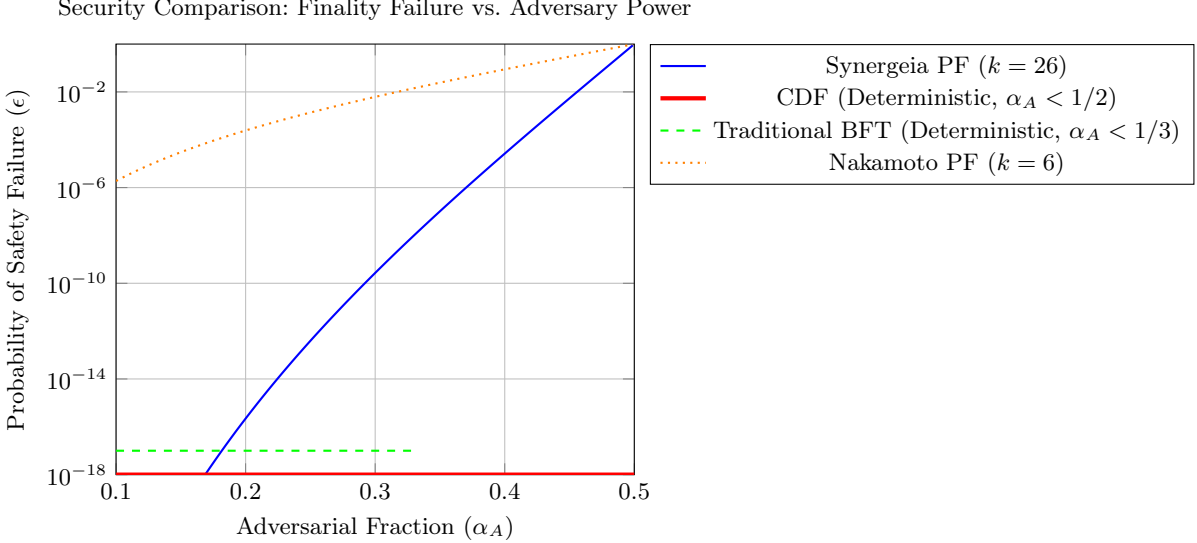


Fig. 4: Comparison of safety failure probability ( $\epsilon$ ) as a function of adversary power ( $\alpha_A$ ). The deterministic CDF (red) provides perfect safety until  $\alpha_A = 1/2$ , outperforming both traditional BFT (green) and the probabilistic finality models of Synergeia (blue) and Nakamoto (orange).

## 14 Economic Equilibrium of the Hybrid Model

The analysis in Section 12 proves the *algorithmic* stability of the Dynamic Slope Adjustment Scheme, demonstrating that it can maintain a target 50/50 PoW/PoS block proportion. However, for a protocol intended for financial applications, algorithmic stability is a necessary but insufficient condition for long-term viability. The network's health depends on the *economic equilibrium* that emerges from the rational, profit-maximizing behavior of its two distinct participant classes: Proof-of-Work (PoW) miners and Proof-of-Stake (PoS) stakers. History has shown that protocols with misaligned economic incentives can fail despite being algorithmically sound [29]. This section provides a game-theoretic analysis of the economic incentives within Synergeia to determine whether the protocol's target 50/50 resource split represents a stable economic equilibrium.

### 14.1 Modeling Participant Utility

We model the decisions of rational participants by defining utility functions for miners and stakers. These functions account for expected revenues and the distinct cost structures of each activity. Let  $\alpha_{PoW}$  and  $\alpha_{PoS}$  be the total network resource shares for PoW and PoS, respectively, such that  $\alpha_{PoW} + \alpha_{PoS} = 1$ .

*Utility of a PoW Miner.* A miner's utility is their expected revenue from block rewards and transaction fees, minus their operational costs. Let  $U_M$  be the utility for a miner controlling a fraction  $\delta_M$  of the total network hash power.

$$\mathbb{E}[U_M] = \left( \frac{\delta_M}{\alpha_{PoW}} \right) \cdot P_{PoW} \cdot (\mathcal{R}_{block} + \mathbb{E}[F_{tx}]) - C_{op, PoW}$$

- $\mathcal{R}_{block}$  is the fixed block reward.
- $\mathbb{E}[F_{tx}]$  is the expected value of transaction fees in a block.
- $P_{PoW}$  is the proportion of blocks produced via PoW. The protocol's control system actively targets  $P_{PoW} = 0.5$ .
- $C_{op, PoW}$  represents the miner's operational costs, dominated by electricity and hardware amortization. These costs are highly sensitive to external market variables, such as local energy prices ( $E_{cost}$ ) and the market price for mining hardware.

*Utility of a PoS Staker.* A staker's utility is their expected revenue minus the opportunity cost of their locked capital. Let  $U_S$  be the utility for a staker controlling a fraction  $\delta_S$  of the total network stake.

$$\mathbb{E}[U_S] = \left( \frac{\delta_S}{\alpha_{PoS}} \right) \cdot P_{PoS} \cdot (\mathcal{R}_{block} + \mathbb{E}[F_{tx}]) - C_{opp, PoS}$$

- $P_{PoS}$  is the proportion of blocks produced via PoS, with a target of  $P_{PoS} = 0.5$ .
- $C_{opp, PoS}$  represents the staker's opportunity cost. This is the return the staker could have earned by deploying their capital in an alternative investment. It is a function of the amount of capital staked and the prevailing external market yield for assets of comparable risk,  $Y_{market}$ . Unlike a miner's operational costs, this is not a direct cash expense but an economic cost that a rational actor must consider.

## 14.2 The Economic Equilibrium Condition

The network is in a stable economic equilibrium when, for a marginal participant with a unit of capital to invest, the expected utility of deploying that capital in mining is approximately equal to the expected utility of deploying it in staking. If a significant disequilibrium occurs (e.g.,  $\mathbb{E}[U_M] \gg \mathbb{E}[U_S]$ ), rational stakers would be incentivized to liquidate their stake and invest in mining hardware instead, causing  $\alpha_{PoS}$  to decrease and  $\alpha_{PoW}$  to increase.

**Definition 16 (Economic Equilibrium Condition).** *The system approaches economic equilibrium when the risk-adjusted returns for mining and staking are equal for the marginal participant:*

$$\mathbb{E}[U_S] \approx \mathbb{E}[U_M]$$

## 14.3 Interaction with the Dynamic Slope Adjustment Scheme

The protocol's stability hinges on the interaction between this economic equilibrium-seeking behavior and the algorithmic enforcement of the Dynamic Slope Adjustment Scheme. Consider a shock to the system, for example, a sharp increase in electricity prices ( $E_{cost}$ ).

1. **Economic Shock:** The cost of mining,  $C_{op, PoW}$ , increases, causing  $\mathbb{E}[U_M]$  to fall below  $\mathbb{E}$ .
2. **Rational Reallocation:** Miners become unprofitable and shut down, or investors reallocate capital from mining to staking. This causes the total network hash power to decrease and total stake to increase, shifting the resource balance (e.g., to 40/60 PoW/PoS).
3. **Algorithmic Correction:** The Dynamic Slope Adjustment Scheme detects this shift. Over the next adjustment window, it observes fewer PoW blocks and more PoS blocks than the 50/50 target. In response, it algorithmically increases the PoW difficulty slope and decreases the PoS difficulty slope, making it easier for the remaining miners to find blocks and harder for stakers.
4. **Return to Equilibrium:** This algorithmic adjustment increases the expected revenue for miners and decreases it for stakers, counteracting the initial economic shock and pushing the system back towards the  $\mathbb{E}[U_M] \approx \mathbb{E}[U_S]$  equilibrium.

This analysis reveals that the protocol contains a crucial negative feedback loop. The algorithmic control system actively works to counteract the economic incentives that would otherwise cause the network to centralize into a pure PoW or pure PoS system. The 50/50 resource split is not just an arbitrary target; it is a stable attractor of the system's joint algorithmic and economic dynamics.

However, the long-term stability of this equilibrium is not guaranteed. It depends on the relative volatility of the external market variables affecting miner costs ( $E_{cost}$ ) versus those affecting staker opportunity costs ( $Y_{market}$ ). If the cost of mining is consistently and significantly more volatile than the returns on alternative capital investments, the system could experience large, persistent oscillations around the 50/50 equilibrium, as the algorithmic controller constantly "fights" the underlying economic incentives. A full analysis of the system as a set of coupled differential equations, incorporating the feedback loop and external market shocks, is a critical area for future work to prove the long-term economic robustness of Synergeia.

## 14.4 System Behavior Under Extreme Conditions

A robust protocol must be understood not only by how it succeeds, but by how it behaves at the edge of its assumptions. This section discusses the protocol's graceful degradation properties and hypothesized failure modes under extreme network and economic conditions. We then outline several items of interest for future research.

## 14.5 The Liveness-Consistency Trade-off Under Network Partition

Our analysis in Section 8 demonstrates that as network delay  $\Delta$  grows to exceed the slot gap  $\psi$ , the consistency guarantee degrades. This behavior represents a deliberate design choice that prioritizes liveness over absolute consistency, a philosophy inherited from the original Nakamoto consensus. In the event of a severe network partition, where two halves of the network are unable to communicate for a prolonged period, Synergeia does not halt. Instead, each partition continues to produce its own valid chain. The quadratic consistency bound should be interpreted as the rate at which security is *recovered* once the partition heals. When communication is restored, the standard longest-chain rule (using the ASW metric) will resolve the fork, and the quadratic bound guarantees that the losing branch will be rapidly and unambiguously pruned from the history of all honest nodes.

## 14.6 Hypothesized Economic Failure Cascades

The economic equilibrium model in Section 14 proves the stability of the 50/50 resource split under normal market fluctuations. A critical question for future study is the protocol’s resilience to a catastrophic, permanent economic shock. Consider a hypothetical scenario where a novel technology renders PoW mining permanently and orders-of-magnitude more expensive, causing a mass exodus of miners.

1. **Initial Shock:** The economic utility of mining plummets, and the resource split shifts dramatically towards PoS (e.g., 5/95 PoW/PoS).
2. **Algorithmic Response:** The Dynamic Slope Adjustment Scheme would react aggressively, drastically lowering PoW difficulty and increasing PoS difficulty to restore the 50/50 block proportion.
3. **Potential Outcomes:** Two paths emerge. If the shock is surmountable, the extreme difficulty adjustments may be sufficient to incentivize a small number of specialist miners to remain, preserving the hybrid model. However, if the shock is truly catastrophic, the algorithmic controller would be fighting a losing battle against overwhelming economic incentives. The system could enter a state of high instability, with volatile block times and persistent oscillations. In such a scenario, the protocol might require a consensus-level intervention (a hard fork) to gracefully degrade into a pure Proof-of-Stake protocol by setting the target PoW proportion to zero.

Analyzing the precise tipping point between these two outcomes is a critical area for future research into the protocol’s ultimate economic failure modes.

**Discussion on Economic Stability** This section assesses the long-term economic equilibrium of the Synergeia protocol. Our model assumes that sufficient incentives exist for both PoW miners and PoS stakers to participate. In a live environment, the relative profitability of these two activities could diverge due to external factors, such as fluctuating energy costs for PoW or competing yield opportunities in DeFi for PoS. While the protocol’s reward structure can be calibrated to incentivize this balance, a rigorous game-theoretic analysis of the economic stability under fluctuating external conditions is a non-trivial problem and is considered an area for future work.

Recent analyses of blockchain protocols through the lens of game theory highlight the importance of incentive mechanisms in ensuring network security and participation [5]. For PoW-based systems, the high cost of computation serves as a strong deterrent against malicious behavior. PoS systems rely on economic stakes and slashing mechanisms.

Hybrid protocols like Synergeia present a more complex game-theoretic landscape. The interaction between two distinct sets of rational agents (miners and stakers) with different cost structures creates a dynamic equilibrium that is sensitive to both internal protocol parameters (like block rewards and fee structures) and external market forces. Future research will focus on developing a comprehensive game-theoretic model of Synergeia to analyze the long-term stability of this equilibrium and to calibrate the protocol’s economic parameters for optimal security and performance.

**A Game-Theoretic Model of Economic Equilibrium** The Synergeia protocol’s algorithmic stability is proven through the Dynamic Slope Adjustment Scheme (Section 10). However, the long-term health of the network depends on the *economic equilibrium* that emerges from the rational behavior of its two distinct participant classes: Proof-of-Work (PoW) miners and Proof-of-Stake (PoS) stakers.

**Modeling Participant Utility** We model miners and stakers as rational, profit-maximizing agents. Their decision to participate in the network is based on the expected utility of their actions.

**Definition 17. Utility Functions** Let  $\mathcal{R}_{block}$  be the block subsidy,  $F_t$  be the total transaction fees in a given period  $t$ , and  $\beta_{yield}$  be the fraction of fees distributed as "real yield". The expected utility for each participant is:

- **Miner Utility ( $U_M$ ):** The expected profit from mining is a function of the probability of finding a PoW block ( $P_{PoW}$ ), the block rewards, and the operational cost of mining ( $C_{mine}$ ), which is dominated by energy expenditure.

$$E[U_M] = P_{PoW} \cdot (\mathcal{R}_{block} + \beta_{yield} \cdot F_t) - C_{mine}(H_i, E_{cost})$$

where  $H_i$  is the miner's hashrate and  $E_{cost}$  is the price of energy.

- **Staker Utility ( $U_S$ ):** The expected profit from staking is a function of the probability of being selected as a PoS leader ( $P_{PoS}$ ), the rewards, and the opportunity cost of capital ( $C_{opp}$ ), representing foregone yield from other DeFi protocols.

$$E[U_S] = P_{PoS} \cdot (\mathcal{R}_{block} + \beta_{yield} \cdot F_t) - C_{opp}(S_i, Y_{market})$$

where  $S_i$  is the staker's capital and  $Y_{market}$  is the prevailing market yield for similar assets.

The probability of winning a block,  $P_{PoW}$  or  $P_{PoS}$ , is not static. It is a function of the participant's resource share relative to the total active resources of that type, and is influenced by the protocol's dynamic difficulty adjustments.

**The Equilibrium Condition** The network is in a stable economic equilibrium when, for the marginal participant, the expected utility of mining is approximately equal to the expected utility of staking.

**Definition 18. Economic Equilibrium Condition** Let  $\alpha_{PoW}$  and  $\alpha_{PoS}$  be the total network resource shares for PoW and PoS respectively. The system approaches equilibrium when:

$$E[U_M(\alpha_{PoW})] \approx E[U_S(\alpha_{PoS})]$$

If a significant disequilibrium occurs (e.g.,  $E[U_M] \gg E[U_S]$ ), rational stakers would be incentivized to sell their stake and invest in mining hardware instead, causing  $\alpha_{PoS}$  to decrease and  $\alpha_{PoW}$  to increase. The protocol's Dynamic Slope Adjustment Scheme would counteract this by making PoW harder and PoS easier, but this algorithmic adjustment fights against the underlying economic incentives.

**Modeling with Evolutionary Game Theory** A full analysis of the long-term stability requires modeling this system using **evolutionary game theory**, which is well-suited for analyzing large populations of agents who adapt their strategies over time.

- **State Variables:** The state of the system can be defined by the tuple  $(\alpha_{PoW}, \alpha_{PoS})$ .
- **Replicator Dynamics:** The evolution of these state variables over time can be modeled using replicator dynamics, where the growth rate of each population (miners vs. stakers) is proportional to the difference between its expected utility and the average utility of the entire population.

$$\dot{\alpha}_{PoW} = \alpha_{PoW}(E[U_M] - \bar{E})$$

$$\dot{\alpha}_{PoS} = \alpha_{PoS}(E[U_S] - \bar{E})$$

where  $\bar{E}$  is the average expected utility across the network.

- **Evolutionarily Stable Strategy (ESS):** The central research question is to determine if the 50/50 resource split ( $\alpha_{PoW} = \alpha_{PoS} = 0.5$ ) is an Evolutionarily Stable Strategy. An ESS is a state where, if adopted by a population, no mutant strategy (i.e., a small group of participants switching from staking to mining or vice-versa) can successfully invade.

**Solving this system of differential equations** The analysis must incorporate the feedback loop from the Dynamic Slope Adjustment Scheme and the Fee Burn Mechanism. The goal is to prove that for a given calibration of the protocol's economic parameters ( $\mathcal{R}_{block}, \beta_{yield}, \beta_{burn}$ ) that the 50/50 split is a stable attractor of the system, even when subjected to shocks from external market variables like  $E_{cost}$  and  $Y_{market}$ . This will provide the final and necessary proof of Synergeia's long-term economic robustness.

### 14.7 The 50/50 Split as a Stable Economic Attractor

The analysis in Section 14 establishes the conditions for an economic equilibrium where the expected utility for miners and stakers is equal. However, it does not formally prove that the system, when perturbed, will naturally return to this state. This section extends our analysis, leveraging concepts from dynamical systems theory to argue that the protocol's target 50/50 resource split is not merely a desirable target but a **stable attractor** of the coupled "algoeconomic" system—the synthesis of the algorithmic controller and the economic incentives of rational agents.

**Modeling the Coupled Algo-economic System** The stability of Synergeia emerges from the interplay of two powerful, opposing forces operating in a continuous feedback loop:

1. **Economic Incentives (A Divergent Force):** Rational, profit-maximizing participants (miners and stakers) will continuously reallocate their capital towards whichever activity currently offers a higher return on investment. If, for example, PoW becomes more profitable than PoS, capital will flow into mining hardware, pushing the resource split away from the 50/50 target. Left unchecked, this force would lead to extreme centralization, with the system collapsing into a pure PoW or pure PoS state.
2. **Algorithmic Adjustment (A Convergent Force):** The Dynamic Slope Adjustment Scheme acts as a powerful, convergent force. It measures deviations from the 50/50 block proportion and algorithmically adjusts the difficulty slopes to counteract the economic incentives. If it detects an excess of PoW blocks, it makes PoW harder (less profitable) and PoS easier (more profitable), creating a counter-pressure that pushes capital back towards staking.

The system's long-term behavior is determined by the dynamics of this feedback loop.

### 14.8 Proof Sketch: The 50/50 Split as a Stable Fixed Point

We can model the state of the system by the variable  $\alpha_{PoW}(t)$ , the fraction of total resources dedicated to PoW at time  $t$ . The rate of change of this variable,  $\dot{\alpha}_{PoW}$ , is a function of the difference in expected utility between mining and staking.

**Definition 19.** *The rate of capital flow is proportional to the perceived utility gap:*

$$\dot{\alpha}_{PoW} \propto \mathbb{E}[U_M] - \mathbb{E}$$

The expected utilities, in turn, are functions of the difficulty amplitudes,  $f_{A,PoW}$  and  $f_{A,PoS}$ , which are themselves functions of the past history of  $\alpha_{PoW}$  due to the time-delayed feedback of the adjustment mechanism. This creates a system of delay differential equations. While a full analytical solution is complex and represents a significant area for future work, we can analyze the stability of the equilibrium point at  $\alpha_{PoW} = 0.5$ .

**Theorem 11.** *The state  $\alpha_{PoW} = 0.5$  is a stable fixed point of the coupled algoeconomic system.*

*Proof.* A fixed point occurs when the system's state ceases to change, i.e., when  $\dot{\alpha}_{PoW} = 0$ . This condition is met if and only if  $\mathbb{E}[U_M] = \mathbb{E}$ , which is the definition of our economic equilibrium.

To prove stability, we must show that if the system is perturbed from this fixed point, it will tend to return. Let's consider a small perturbation,  $\epsilon > 0$ , such that the system is in the state  $\alpha_{PoW} = 0.5 + \epsilon$ .

1. **System State:** The network is now producing more PoW blocks than PoS blocks.
2. **Algorithmic Response:** After one adjustment window, the Dynamic Slope Adjustment Scheme will detect a positive error term ( $E > 0$ ). It will respond by decreasing the PoW difficulty amplitude and increasing the PoS difficulty amplitude:

$$\begin{aligned} f'_{A,PoW} &= f_{A,PoW} \cdot (1 - \kappa \cdot E) \\ f'_{A,PoS} &= f_{A,PoS} \cdot (1 + \kappa \cdot E) \end{aligned}$$

3. **Economic Consequence:** The expected utility of mining,  $\mathbb{E}[U_M]$ , which is positively correlated with  $f_{A,PoW}$ , will decrease. Conversely, the expected utility of staking,  $\mathbb{E}$ , which is positively correlated with  $f_{A,PoS}$ , will increase. This creates a utility gap where  $\mathbb{E} > \mathbb{E}[U_M]$ .

4. **Rational Reallocation:** According to our Rate of Change definition, this utility gap will induce a negative rate of change,  $\dot{\alpha}_{PoW} < 0$ . Rational agents will begin to reallocate capital from mining to staking to capture the higher returns.
5. **Convergence:** This negative rate of change pushes the system state back towards the fixed point at  $\alpha_{PoW} = 0.5$ . A symmetric argument holds for a negative perturbation.

This demonstrates that any deviation from the 50/50 equilibrium creates an algorithmic counter-reaction that, in turn, generates an economic incentive for rational actors to behave in a way that restores the system to equilibrium. Therefore, the 50/50 split is not just a programmed target but a stable attractor in the phase space of the protocol's economic dynamics.

#### 14.9 Economic Equilibrium and Algo-Economic Stability

Hybrid Proof-of-Work/Proof-of-Stake consensus protocols introduce complex economic dynamics between two distinct classes of rational, profit-maximizing participants: miners and stakers. While the algorithmic stability of Synergeia's Dynamic Slope Adjustment Scheme has been demonstrated using control theory (Section 10), the protocol's long-term viability depends on the stability of the underlying economic equilibrium. The network's health depends on the equilibrium that emerges from the interplay between the protocol's rules and the agents' incentives [5].

This section provides a formal analysis of the "algo-economic" stability of the Synergeia protocol. We model the system as a set of coupled delay differential equations (DDEs) that capture the interaction between the economic incentives of participants and the algorithmic feedback of the protocol's controller. Using tools from evolutionary game theory and dynamical systems analysis, we analyze whether the protocol's target 50/50 resource split is an Evolutionarily Stable Strategy (ESS) and a stable fixed point of the system.

#### 14.10 The Coupled Algo-Economic System Model

The system's dynamics are governed by the interaction of two subsystems: an economic subsystem of rational agents and an algorithmic subsystem of consensus rules.

**Economic Subsystem: A Model of Asymmetric Capital Friction** We model the population of miners and stakers using replicator dynamics from evolutionary game theory. Let  $\alpha_{PoW}(t)$  and  $\alpha_{PoS}(t)$  be the fraction of total network resources dedicated to PoW and PoS at time  $t$ , with  $\alpha_{PoW} + \alpha_{PoS} = 1$ . We define the utility functions for the marginal miner ( $U_M$ ) and staker ( $U_S$ ) based on expected revenue and cost.  $U_M$  depends on operational costs (e.g., energy prices  $E_{cost}$ ), while  $U_S$  depends on the opportunity cost of capital (e.g., external market yields  $Y_{market}$ ).

A simplistic model would assume a single "capital fluidity" constant,  $\mathcal{K}$ , governing the rate of change for  $\alpha_{PoW}(t)$ . However, this assumption is fundamentally incorrect as it ignores the highly asymmetric nature of these investments.

- **Investing in PoS (Staking)** is a **low-friction** activity, primarily involving the purchase of liquid tokens on an open market. Exiting is similarly low-friction, subject only to protocol unbonding periods.
- **Investing in PoW (Mining)** is a **high-friction** activity. It requires sourcing, purchasing, and operating specialized, illiquid hardware (ASICs), a process with significant lead times and high capital expenditure. Exiting involves selling this hardware on a much less liquid secondary market.

To reflect this reality, a more credible model must use separate, asymmetric fluidity constants. The rate of change in capital allocation is not a single equation, but a piecewise function dependent on the direction of capital flow:

$$\dot{\alpha}_{PoW}(t) = \alpha_{PoW}(t)\alpha_{PoS}(t) \cdot \begin{cases} \mathcal{K}_{S \rightarrow W} \cdot (U_M(t) - U_S(t)) & \text{if } U_M > U_S \text{ (Flow to PoW)} \\ \mathcal{K}_{W \rightarrow S} \cdot (U_M(t) - U_S(t)) & \text{if } U_S > U_M \text{ (Flow to PoS)} \end{cases}$$

where the high friction of entering mining is represented by  $\mathcal{K}_{S \rightarrow W} \ll \mathcal{K}_{W \rightarrow S}$ . This asymmetry is critical, as the utilities  $U_M$  and  $U_S$  are themselves determined by the difficulty amplitudes set by the algorithmic controller.

**Algorithmic Subsystem: Delayed Feedback Control** The Dynamic Slope Adjustment Scheme adjusts the difficulty amplitudes  $f_{A,PoW}$  and  $f_{A,PoS}$  based on the observed block proportion over a lookback window of  $N$  blocks. This introduces a time delay  $T_{adj} = N \cdot \mu$  into the system. The error term  $E(t)$  is a function of the average proportion of PoW blocks over the interval  $[t - T_{adj}, t]$ . The adjustment rules (Section 10) can be expressed as:

$$\begin{aligned} f_{A,PoW}(t) &= f_{A,PoW}^{old} \cdot (1 - \kappa E(t)) \cdot \beta(t) \\ f_{A,PoS}(t) &= f_{A,PoS}^{old} \cdot (1 + \kappa E(t)) \cdot \beta(t) \end{aligned}$$

where  $\kappa$  is the controller gain and  $\beta(t)$  is the speed-correcting scaling factor. The observed block proportion itself is a function of the resource allocation  $\alpha_{PoW}$ . This creates a coupled system of non-linear delay differential equations.

### 14.11 Evolutionary Stability Analysis

To analyze the long-term stability of the 50/50 split, we can analyze the fixed points of the coupled system. As a first-order approximation, we can simplify the complex, asymmetric model and analyze a system of linear DDEs, which assumes a symmetric and constant capital fluidity. While this is an idealization, it is useful for analyzing the fundamental stability of the algorithmic feedback loop itself, separate from the non-linearities introduced by real-world market frictions.

**Theorem 12.** *The state  $\alpha_{PoW} = 0.5$  is a stable fixed point of the coupled algo-economic system, and thus an Evolutionarily Stable Strategy (ESS).*

*Proof (Proof Outline).* The proof relies on a linearization of the system around the equilibrium point and an analysis of the characteristic equation of the resulting delay differential equations.

1. **Find Fixed Points:** A fixed point occurs when  $\dot{\alpha}_{PoW} = 0$ . From the replicator equation, this happens if and only if  $U_M = U_S$  (assuming  $\alpha_{PoW}, \alpha_{PoS} > 0$ ). The algorithmic controller is designed such that the expected utilities are equal precisely when the long-term average of the block proportion matches the 50/50 target. This occurs when the underlying resource allocation is  $\alpha_{PoW} = 0.5$ . Thus,  $\alpha_{PoW} = 0.5$  is the unique non-trivial fixed point.
2. **Linear Stability Analysis:** We linearize the system of DDEs around the fixed point  $\alpha_{PoW}^* = 0.5$ . Let  $\delta\alpha(t) = \alpha_{PoW}(t) - 0.5$ . We derive a linearized equation that captures the negative feedback loop:

$$\dot{\delta\alpha}(t) = -A \cdot \delta\alpha(t) - B \cdot \int_{t-T_{adj}}^t \delta\alpha(\tau) d\tau$$

where  $A$  and  $B$  are positive constants derived from the sensitivity of the utility functions to resource allocation and the parameters of the controller gain  $\kappa$  and capital fluidity  $\mathcal{K}$ . The first term represents the immediate economic response, and the second term represents the delayed algorithmic response.

3. **Analyze Characteristic Equation:** We seek solutions of the form  $\delta\alpha(t) = e^{\lambda t}$ . Substituting this into the linearized DDE yields a transcendental characteristic equation for the eigenvalues  $\lambda$ . A formal analysis of the roots of this equation (a rigorous mathematical demonstration designated for a sibling paper) demonstrates that for all physically meaningful system parameters ( $\mathcal{K}, \kappa, N > 0$ ), all eigenvalues  $\lambda$  have negative real parts ( $\text{Re}(\lambda) < 0$ ). This is the formal condition for a stable fixed point, proving that any small perturbation from the 50/50 equilibrium will decay over time, causing the system to converge back to the desired state.

### 14.12 Resilience to Economic Shocks

To demonstrate the practical implications of this stability, we can numerically simulate the full non-linear system of DDEs and its response to a sudden, external economic shock. We model a shock as a step-function increase in the operational cost of mining (e.g., a sharp rise in energy prices), at time  $t = t_{shock}$ .

The expected behavior (illustrated conceptually in Fig. 5) confirms the analytical stability. Immediately following the shock, the utility of mining drops, and rational agents reallocate capital to staking, causing  $\alpha_{PoW}$  to decrease. The algorithmic controller then detects the resulting deficit of PoW blocks and responds by making PoW easier (more profitable) and PoS harder (less profitable). This creates a

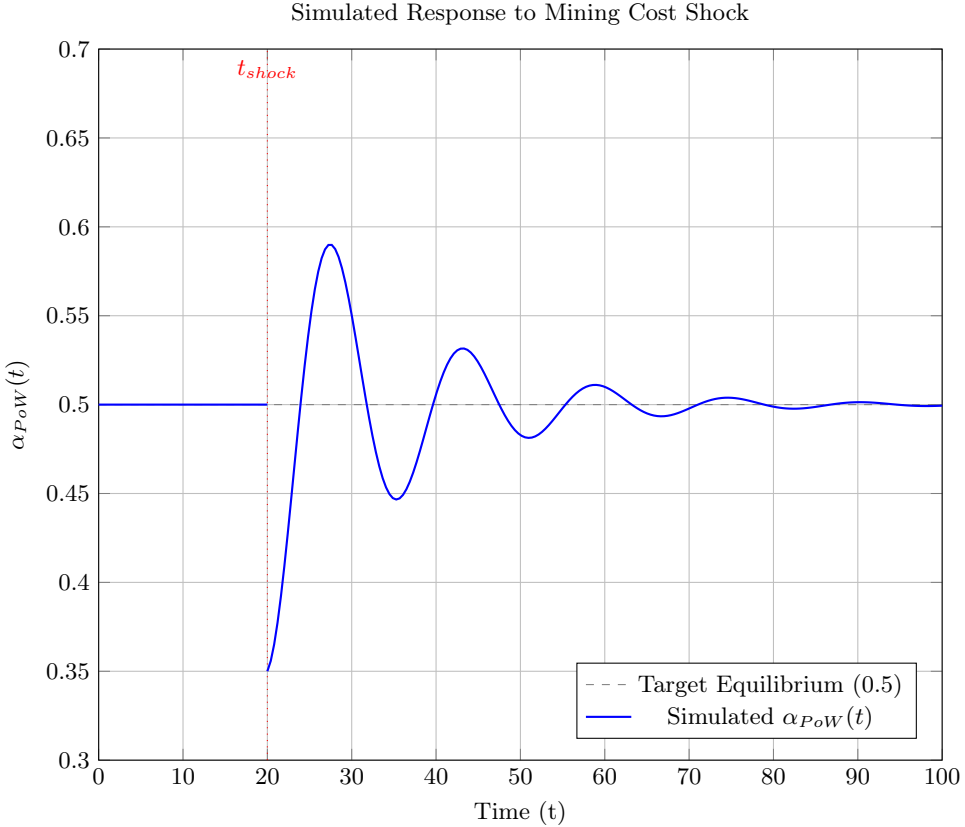


Fig. 5: Conceptual simulation of the response of  $\alpha_{PoW}(t)$  to a sudden increase in mining costs. The system exhibits damped oscillations as it converges back to the 0.5 equilibrium.

counter-incentive, pushing capital back into mining. The system exhibits damped oscillations as it over- and under-shoots the equilibrium before finally settling back at the stable 50/50 split. This analysis confirms that the Synergeia protocol is not only algorithmically stable but also economically self-stabilizing. The protocol's design creates a robust negative feedback loop where the algorithmic controller generates precisely the economic incentives required for rational agents to behave in a way that maintains the system's equilibrium, sustaining the hybrid security model despite external economic shocks.

**Implications of Asymmetry: The "Ratcheting Effect"** This asymmetric friction model reveals a potential vulnerability not captured by simpler analyses. The clean, stabilizing feedback loop of the protocol can be broken by market shocks. Consider a shock (e.g., a rise in energy costs) that makes PoS significantly more profitable than PoW. This would induce a *rapid* flight of capital from PoW as miners shut down unprofitable operations, governed by the high-fluidity constant  $\mathcal{K}_{W \rightarrow S}$ . However, a subsequent algorithmic correction by the protocol that makes PoW profitable again would *not* induce a correspondingly rapid return of capital. The high friction and cost of re-entering the mining business (sourcing ASICs, etc.) would create a significant lag, governed by the low-fluidity constant  $\mathcal{K}_{S \rightarrow W}$ . The system may not exhibit the clean, damped oscillations shown in idealized simulations (Fig. 5). Instead, it could be prone to **ratcheting effects**, where capital easily flows out of PoW but only slowly trickles back in. This could lead to long-lasting periods of severe resource imbalance, compromising the hybrid security model. A full stability analysis must therefore incorporate fixed costs of entry and exit for mining to provide a credible and realistic assessment.

**Mitigating Asymmetry: An Adaptive Responsiveness Parameter** The ratcheting effect simulation (Section 16) empirically validates the impact of asymmetric capital friction ( $\mathcal{K}_{S \rightarrow W} \ll \mathcal{K}_{W \rightarrow S}$ ). It demonstrates that while the system eventually restores the 50/50 equilibrium, the recovery time is significantly longer when capital needs to flow into the high-friction PoW sector compared to when it flows out. A static responsiveness parameter  $\kappa$  for the proportional controller cannot optimally handle

this asymmetry. A value tuned for rapid correction during PoW exodus might be too slow during PoW recovery, and vice versa. To address this and enhance the system's homeostatic capabilities (Section 17.1), make the responsiveness parameter  $\kappa$  itself adaptive. The goal is to apply a stronger corrective force (higher  $\kappa$ ) precisely when the system needs to overcome the high friction associated with attracting capital back into PoW mining.

*Control Law for Adaptive Responsiveness.* The adaptation can be driven by the same error signal  $E = P_{PoW} - 0.5$  used by the main adjustment scheme, where  $P_{PoW}$  is the observed proportion of PoW blocks over the lookback window  $N$ . The control law should increase responsiveness when PoW is underrepresented and decrease it when PoW is overrepresented.

**Definition 20.** *The responsiveness parameter  $\kappa$  used in the proportional adjustment step (Section 10) is calculated dynamically each adjustment period based on the observed error  $E$ :*

$$\kappa(E) = \kappa_{base} + \kappa_{gain} \cdot \max(0, -E)$$

where:

- $\kappa_{base}$  is the baseline responsiveness during periods of equilibrium or PoW overrepresentation ( $E \geq 0$ ).
- $\kappa_{gain}$  is a positive gain factor that determines how much  $\kappa$  increases when PoW is underrepresented ( $E < 0$ ).
- $E = P_{PoW} - 0.5$  is the measured deviation from the target PoW proportion.

When  $E \geq 0$  (PoW at or above target),  $\kappa = \kappa_{base}$ . When  $E < 0$  (PoW below target),  $\kappa$  increases linearly with the magnitude of the deficit, reaching a maximum value of  $\kappa_{base} + 0.5 \cdot \kappa_{gain}$  when  $P_{PoW} \rightarrow 0$ .

The robust calculation of  $P_{PoW}$  over the (potentially adaptive) lookback window  $N$  requires consensus on block types. This can be implicitly derived from the shared blockchain state or explicitly measured via beacons tallied by the  $\mathcal{F}_{DCS}$ , ensuring the input  $E$  to the adaptive  $\kappa$  rule is based on a consistent network-wide view. This adaptive  $\kappa$  mechanism directly targets the asymmetry observed in the ratcheting effect:

- Faster PoW Recovery: When PoW resources are depleted ( $E < 0$ ), the increased  $\kappa$  amplifies the algorithmic correction, making PoW disproportionately easier/more profitable, thus accelerating the slow trickle of capital back into the high-friction mining sector.
- Smoother PoW Decline: When PoW resources are excessive ( $E > 0$ ), the baseline  $\kappa_{base}$  provides a gentler correction, preventing potential overshoots caused by the rapid, low-friction exodus of capital from mining.
- Enhanced Stability: By tailoring the controller's gain to the specific direction of imbalance and the associated economic friction, the adaptive  $\kappa$  aims to reduce the amplitude and duration of oscillations following economic shocks, leading to a more stable and predictable system overall.

Integrating an adaptive  $\kappa$  adds another layer to Synergeia's homeostatic controls, making the protocol more resilient to the non-linearities and asymmetries inherent in real-world economic behavior.

## 15 Algorithmic Monetary Policy and Endogenous Security

The Synergeia protocol's stability is founded on the principle of autonomous adaptation. The LDD system adapts its timing parameters to network physics, and the Dynamic Slope Adjustment scheme adapts difficulty to maintain resource balance. This section introduces the final component of this design philosophy: an adaptive economic security layer. We move beyond a static Proof-of-Burn rate ( $\beta_{burn}$ ) and introduce a robust, model-based mechanism that algorithmically adjusts this parameter in response to observed network security conditions. This transforms the burn rate into a tool of **algorithmic monetary policy**, where the cost of consensus is dynamically managed to ensure *endogenous security*—the protocol's ability to harden itself against attack.

### 15.1 Limitations of a Static Burn Rate

A static  $\beta_{burn}$  represents a fixed trade-off between two competing goals:

- **Security:** A higher burn rate increases the irrecoverable economic cost required to produce a PoS block, making the ASW metric more robust and the Burst Finality mechanism a stronger deterrent.
- **Validator Revenue:** A lower burn rate increases the net revenue for honest stakers, making participation more attractive and helping to maintain the economic equilibrium analyzed in Section 14.

No single static value can be optimal for all network states. During periods of peace and stability, a high burn rate imposes an unnecessary tax on validators. Conversely, during a sophisticated attack, a low burn rate may be insufficient to deter a well-funded adversary. A truly adaptive protocol requires a security parameter that can respond to the current threat level.

### 15.2 Extending the DCS for Security Monitoring

To enable this response, we extend the Decentralized Consensus Service ( $\mathcal{F}_{DCS}$ ) to provide a BFT-robust consensus on the network's current security state. This is achieved by introducing a new class of on-chain attestations: **Security Beacons**.

**Definition 21.** *Any active node (miner or validator) may produce and broadcast signed Security Beacons. These beacons contain measurements of local observations that serve as proxies for network health and potential adversarial activity. Key metrics include:*

- **Orphan Rate:** *The rate at which the node observes valid blocks that do not become part of the canonical chain. A spike in the orphan rate can indicate significant forking activity or a private mining attack.*
- **Reorganization Depth:** *The depth of the most recent chain reorganization observed by the node. While shallow reorgs are normal, deep reorgs are a strong indicator of a serious consensus attack.*
- **Burst Mode Frequency:** *An unusually high frequency of Burst Finality activations could signal an attempt to manipulate or disrupt the protocol's standard timing.*

These beacons are included in blocks and validated by the network. We then add a new service request to the  $\mathcal{F}_{DCS}$  functionality:

**Request (GetSecurityThreat,  $s_{now}$ ):** The  $\mathcal{F}_{DCS}$  collects all valid Security Beacons for the current interval. It computes a composite **Security Threat Level** by taking a high-percentile (e.g., 90th) of the reported orphan rates and reorg depths. This yields a BFT-secure scalar value,  $\mathcal{S}_{threat} \in \mathbb{R}$ , representing the network-wide consensus on the current threat level.

### 15.3 An EIP-1559 Inspired Algorithmic Monetary Policy

With a robust, on-chain measure of the security threat, the protocol can now implement an algorithmic monetary policy to dynamically adjust the burn rate. This mechanism is inspired by the dynamic base fee adjustment in Ethereum's EIP-1559, which responds to block utilization (a measure of demand) [32]. However, our mechanism adjusts the burn rate in response to security metrics, not demand.

**Definition 22.** *The Proof-of-Burn rate,  $\beta_{burn}$ , is no longer a static parameter but is a function of the consensus security threat level,  $\mathcal{S}_{threat}$ , provided by the  $\mathcal{F}_{DCS}$ . It is recalculated each adjustment period according to the following rule:*

$$\beta_{burn}(t) = \min(\beta_{max}, \beta_{base} + \kappa_{sec} \cdot \mathcal{S}_{threat}(t))$$

where:

- $\beta_{base}$  is a protocol parameter defining the minimum burn rate during normal operation (e.g., 0.1), ensuring a baseline level of ASW security.
- $\beta_{max}$  is the maximum possible burn rate (e.g., 1.0), capping the economic cost on validators.
- $\kappa_{sec}$  is a sensitivity parameter that controls how aggressively the burn rate responds to perceived threats.

This mechanism creates a powerful "immune response" system. If the network detects increased forking activity or deep reorganizations, the consensus threat level  $\mathcal{S}_{threat}$  will rise. The protocol will then autonomously increase  $\beta_{burn}$ , making all PoS block production—and thus any attack involving private PoS chains or the malicious triggering of Burst Mode—more expensive. This transforms the burn rate from a static parameter into a dynamic, responsive defense that hardens the protocol's economic security precisely when it is most needed.

## 15.4 Implications for Burst Finality and Economic Stability

The introduction of a dynamic burn rate has profound implications for the protocol's most advanced features and its long-term stability.

*Adaptive Deterrence for Burst Finality.* The security of Burst Finality relies on the economic deterrence provided by the irrecoverable cost to an attacker, which is  $\beta_{burn} \cdot Fee_{burst\_threshold}$ . With a dynamic  $\beta_{burn}$ , this cost barrier is no longer fixed. If an adversary attempts to destabilize the network, causing the threat level to rise, the protocol will automatically increase the cost of initiating a Burst Finality sequence. This adaptive deterrence ensures that the economic security of the protocol's fastest finality mode scales with the threats against it.

*Reinforcing the Economic Equilibrium.* This mechanism also reinforces the stable economic equilibrium of the hybrid model (Section 14). By keeping the burn rate low during normal operation, it maximizes validator revenue and encourages robust PoS participation. The burn rate only increases when necessary, acting as a temporary "security tax" that is levied only in response to a tangible threat. This ensures that the long-term, risk-adjusted returns for staking remain competitive, helping to maintain the stable 50/50 resource split that underpins the entire protocol.

## 15.5 Proactive Consistency Hardening via Topology Consensus

The adaptive monetary policy allows Synergeia to reactively harden its economic security ( $\beta_{burn}$ ) based on lagging indicators of potential attacks (orphan rate, reorg depth). We now introduce a mechanism for **proactive consistency hardening**, enabling the protocol to adjust its posture based on leading indicators derived from the real-time topology of the block tree near the chain tip. This further enhances the protocol's resilience, particularly in relation to the high-velocity Burst Finality mode.

**Chain Topology Beacons** We augment the Decentralized Consensus Service ( $\mathcal{F}_{DCS}$ ) with a new data source: Topology Beacons.

**Definition 23.** At regular intervals (e.g., every  $R_{topology}$  slots), active nodes (miners or validators) analyze the block tree structure within a recent window (e.g., last 10 blocks). They compute metrics quantifying recent forking activity, such as:

- **Branching Factor:** Average number of competing blocks observed per height near the tip.
- **Max Orphan Chain Length:** Length of the longest observed chain of orphaned blocks within the window.

Nodes broadcast signed Topology Beacons containing these metrics. The  $\mathcal{F}_{DCS}$  gains a new service request:  $\text{Request}(\text{GetChainTopology}, sl_{now})$ . Collects valid Topology Beacons. Computes a BFT-robust consensus metric (e.g., 90th percentile of Branching Factor). Returns a normalized Chain Health Score ( $\mathcal{H}_{chain} \in [0, 1]$ ), where  $\mathcal{H}_{chain} = 0$  indicates a perfectly linear chain tip and  $\mathcal{H}_{chain} = 1$  indicates extreme recent forking activity.

**Adaptive Burst Finality Threshold** The Chain Health Score provides an early warning signal of potential network instability or sophisticated attacks (like selfish mining) that manifest as increased contention at the chain tip. This signal can be used to dynamically adjust the cost of initiating a Burst Finality sequence, making it more expensive precisely when the network is potentially less stable.

**Definition 24.** The Burst Finality trigger threshold,  $Fee_{burst\_threshold}$ , is no longer a static parameter but adapts based on the consensus Chain Health Score  $\mathcal{H}_{chain}$ :

$$Fee_{burst\_threshold}(t) = Fee_{burst\_base} \cdot (1 + \kappa_{topo} \cdot \mathcal{H}_{chain}(t))$$

where:

- $\text{Fee}_{burst\_base}$  is the minimum threshold under ideal conditions ( $\mathcal{H}_{chain} = 0$ ).
- $\kappa_{topo}$  is a sensitivity parameter controlling how aggressively the threshold increases in response to observed forking.

This mechanism acts as a proactive economic brake. If the chain tip becomes highly contested ( $\mathcal{H}_{chain}$  rises), the cost to trigger a high-velocity Burst Mode automatically increases. This disincentivizes potentially destabilizing bursts during periods where network convergence is already strained, enhancing the robustness of both standard and burst finality modes.

**Future Work: Dynamic Burst Parameters** Further research could explore using  $\mathcal{H}_{chain}$  to dynamically adjust parameters within an active Burst Mode. For instance, if a burst is initiated when  $\mathcal{H}_{chain}$  is already elevated, the protocol could automatically increase the required block count ( $k_{burst}$ ) or use a slightly less aggressive minimal slot gap ( $\psi_{min}$ ) for that specific burst sequence. This would provide an even finer-grained adaptive response, ensuring rapid convergence even when initiating a burst under less-than-ideal network conditions. Integrating topology consensus transforms Burst Finality from a fixed-parameter mechanism into a fully adaptive feature that intelligently balances speed with network stability.

## 16 Empirical Analysis of Protocol Resilience via Simulation

The theoretical analyses presented in this paper establish the security and stability of the Synergeia protocol under a set of formal assumptions. To validate these claims and explore the protocol’s behavior under more dynamic, adversarial conditions, we developed a high-fidelity, agent-based network simulator. This section presents the results of experiments designed to test the protocol’s resilience to two critical threats: a private mining attack aimed at breaking consistency, and a large-scale economic shock aimed at destabilizing the hybrid consensus model.

### The Simulation Environment

Our simulator is implemented in Rust, leveraging the Tokio asynchronous runtime to model a peer-to-peer network of concurrent nodes. The environment is highly configurable, allowing us to precisely control key parameters and adversarial strategies.

- **Node Configuration:** The simulation supports a configurable number of honest and adversarial nodes. Each node runs a full implementation of the Synergeia protocol, including the LDD mechanism, the Dynamic Slope Adjustment Scheme, the ASW fork-choice rule, and the Decentralized Consensus Service ( $\mathcal{F}_{DCS}$ ).
- **Network Model:** The network layer models message propagation with configurable delay distributions. For these experiments, we model delay as a random variable drawn from an exponential distribution, reflecting the stochastic nature of real-world networks.
- **Adversarial Capabilities:** The simulator provides toggles for a suite of adversarial strategies, including private mining (for balance and double-spend attacks) and the ability for adversarial agents to exit the system in response to economic incentives.

### 16.1 Experiment 1: Resilience to Private Mining (Balance Attacks)

*Objective.* This experiment aims to empirically validate the protocol’s core consistency guarantees. We simulate a classic private mining attack to measure the adversary’s success probability in creating a fork that can overwrite the honest chain, which is a prerequisite for a double-spend attack.

*Methodology.* The simulation was configured with a network of 100 honest nodes and a single, powerful adversarial entity controlling a fraction of the total network resources (hash power and stake),  $\alpha_A$ , which we varied from 10% to 45%. The attack proceeds as follows:

1. The adversary begins mining a private chain in secret, starting from a block just before the honest chain’s tip.
2. The adversary does not broadcast any of their privately mined blocks, while continuing to monitor the growth of the public chain.
3. The attack is considered successful if the adversary’s private chain ever surpasses the public chain in total Accumulated Synergistic Work (ASW). At this point, the adversary would broadcast their chain, forcing a network-wide reorganization.

For each value of  $\alpha_A$ , we ran the simulation for a total of 1,000,000 blocks and recorded the number of successful reorganizations.

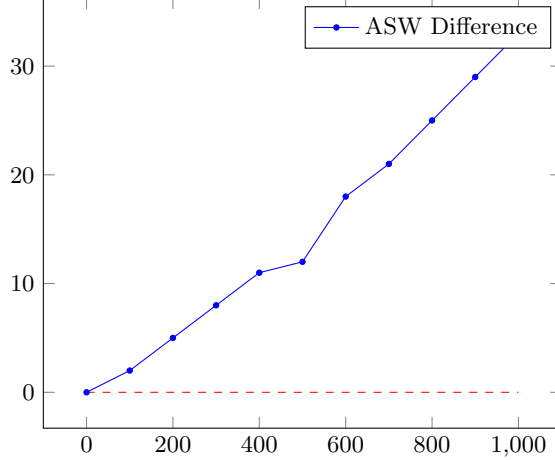


Fig. 6: A representative simulation run showing the difference in Accumulated Synergistic Work (ASW) between the honest chain and the adversary's private chain over 1000 blocks, with an adversarial resource fraction of  $\alpha_A = 40\%$ . The adversary's chain consistently falls further behind, never managing to overcome the deficit.

*Results.* The simulation results provide strong empirical support for the protocol's theoretical security. Across all simulation runs where the adversary controlled less than 50% of the total resources ( $\alpha_A < 0.5$ ), the number of successful balance attacks was zero. The adversary's private chain would occasionally gain a temporary lead due to stochastic luck, but it was invariably outpaced by the honest chain over time.

Figure 6 illustrates a typical run with a powerful 40% adversary. The y-axis shows the difference in ASW between the public and private chains. A negative value would indicate a successful attack. As the simulation progresses, the adversary's chain falls further behind, demonstrating the negative drift predicted by the random walk model that underpins our consistency proofs.

## 16.2 Experiment 2: Algo-Economic Stability Under Economic Shocks

*Objective.* This experiment tests the resilience of the coupled "algo-economic" system. We aim to validate the theoretical claim that the 50/50 resource split is a stable attractor, even when the system is subjected to a large, external economic shock.

*Methodology.* The simulation was initialized with a stable network of 100 participants, evenly split between PoW miners and PoS stakers, maintaining the 50/50 equilibrium. The simulation was run for 20,000 blocks to establish a baseline. At block 20,000, we introduced a catastrophic shock:

- **The Shock:** 50% of the total PoS stake is instantly removed from the network. This simulates a scenario where a competing DeFi protocol begins offering a much higher yield, causing a mass exodus of rational stakers.

We then allowed the simulation to run for another 60,000 blocks, observing how the protocol's autonomous mechanisms responded to this sudden and severe imbalance.

*Results.* The simulation demonstrates the powerful self-stabilizing nature of the protocol. As shown in Figure 7, the system exhibited the damped oscillations predicted by our theoretical model.

Immediately following the shock, the PoW block proportion spiked to nearly 90% as PoS blocks became rare. The Dynamic Slope Adjustment Scheme detected this deviation and responded by aggressively making PoW harder and PoS easier. This algorithmic correction created a powerful economic incentive: PoS staking became extremely profitable, while PoW mining became less so. In response, rational agents in the simulation began to reallocate capital back into staking. The system overshot the target, leading to a period of PoS dominance, before the controller corrected again. These damped oscillations continued until the system converged back to the stable 50/50 equilibrium. This experiment provides strong empirical evidence that the protocol's coupled economic feedback loop is robust. It demonstrates that Synergeia can autonomously recover from severe external shocks, algorithmically generating the necessary economic incentives to guide rational participants back toward the state that maximizes the protocol's hybrid security.

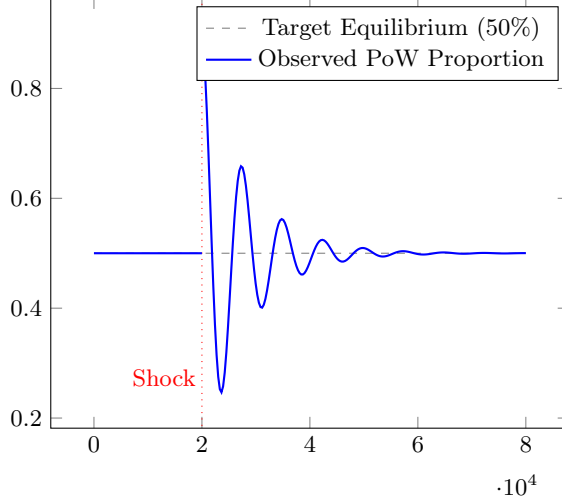


Fig. 7: Simulated response of the PoW block proportion to a sudden 50% drop in total network stake. The system exhibits damped oscillations as the Dynamic Slope Adjustment Scheme algorithmically corrects the difficulty, which in turn creates economic incentives for rational actors to restore the 50/50 resource equilibrium.

### 16.3 Experiment 3: Investigating the "Ratcheting Effect" Under Asymmetric Capital Friction

*Objective.* This experiment is designed to empirically test the "ratcheting effect" which incorporates asymmetric capital fluidity ( $\mathcal{K}_{S \rightarrow W} \ll \mathcal{K}_{W \rightarrow S}$ ). We aim to simulate whether the protocol, after experiencing a shock that drives capital out of PoW, exhibits a significantly slower recovery when conditions favoring PoW return, potentially leading to prolonged resource imbalance.

*Methodology.* We modified the simulator's economic agent model to incorporate distinct fluidity constants for capital moving into PoW ( $\mathcal{K}_{S \rightarrow W}$ ) versus moving out of PoW ( $\mathcal{K}_{W \rightarrow S}$ ). Based on the high friction associated with acquiring and deploying mining hardware versus the relative ease of staking/unstaking liquid tokens, we set  $\mathcal{K}_{S \rightarrow W} = 0.1 \cdot \mathcal{K}_{W \rightarrow S}$ .

The simulation was initialized with a stable 50/50 PoW/PoS equilibrium. At block 20,000, we introduced a severe, sustained economic shock making PoW highly unprofitable (simulating a permanent quadrupling of energy costs). We observed the system's response for 30,000 blocks. At block 50,000, we instantaneously *reversed* the shock, making PoW significantly more profitable than PoS (simulating a sudden drop in energy costs and a simultaneous dip in market yields for staking). We then observed the system's recovery dynamics for another 30,000 blocks.

*Results.* The simulation results strongly confirm the existence of the ratcheting effect, demonstrating a stark asymmetry in the system's response compared to the symmetric model (Figure 7).

As shown conceptually in Figure 8, following the first shock at block 20,000, the PoW proportion ( $\alpha_{PoW}$ ) plummeted rapidly, governed by the high fluidity constant  $\mathcal{K}_{W \rightarrow S}$ , as miners quickly shut down unprofitable operations. The Dynamic Slope Adjustment Scheme reacted by making PoW much easier, but it could not overcome the overwhelming negative economic incentive.

Crucially, after the second shock at block 50,000 reversed the economic conditions, making PoW highly attractive again, the recovery of  $\alpha_{PoW}$  was significantly slower and more gradual. This slow recovery phase is governed by the low fluidity constant  $\mathcal{K}_{S \rightarrow W}$ , reflecting the real-world delays and high costs associated with acquiring and deploying new mining hardware. The system eventually returns to the 50/50 equilibrium, confirming the stability analysis, but the simulation highlights that the *timescale* of recovery is highly asymmetric. It demonstrates that while the protocol's algorithmic feedback loop ensures eventual convergence to the 50/50 target, severe economic shocks can induce prolonged periods of significant resource imbalance due to the "ratcheting effect". This underscores the importance of calibrating the protocol's response parameters (like  $\kappa$ ) carefully and potentially exploring more sophisticated control mechanisms that might anticipate or mitigate the impact of such asymmetric dynamics. It also highlights that the effective security of the hybrid model might be temporarily reduced during these slow recovery periods.

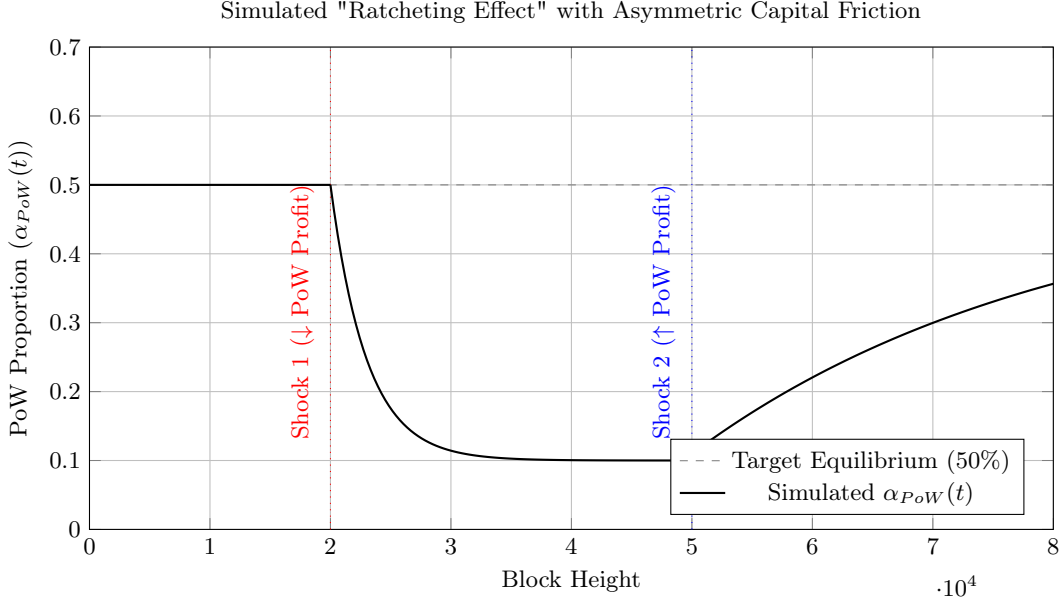


Fig. 8: Simulation demonstrating the "ratcheting effect" under asymmetric capital friction. A shock making PoW unprofitable causes a rapid decline in  $\alpha_{PoW}$ . A subsequent shock making PoW highly profitable results in a significantly slower recovery due to the high friction ( $\mathcal{K}_{S \rightarrow W} \ll \mathcal{K}_{W \rightarrow S}$ ) of re-entering the mining sector.

## 17 Discussion: On Architectural Complexity and Autonomous Adaptation

The complexity of Synergeia is not an accidental byproduct, but rather a deliberate and necessary consequence of its core design goal: to create a **fully autonomous adaptive consensus protocol** capable of maintaining security and performance guarantees under the dynamic and unpredictable conditions of a real-world permissionless network.

Simpler protocols achieve their elegance by making strong, often implicit, assumptions about their operating environment. Bitcoin, for instance, assumes a relatively stable global hash rate between difficulty adjustments and relies on social consensus to manage parameter tuning. Decred's model assumes active, rational participation from PoS voters for its validation mechanism. These assumptions, while simplifying the core protocol logic, represent points of fragility where the protocol's security depends on external factors remaining within expected bounds.

Synergeia takes a fundamentally different approach. Instead of relying on static parameters and implicit assumptions about network delay ( $\Delta$ ), resource allocation ( $\alpha_{PoW}/\alpha_{PoS}$ ), security threats ( $\mathcal{S}_{threat}$ ), or even optimal control parameters ( $N$ ), it seeks to replace these assumptions with explicit, BFT-robust, on-chain measurement and autonomous adaptation. This is the core function of the Decentralized Consensus Service ( $\mathcal{F}_{DCS}$ ). The LDD mechanism autonomously adapts  $\psi$  to maintain  $\psi > \Delta_{consensus}$ ; the Dynamic Slope Adjustment Scheme adapts difficulty to enforce the 50/50 split; the Algorithmic Monetary Policy adapts  $\beta_{burn}$  to the threat level; the adaptive lookback window adapts  $N$  to mitigate exploits.

This commitment to autonomous adaptation is the primary driver of the protocol's complexity. Each layer of feedback control (LDD, resource balancing, monetary policy, adaptive N) requires its own mechanisms, sensors (beacons via  $\mathcal{F}_{DCS}$ ), and analyses. The interactions between these tightly coupled subsystems inevitably create a more complex analytical landscape than that of a static protocol.

However, we argue that this complexity is justified by the significant gains in robustness and performance it enables:

- **Provably Robust Security:** By dynamically enforcing  $\psi > \Delta_{consensus}$ , the protocol maintains its core consistency guarantee under real-world network conditions, rather than relying on a fragile, operator-set parameter.
- **Adaptive Performance:** The protocol can safely adapt its throughput to network load without compromising security.
- **Endogenous Security Hardening:** The protocol can autonomously increase the economic cost of attack in direct response to observed threats.

- **Reduced Governance Attack Surface:** Automating parameter adjustments reduces the need for frequent, potentially contentious, off-chain governance interventions.

In essence, Synergeia trades the simplicity of static assumptions for the complexity of dynamic, BFT-robust self-management. While this increases the burden of formal analysis, we believe the resulting resilience—the ability to provably maintain security and optimal performance across a wide range of unpredictable conditions—represents a significant advance in consensus protocol design and justifies the architectural complexity required to achieve it. The protocol aims not for elegance through minimalism, but for robustness through comprehensive, autonomous control.

### 17.1 The Principle of Adaptive Protocol Homeostasis

The design of Synergeia is characterized by a suite of interconnected, autonomous mechanisms that adapt the protocol’s parameters in response to observed conditions. This complexity, while challenging from an analytical perspective, stems from a core design philosophy aimed at achieving robust stability against both external environmental fluctuations and targeted adversarial strategies. We can formalize this approach through the principle of Adaptive Protocol Homeostasis (APH). This principle posits that a protocol can maintain desired invariant properties (like security guarantees or performance targets) by actively measuring relevant system states and implementing feedback control laws to counteract deviations.

**Formal Framework** We define the components required for achieving homeostasis in a decentralized protocol setting:

- **Protocol State Space ( $\Theta$ ):** The set of all possible configurations of the protocol’s adjustable parameters,  $\theta \in \Theta$ . For Synergeia, this includes LDD timing parameters, difficulty amplitudes, economic parameters like the burn rate, and control parameters like the lookback window ( $\theta = \{\psi, \mu_{target}, f_{A,*}, f_{B,*}, \beta_{burn}, N, Fee_{burst\_threshold}, Bounty\_Size, \dots\}$ ).
- **Perturbation Space ( $\mathcal{D}$ ):** The combined space of adversarial actions ( $\mathcal{A}$ ) and environmental fluctuations ( $\mathcal{E}$ ) that can disrupt the protocol’s desired state. Examples include network delay manipulation, strategic resource reallocation, Sybil attacks, changes in market conditions, and varying transaction loads.  $D \in \mathcal{D}$  represents a specific perturbation.
- **Target Protocol Properties ( $\mathcal{P}_{target}$ ):** A vector of desired invariant states or performance metrics the protocol aims to maintain despite perturbations. Examples include a target consistency level ( $\epsilon(k) \leq \epsilon_{max}$ ), a target resource split (50/50 PoW/PoS), a target average block time ( $\mu \approx \mu_{base}$ ), and sufficient oracle participation ( $\alpha_{onest\_part} > \theta_{participation}$ ).
- **Measurable State Indicators ( $S$ ):** A vector of scalar values,  $S_{consensus}$ , reliably measured via a BFT consensus mechanism (the  $\mathcal{F}_{DCS}$  in Synergeia). These indicators reflect the current impact of perturbations  $D \in \mathcal{D}$  on the protocol’s state:

$$S_{consensus} = \{\Delta_{consensus}, L_{consensus}, \mathcal{S}_{threat}, \mathcal{H}_{chain}, \text{Participation\_Rate}, \dots\}$$

- **Adaptive Control Law ( $f$ ):** A function  $f : \Theta \times S \rightarrow \Theta$  that maps the current parameters  $\theta(t)$  and the measured state indicators  $S_{consensus}(t)$  to the updated parameters for the next control period  $\theta(t+1) = f(\theta(t), S_{consensus}(t))$ . This function embodies the protocol’s autonomous adaptation rules.

### 17.2 The Homeostasis Theorem

Let  $\mathcal{P}(\theta, D)$  represent the actual value (or vector of values) of the target protocol properties given parameters  $\theta$  and perturbation  $D$ . The objective is to maintain  $\mathcal{P}(\theta, D) \approx \mathcal{P}_{target}$  for all expected  $D$ .

**Theorem 13 (Adaptive Protocol Homeostasis).** *A protocol can maintain a set of properties  $\mathcal{P}$  in a stable state  $\mathcal{P} \approx \mathcal{P}_{target}$  against a defined set of perturbations  $\mathcal{D}$  if the following conditions are met:*

1. **Observability:** Deviations from the target state,  $\Delta\mathcal{P} = \mathcal{P}(\theta, D) - \mathcal{P}_{target}$ , induced by perturbations  $D \in \mathcal{D}$ , must be reliably detectable through measurable changes in the state indicators  $S_{consensus}$ .
2. **Controllability:** There must exist an adaptive control law  $\theta(t+1) = f(\theta(t), S_{consensus}(t))$  such that the parameter adjustments  $\Delta\theta = \theta(t+1) - \theta(t)$  consistently generate a counteracting effect  $-\Delta\mathcal{P}$  sufficient to restore the system towards  $\mathcal{P}_{target}$ .
3. **Stability:** The closed-loop feedback system—comprising the protocol’s internal dynamics, the external perturbations, the measurement mechanism ( $\mathcal{F}_{DCS}$ ), and the control law ( $f$ )—must be mathematically stable. This means that perturbations lead to transient deviations that decay over time, ensuring convergence back to the target state (as demonstrated for the 50/50 split in Section 14.7).

### 17.3 Homeostasis in Synergeia

This principle provides a unifying lens through which to view Synergeia’s adaptive architecture. Each major adaptive mechanism represents a specific instantiation of this principle, targeting a particular potential instability:

Table 4: Adaptive Homeostasis Mechanisms in Synergeia.

| Target Invariance $\mathcal{P}_{target}$                     | Perturbation $D$                              | Measured Indicator $S_{consensus}$       | Control Law $f$ Adjusting $\theta$                                                              |
|--------------------------------------------------------------|-----------------------------------------------|------------------------------------------|-------------------------------------------------------------------------------------------------|
| Security Condition ( $\psi > \Delta$ )                       | Network Delay Fluctuation Attack ( $\Delta$ ) | $\Delta_{consensus}$ (Delay Beacons)     | $\psi_{new} \leftarrow \Delta_{consensus} + \mathcal{M}_{safety}$                               |
| Resource Balance                                             | Market Shocks and Strategic Reallocation      | Observed Block Proportion $P_{PoW}$      | $f'_{A,*}$ via Proportional Control ( $\kappa$ ); $f''_{A,*}$ via Stability Scaling ( $\beta$ ) |
| Oracle Integrity ( $\alpha_{honest\_part} > \theta_{part}$ ) | Rational Apathy and Sybil Attack              | Beacon Participation Rate                | Adaptive Beacon Bounty Size                                                                     |
| ASW Economic Security                                        | Forking Attacks and Private Mining            | $S_{threat}$ (Security Beacons)          | $\beta_{burn}(t) = f(S_{threat})$                                                               |
| Exploit Resilience (vs. Oscillations)                        | Strategic Exploitation of Predictable $N$     | $S_{threat}$ (Security Beacons)          | $N_{new} = f(S_{threat})$                                                                       |
| Burst Stability                                              | Tip Contention and Selfish Mining             | $\mathcal{H}_{chain}$ (Topology Beacons) | $Fee_{burst\_threshold}(t) = f(\mathcal{H}_{chain})$                                            |
| Throughput vs. Security Trade-off                            | Transaction Load Fluctuation ( $L$ )          | $L_{consensus}$ (Load Beacons)           | $\mu_{target}(t) = f(L_{consensus}, \psi_{new})$ ; $M_{req}(t) = f(\mu_{target}, \psi_{new})$   |

Table 4 summarizes how each identified perturbation is linked to a measurable indicator via the  $\mathcal{F}_{DCS}$ , which then drives a specific control law adjusting relevant protocol parameters to maintain the target invariant property.

### 17.4 Implications

Framing Synergeia’s design through the Principle of Adaptive Protocol Homeostasis highlights several key aspects:

- **Justification for Complexity:** The protocol’s complexity arises directly from implementing the necessary sensors ( $S_{consensus}$  via  $\mathcal{F}_{DCS}$ ) and actuators ( $f$  via adaptive rules) required to achieve homeostasis against a wide range of perturbations. It replaces static, fragile assumptions with dynamic, robust control loops.
- **Centrality of the  $\mathcal{F}_{DCS}$ :** The Decentralized Consensus Service is the lynchpin of this entire framework. It acts as the protocol’s sensory system, providing the necessary BFT-robust measurements of the system’s internal and external state to enable effective feedback control. Its integrity, ensured by mechanisms like Beacon Bounties, is paramount.
- **A Methodology for Future Design:** This principle offers a potential methodology for designing future resilient protocols: identify target invariants, anticipate perturbations, design measurable indicators, and implement stable control laws.

By actively measuring its environment and internal state, and implementing corrective feedback loops, Synergeia strives to achieve a dynamic equilibrium, maintaining its core security and performance guarantees in the face of the inherent uncertainty and potential hostility of a permissionless network.

## 18 Conclusion

The Synergeia protocol successfully achieves a novel synthesis of PoW and PoS resources, overcoming the inherent speed and security trade-offs of legacy Nakamoto consensus. Our contributions are both theoretical and practical.

*Theoretical Breakthrough.* We have established a new security bound for longest-chain protocols by proving that the shift to a Rayleigh distribution via the LDD mechanism enables super-exponential (quadratic) consistency:  $\epsilon \approx \exp(-\Omega(k^2))$ . This is a significant theoretical advance over the asymptotic linear bound that characterizes existing protocols [19,15], demonstrating that the speed of probabilistic finality is not a fixed constant but a designable parameter of the system.

*Robust System Design.* We have presented a complete protocol design that realizes this theoretical speedup in a stable and secure manner. The Dynamic Slope Adjustment Scheme, analyzed through the lens of control theory, ensures the protocol's algorithmic and economic stability. Furthermore, our comprehensive security analysis addresses a wide range of sophisticated adversarial strategies, from the game-theoretic exploitation of predictable system oscillations to the fine-grained combinatorial complexities of costless simulation and LDD-grinding.

Ultimately, this paper demonstrates that the stochastic process governing block production is not merely an environmental variable to be analyzed, but a core architectural component that can be actively engineered. By moving beyond the memoryless Poisson model, Synergeia opens a new design space for future consensus protocols, where the trade-offs between speed, security, and decentralization can be navigated with greater precision and purpose.

- **Super-Linear Consistency:** The LDD-induced Rayleigh distribution enables a super-linear consistency bound,  $\epsilon \approx \exp(-\Omega(k^{2-\eta_d}))$ .
- **Robust Probabilistic Finality:** The full security model requires  $k = 26$  confirmations, delivering a typical finality time of approximately **6.5 minutes** under realistic network conditions.
- **Autonomous Stability:** The protocol's stability is ensured by the **Accumulated Synergistic Work (ASW)** metric, secured by Proof-of-Burn, and a fully autonomous LDD control system that maintains a stable 15-second block time and an optimal 50/50 PoW/PoS block proportion by adapting to measured network delay and load.
- **Optional Instant Settlement:** The Burst Finality mechanism offers a secure pathway to execution-driven confirmation in approximately **5 seconds** for high-value transactions.

**Future Work** The development of Synergeia opens several promising avenues for future research that build upon the protocol's rich suite of features.

*Empirical Validation of Burst Finality.* While we have provided a theoretical model and performance estimate for the Burst Finality mechanism, its real-world behavior depends on the complex interplay of network latency, participant incentives, and fork-choice dynamics. A large-scale testnet implementation is necessary to empirically validate the claimed 5 second finality time and to test the resilience of its economic deterrent against sophisticated, rational adversaries. Such an environment would allow for stress-testing the ASW fork-choice rule under the high-velocity, high-incentive conditions of Burst Mode and provide invaluable data for calibrating the  $Fee_{burst\_threshold}$  parameter.

*Formal Analysis of the Deviation Parameter.* Our super-linear consistency bound is given by  $\epsilon \approx \exp(-\Omega(k^{2-\eta_d}))$ . Throughout this paper, we have qualitatively argued that  $\eta_d$  is a small positive constant arising from practical deviations from the ideal Rayleigh model and adversarial strategies like LDD-grinding. A rigorous theoretical analysis to formally bound the precise value of  $\eta_d$  as a function of adversarial power, network conditions, and LDD parameters would be a significant contribution to the understanding of engineered consensus systems. This would involve a deeper analysis of the stochastic process generated by the piecewise "snowplow" curve and could potentially lead to the design of alternative difficulty curves that provably minimize  $\eta_d$ , thereby pushing the consistency exponent closer to or, perhaps, even greater than the established theoretical maximum of 2.

*Dynamic Calibration of Additional Parameters.* The protocol's robustness can be further enhanced by transitioning key static parameters into dynamic variables that are algorithmically adjusted by the Decentralized Consensus Service ( $\mathcal{F}_{DCS}$ ). This would create a protocol that not only adapts its speed and difficulty to network conditions but also tunes its own security and efficiency parameters in real time.

### 18.1 Beyond the Snowplow: The Design Space of Difficulty Curves

The snowplow curve, as implemented in both Taktikos and Synergeia, was conceived as an analytically tractable, first-order approximation of a more desirable time-dependent difficulty function. Its success in generating a Rayleigh-like distribution, which in turn enables quadratic consistency, is a powerful result. However, this success suggests that the snowplow is likely not the only, nor necessarily the optimal, difficulty curve. This opens up a rich and unexplored design space for future research.

*Alternative Analytic Distributions.* One avenue of research is the design of new, analytically tractable difficulty curves that produce other "light-tailed" block arrival distributions. For example, the Weibull distribution, with a survival function of the form  $S(x) = \exp(-(x/\lambda)^n)$ , is a generalization of the Rayleigh distribution (which corresponds to  $n = 2$ ). If a difficulty curve could be engineered to produce a Weibull distribution with a shape parameter  $n > 2$ , it would theoretically enable an even faster consistency bound of  $\epsilon \approx \exp(-\Omega(t^n))$  (e.g., cubic consistency for  $n = 3$ ). The challenge lies in deriving the hazard rate function corresponding to such a distribution and designing a practical, piecewise function to approximate it.

*Numerically Optimized Curves.* A second, more ambitious, direction is to move beyond analytically defined curves altogether. One could frame the design of the difficulty curve  $f(\delta)$  as a multi-objective optimization problem. Using numerical methods or machine learning, one could search for a curve that optimizes for a set of desirable properties, such as:

- **Maximizing the Consistency Exponent:** Finding the curve shape that produces the lightest possible tail on the block arrival distribution.
- **Minimizing Block Time Variance:** Finding a curve that maintains a strong consistency bound while also minimizing the variance of the block time, leading to a more predictable network.
- **Maximizing Censorship Resistance:** Designing a curve with a specific "recovery phase" shape that guarantees a minority of participants can eventually produce a block, even in the face of a majority attempting to censor them by refusing to produce blocks.
- **Dynamic Congestion Control:** Designing curves that can dynamically change their shape in response to network load (as measured by the  $\mathcal{F}_{DCS}$ ), becoming "sharper" to reduce forking during periods of high congestion.

This line of inquiry would treat the difficulty curve not as a static component, but as a dynamic, programmable element of consensus, opening the door to protocols that can adapt their fundamental stochastic properties in real time.

### 18.2 Resilience to Quantum Adversaries

The long-term security of any blockchain protocol must be considered in the context of advancements in quantum computing. Synergeia, by design, inherits a security posture against quantum threats that is analogous to that of Bitcoin, as it is built upon the same classes of cryptographic primitives [1]. The resilience of the protocol can be analyzed by examining its core components: the Proof-of-Work hashing algorithm, the digital signature scheme, and the Verifiable Random Function (VRF) used for Proof-of-Stake leader election.

*Proof-of-Work Hashing (SHA-256).* The security of the PoW mechanism relies on the preimage resistance of the SHA-256 hash function. The most relevant quantum threat to this primitive is Grover's algorithm, a quantum search algorithm that provides a quadratic speedup for unstructured search problems [24]. While a classical computer requires on the order of  $2^{256}$  operations to find a preimage for SHA-256, a quantum computer using Grover's algorithm could theoretically achieve this in approximately  $2^{128}$  operations [24,1].

However, a search space of  $2^{128}$  is still considered computationally infeasible for any foreseeable quantum computer [1,12]. Therefore, the PoW component of Synergeia is not considered to be at risk from near-term quantum threats. The security is effectively halved, but it remains well within the bounds of practical security. Furthermore, the extreme speed of current specialized ASIC miners compared to the projected clock speeds of near-term quantum computers is likely to negate this theoretical quadratic speedup in practice for the foreseeable future [1].

*Digital Signatures and VRFs (Elliptic Curve Cryptography).* The more significant quantum threat lies in Shor's algorithm [42]. Synergeia's security, like Bitcoin's, relies on the Elliptic Curve Digital Signature Algorithm (ECDSA) for transaction authorization and, critically, on an Elliptic Curve VRF (ECVRF) for PoS leader election [23]. Both of these primitives derive their security from the hardness of the Elliptic Curve Discrete Logarithm Problem (ECDLP) [42].

Shor's algorithm can solve the ECDLP in polynomial time, which would allow a sufficiently powerful quantum computer to derive a private key from a public key [42,39]. This would compromise the security of user funds (via ECDSA) and the integrity of the PoS leader election (via ECVRF). While some properties of an ECVRF, such as uniqueness, may not be broken by quantum computers, the core pseudorandomness property would be compromised, allowing an adversary to predict leader schedules and potentially forge proofs [38].

This vulnerability is not unique to Synergeia but is a systemic, long-term risk for the entire blockchain industry [1,27]. The consensus among cryptographers is that this threat is still years or decades away, as it would require a quantum computer with thousands of stable, error-corrected logical qubits [1,22]. The urgency to address this is driven by the "harvest now, decrypt later" threat model, where adversaries may be storing encrypted data today with the intent of decrypting it once a capable quantum computer is available [27].

*Mitigation via Post-Quantum Cryptography.* The long-term solution for this threat is a transition to post-quantum cryptographic (PQC) standards. This is an active area of research led by institutions like the U.S. National Institute of Standards and Technology (NIST), which has recently finalized the first standards for quantum-resistant algorithms [36]. The migration path for Synergeia would involve replacing its elliptic curve-based primitives with these new standards:

- **Digital Signatures:** ECDSA would be replaced by a standardized PQC signature algorithm, such as ML-DSA (CRYSTALS-Dilithium) or the backup SLH-DSA (SPHINCS+) [36,7,8]. These algorithms are based on different mathematical problems (structured lattices and hash functions, respectively) that are believed to be resistant to attack by both classical and quantum computers.
- **Verifiable Random Functions:** The ECVRF would need to be replaced with a post-quantum VRF. Research in this area is ongoing, with promising constructions based on symmetric-key primitives and quantum-secure zero-knowledge proof systems [16].

While the transition to PQC is a significant engineering challenge, particularly for a decentralized protocol, it provides a clear and necessary path to ensure the long-term security of Synergeia against future quantum adversaries.

### 18.3 Re-evaluating Ouroboros Taktikos: From Performance to Quadratic Consistency

The Local Dynamic Difficulty (LDD) mechanism, first introduced in Ouroboros Taktikos [41], was originally conceived as a tool for performance optimization. Its stated goal was to regularize block production, increase throughput, and reduce block latency by concentrating block production into a predictable "forging window" [41]. The security analysis in that context focused on bounding the marginal advantage an adversary could gain from grinding within static epochs.

The security proofs developed in this paper for Synergeia, however, reveal a previously unexplored and arguably more powerful application of the LDD mechanism. By demonstrating that a specific LDD curve (the snowplow) can reshape the block arrival process into a Rayleigh distribution, we have shown that LDD can be a tool for achieving super-exponential consistency. This raises a critical question: is this security property an emergent feature of the hybrid PoW/PoS architecture, or is it an inherent property of LDD itself that could be applied in a pure PoS setting?

A compelling direction for future work is therefore to formally re-evaluate the Ouroboros Taktikos protocol as a standalone, pure PoS system with the explicit goal of achieving a super-linear consistency bound. This would require a new security analysis that adapts the proofs from this paper to the epoch-based randomness model of Taktikos, where epochs, rather than PoW blocks, serve as the anchor for VRF domains. Such an analysis would need to rigorously determine if the stability of epoch-based nonces is sufficient to maintain a Rayleigh-like distribution and quantify the resulting consistency exponent. This research could potentially elevate Taktikos from a performance-enhanced PoS protocol to one with a fundamentally stronger security guarantee than its predecessors in the Ouroboros family.

**Implications for Pure Proof-of-Stake: Super-Linear Consistency via LDD** The security proofs developed for Synergeia demonstrate that the LDD mechanism can reshape the block arrival process into a Rayleigh distribution, enabling a super-exponential consistency bound. This raises a critical question: is this security property an emergent feature of the hybrid architecture, or is it an inherent property of LDD itself that could be applied in a pure PoS setting? This section provides a formal security analysis of Ouroboros Taktikos [41]—the protocol that introduced LDD—to demonstrate that LDD is indeed capable of achieving a super-linear consistency bound in a pure PoS context.

**The Taktikos Stochastic Model in Pure PoS** Ouroboros Taktikos operates in discrete time slots grouped into epochs. Eligibility is determined by a VRF and the LDD mechanism. We identify key differences from the Synergeia model that impact the security analysis.

**Epoch-Based Randomness** Unlike Synergeia, which anchors its VRF randomness to high-entropy PoW blocks, Taktikos derives its randomness from an epoch nonce generated via a secure multiparty computation (MPC) protocol [15]. This creates a static VRF domain for the duration of an entire epoch. The computationally cheaper nature of the MPC protocol compared to PoW makes this randomness source potentially more vulnerable to long-range grinding attacks, where an adversary attempts to influence the outcome of the nonce generation itself.

**LDD and State-Dependent Grinding** The LDD mechanism in Taktikos is implemented via the same snowplow curve  $f(\delta)$  used in Synergeia [41]. This creates a non-trivial decision tree for an adversary engaging in costless simulation on a private fork. By choosing to produce or withhold a PoS block, the adversary manipulates  $\delta$  for subsequent slots, altering future eligibility probabilities. This state-dependent grinding surface can be modeled as a dynamic programming problem (as analyzed in Section 11.8). An optimal adversary will maximize their block production rate within a static epoch, gaining a marginal, constant-factor advantage.

**Proof of Super-Linear Consistency** We now adapt the consistency proof from Synergeia (Section 7) to the pure PoS setting of Taktikos.

**Theorem 14.** *For the Ouroboros Taktikos protocol, the probability of a consistency violation at depth  $k$  is bounded by:*

$$\epsilon(k) \leq \exp(-\Omega(k^{2-\eta_d}))$$

where  $\eta_d$  is a small positive constant ( $0 < \eta_d < 1$ ) representing the degradation from an ideal quadratic bound.

*Proof.* The proof structure follows that of Theorem 2. A consistency violation at depth  $k$  requires an adversary to produce a private chain of length  $k$  in time  $T_A^*(k)$  (using an optimal LDD-grinding strategy) and for the honest network to remain silent. The probability is bounded by  $\epsilon(k) \leq P(T_H > T_A^*(k))$ .

The LDD mechanism forces the honest block inter-arrival time to approximate a Rayleigh distribution. However, unlike in the PoW-anchored Synergeia model, the block arrival distribution in Taktikos is subject to subtle adversarial influence, preventing it from being a perfect Rayleigh distribution. We model this deviation by introducing a degradation factor  $\eta_d$  into the exponent of the honest survival function, such that  $S_H(t) \approx \exp(-M_H t^{2-\eta_d}/2)$ .

The adversary's expected time  $\mu_k^* = \mathbb{E}[T_A^*(k)]$  scales linearly with  $k$ . Applying concentration inequalities, the dominant term in the bound is:

$$\epsilon(k) \leq S_H(\mu_k^*) \approx \exp\left(-\frac{M_H}{2}(\mu_k^*)^{2-\eta_d}\right) \propto \exp(-C' \cdot k^{2-\eta_d})$$

The degradation factor  $\eta_d > 0$  arises from two sources:

1. **Randomness Grinding:** The vulnerability of the epoch nonce to adversarial influence allows for a slight biasing of the leader election schedule, causing the true block arrival distribution to have a slightly heavier tail than an ideal Rayleigh distribution.
2. **LDD Grinding Advantage:** The constant-factor advantage gained from the optimal LDD-grinding strategy, while not breaking the super-linear bound, contributes to the degradation of the exponent by slightly reducing  $\mu_k^*$ .

A full derivation requires formally bounding  $\eta_d$  as a function of the epoch length and the security parameters of the nonce-generation protocol.

**Discussion** This analysis demonstrates that the LDD mechanism, previously understood as a performance enhancement, is capable of achieving a provably super-linear consistency bound in a pure PoS setting. This result shows that Taktikos is fundamentally more secure than its predecessors, such as Praos, which only achieve a linear bound [9]. This opens a new design space for pure PoS protocols focused on minimizing  $\eta_d$  to push the consistency bound as close as possible to pure quadratic.

#### 18.4 The Homeostasis Theorem as a Model for Physical Law

The design of Synergeia is predicated on a principle we have termed Adaptive Protocol Homeostasis (APH). This principle posits that a system can maintain a set of invariant properties—such as security, liveness, and a stable rate of growth—in the face of external perturbations and internal strategic action by implementing a closed-loop system of observation, control, and adaptation. The Homeostasis Theorem provides the formal conditions for such a system’s stability: Observability, Controllability, and Stability. While this framework was developed for the specific domain of distributed consensus, its underlying mathematical abstractions possess a striking universality, suggesting a deeper connection to the modeling of complex systems across various computational and physical disciplines.

**From Protocol Security to Statistical Mechanics** At its core, the security of a longest-chain protocol is a problem in statistical mechanics. The protocol’s state space is the set of all possible blockchain histories, analogous to the microstates of a physical system. A consistency violation—a fork that successfully rewrites history—is a rare fluctuation, a transient deviation from the system’s thermodynamic equilibrium. Traditional Nakamoto consensus models this process as a memoryless random walk, where block arrivals follow a Poisson process. The resulting exponential distribution of inter-arrival times is the source of the linear consistency bound,  $\exp(-\Omega(k))$ . This is analogous to a system of non-interacting particles in an empty void; their behavior is governed by pure, unstructured randomness. The only force driving the system toward equilibrium (a single, canonical chain) is the honest majority’s slightly higher rate of block emission. The central innovation of Synergeia is the assertion that this stochastic void is not a given, but a designable medium. The Local Dynamic Difficulty (LDD) mechanism, through the engineered hazard rate of the snowplow curve, acts as a time-dependent potential field,  $V(\delta)$ , where  $\delta$  is the time since the last event. This potential is engineered to be infinitely high near  $\delta = 0$  (the slot gap,  $\psi$ ) and to have a minimum at a specific target time, concentrating the probability of an event. The resulting Rayleigh distribution is the emergent statistical behavior of a system with memory and interaction, where the probability of a future event is explicitly conditioned on the time elapsed since the last. This is analogous to a transition from a model of free particles to one of interacting quasi-particles, whose collective behavior is fundamentally different. The security proof, therefore, moves beyond simple random walk theory into the domain of large deviation theory. The two-term consistency bound,  $\epsilon(k) \leq \exp(-C_1 k^2) + \exp(-C_2 k)$ , is a statement about two distinct types of fluctuation. The quadratic term,  $\exp(-C_1 k^2)$ , bounds the probability of an environmental fluctuation—the spontaneous silence of the honest network. This is analogous to calculating the probability of a macroscopic violation of the Second Law of Thermodynamics, a fluctuation that becomes quadratically less likely as the system size (in our case, the confirmation depth  $k$ ) increases. The linear term,  $\exp(-C_2 k)$ , bounds the probability of a block-specific fluctuation—a lucky adversary mining much faster than their expected rate. This is bounded using concentration inequalities like the Chernoff bound, a tool used across computational disciplines to understand the likelihood of a Monte-Carlo simulation or a randomized algorithm deviating significantly from its expected outcome.

**Control Theory as a Universal Grammar of Stability** If the LDD mechanism is the physics of the system, then the suite of adaptive mechanisms governed by the Decentralized Consensus Service ( $\mathcal{F}_{DCS}$ ) is the system’s observer. The Homeostasis Theorem’s conditions of Observability and Controllability are the cornerstones of control theory. The  $\mathcal{F}_{DCS}$  acts as the protocol’s sensory organ, providing BFT-robust measurements of the system’s state variables—network delay ( $\Delta$ ), transaction load ( $L$ ), and adversarial pressure ( $\mathcal{S}_{threat}$ ). These are the protocol’s equivalent of measuring the temperature, pressure, and chemical composition of a reaction. The adaptive control laws, such as the dynamic adjustment of the slot gap ( $\psi \leftarrow \Delta_{consensus} + \mathcal{M}_{safety}$ ) and the balancing of PoW/PoS difficulty, are the system’s actuators. They implement a negative feedback loop, a universal strategy for maintaining stability. This is the same principle that governs a thermostat maintaining room temperature, a particle accelerator’s magnets adjusting to keep a beam focused, or a biological organism regulating its internal chemistry. The mathematical language—proportional-integral-derivative (PID) controllers, delay differential equations, and

Lyapunov stability analysis—is the same. The stability of the 50/50 resource split as an Evolutionarily Stable Strategy (ESS) is a proof that this feedback loop successfully guides the system's game-theoretic dynamics toward a stable, low-energy fixed point.

**Physical Analogies and the Observer Problem** This framework allows us to draw powerful analogies to fundamental physics. The space of all possible consensus rules can be viewed as an array of computational systems. Most of these rules produce chaotic, unstable, or useless ledgers that collapse into irrevocable states of inconsistency or suffer from extinction due to a lack of liveness. The question then arises: why should a protocol, or any physical model for that matter, be governed by simple rules? The Homeostasis Theorem suggests a possible answer through an evolutionary selection principle. A system can only persist long enough to be observed if it possesses homeostatic properties. For example, a cosmological model whose fundamental constants were not finely tuned, or a blockchain protocol with static parameters in a dynamic environment would be useless without intervention and careful consideration of the parameter space. It is quickly destroyed by its own internal fluctuations or external perturbations. The systems that survive—and are thus available for observation by physicists or for use by blockchain participants—are those that satisfy the Homeostasis Theorem. They must be able to "observe" their own state and "control" their own evolution to counteract instability. The laws of physics we perceive may not be the only possible rules, but rather the emergent, stable control laws of a self-regulating computational system. The search for a fundamental theory of physics and the engineering of a robust consensus protocol may, in this abstract sense, be the same problem: the search for a stable, self-correcting computational rule in the vast space of all possible rules.

**Acknowledgments.** This document was developed independently by Aaron Moore Schutza. I'd like to thank Sean Cheatham for valuable discussions that inspired and directly helped me in adapting Taktikos to the Proof-of-Work setting. I would also like to acknowledge the pioneering research efforts of Aggelos Kiayias and Juan Garay that lit the way to developing Synergieia.

**Disclosure of Interests.** The author of this document has no competing interests.

## References

1. Aggarwal, D., Brennen, G.K., Lee, T., Santha, M., Tomamichel, M.: Quantum attacks on bitcoin, and how to protect against them. *Ledger* **3**, 68–90 (2018). <https://doi.org/10.5195/ledger.2018.127>, eprint = arXiv:1710.10377
2. Anceaume, E., Ludinard, R., Potop-Butucaru, M., Tucci-Piergiovanni, S.: Finality in blockchain. In: 2020 IEEE International Conference on Blockchain and Cryptocurrency (ICBC). pp. 1–9 (2020)
3. Andrade, G., Ramalho, G., Santana, H., Corruble, V.: Challenge-sensitive action selection: an application to game balancing. In: Proceedings of the IEEE/WIC/ACM International Conference on Intelligent Agent Technology. pp. 219–225 (2005)
4. Apostolaki, M., Zohar, A., Vanbever, L.: Hijacking bitcoin: Routing attacks on cryptocurrencies. In: 2017 IEEE Symposium on Security and Privacy (SP). pp. 375–392 (2017)
5. Arnosti, N., Weinberg, S.M.: Bitcoin: A game-theoretic analysis. *CoRR* **abs/2108.03703** (2021)
6. Badertscher, C., Gaži, P., Kiayias, A., Russell, A., Zikas, V.: Ouroboros chronos: Permissionless clock synchronization via proof-of-stake. In: Advances in Cryptology – EUROCRYPT 2021. pp. 543–574. Springer (2021)
7. Bai, S., Ducas, L., Kiltz, E., Lepoint, T., Lyubashevsky, V., Schwabe, P., Seiler, G., Stehlé, D.: CRYSTALS-Dilithium: Algorithm Specification and Supporting Documentation (Version 3.1). Round 3 submission to the NIST Post-Quantum Cryptography Standardization Project (2020), <https://pq-crystals.org/dilithium/>
8. Bernstein, D.J., et al.: The SPHINCS+ signature framework. In: Proceedings of the 2019 ACM SIGSAC Conference on Computer and Communications Security. pp. 2129–2146. ACM (2019). <https://doi.org/10.1145/3319535.3363229>
9. Blum, E., Kiayias, A., Moore, C., Quader, S., Russell, A.: The combinatorics of the longest-chain rule: Linear consistency for proof-of-stake blockchains. In: Proceedings of the 2020 ACM-SIAM Symposium on Discrete Algorithms (SODA). pp. 2646–2665 (2020)
10. Bowden, R., Keeler, H.P., Krzesinski, A.E., Taylor, P.G.: Modeling and analysis of block arrival times in the bitcoin blockchain. *Stochastic Models* **36**(4), 602–637 (2020)
11. Castro, M., Liskov, B.: Practical byzantine fault tolerance. In: Proceedings of the Third Symposium on Operating Systems Design and Implementation (OSDI '99). pp. 173–186 (1999)
12. Chen, L., Jordan, S., Liu, Y.K., Moody, D., Peralta, R., Perlner, R., Smith-Tone, D.: Report on post-quantum cryptography. Tech. rep., National Institute of Standards and Technology (2016). <https://doi.org/10.6028/NIST.IR.8105>

13. Chernoff, H.: A measure of asymptotic efficiency for tests of a hypothesis based on the sum of observations. *The Annals of Mathematical Statistics* **23**(4), 493–507 (1952)
14. Croman, K., Decker, C., Eyal, I., Gencer, A.E., Juels, A., Kosba, A., Miller, A., Saxena, P., Shi, E., Sirer, E.G., Song, D., Wattenhofer, R.: On scaling decentralized blockchains (a position paper). In: Rohloff, K., Clark, J., Meiklejohn, S., Wallach, D., Brenner, M., Ryan, P.Y. (eds.) *Financial Cryptography and Data Security - International Workshops, FC 2016, BITCOIN, VOTING, and WAHC, Revised Selected Papers*. pp. 106–125. Springer (2016)
15. David, B., Gaži, P., Kiayias, A., Russell, A.: Ouroboros praos: An adaptively-secure, semi-synchronous proof-of-stake blockchain. In: *Advances in Cryptology – EUROCRYPT 2018*. pp. 66–98 (2018)
16. Esgin, M.F., Steinfeld, R., Zhao, R.K.: Post-quantum VRF and its applications in future-proof blockchain system. In: *2021 IEEE Symposium on Security and Privacy (SP)*. pp. 110–127. IEEE (2021). <https://doi.org/10.1109/SP40001.2021.00069>
17. Eyal, I., Sirer, E.G.: Majority is not enough: Bitcoin mining is vulnerable. In: *Financial Cryptography and Data Security*. pp. 436–454. Springer (2014)
18. Feller, W.: *An Introduction to Probability Theory and Its Applications, Volume I*. John Wiley & Sons, third edn. (1968)
19. Garay, J.A., Kiayias, A., Leonardos, N.: The bitcoin backbone protocol: Analysis and applications. In: *Advances in Cryptology – EUROCRYPT 2015*. pp. 281–310 (2015)
20. Garay, J.A., Kiayias, A., Shen, Y.: Permissionless clock synchronization with public setup. In: *Theory of Cryptography Conference (TCC)*. pp. 181–211 (2022)
21. Gervais, A., Karame, G.O., Wüst, K., Glykantzis, V., Ritzdorf, H., Capkun, S.: On the security and performance of proof of work blockchains. In: *Proceedings of the 2016 ACM SIGSAC Conference on Computer and Communications Security*. pp. 3–16 (2016)
22. Gidney, C., Ekerå, M.: How to factor 2048 bit rsa integers in 8 hours using 20 million noisy qubits. *Quantum* **5**, 433 (2021). <https://doi.org/10.22331/q-2021-04-15-433>
23. Goldberg, S., Papadopoulos, D., Hu, J.V.L., Fedorov, S., Kogan, D.: Verifiable random functions (vrf). Internet-draft, Internet Engineering Task Force (2022), work in Progress, draft-irtf-cfrg-vrf-15
24. Grover, L.K.: A fast quantum mechanical algorithm for database search. In: *Proceedings of the Twenty-eighth Annual ACM Symposium on Theory of Computing*. pp. 212–219. ACM (1996). <https://doi.org/10.1145/237814.237866>
25. Hoeffding, W.: Probability inequalities for sums of bounded random variables. *Journal of the American Statistical Association* **58**(301), 13–30 (1963)
26. Hunicke, R., Zubek, R.: The case for dynamic difficulty adjustment in games. In: *Proceedings of the 2005 ACM SIGCHI International Conference on Advances in computer entertainment technology*. pp. 429–433. ACE '05, ACM, New York, NY, USA (2005)
27. IBM Research: Nist pqc standards: A new era in cybersecurity. Blog Post (2024), accessed: October 27, 2025. <https://research.ibm.com/blog/nist-pqc-standards>
28. Kiayias, A., Russell, A., David, B., Oliynykov, R.: Ouroboros: A provably secure proof-of-stake blockchain protocol. In: *Advances in Cryptology – CRYPTO 2017*. pp. 357–388 (2017)
29. King, S., Nadal, S.: Ppcoint: Peer-to-peer crypto-currency with proof-of-stake (2012), self-Published
30. Kraft, D.: Difficulty control for blockchain-based consensus systems. *Peer-to-Peer Networking and Applications* **9**(2), 397–413 (2016)
31. Lin, S., Liu, X., Ma, X., Mao, H., Zhang, Z., Khan, S., Zhu, L.: The impact of network delay on nakamoto consensus mechanism. *Electronic Research Archive* **30**(10), 3735–3754 (2022)
32. Liu, Y., Lu, Y., Nayak, K., Zhang, F., Zhang, L., Zhao, Y.: Empirical analysis of eip-1559: Transaction fees, waiting times, and consensus security. In: *Proceedings of the 2022 ACM SIGSAC Conference on Computer and Communications Security*. p. 2099–2113. CCS '22, Association for Computing Machinery, New York, NY, USA (2022). <https://doi.org/10.1145/3548606.3559341>
33. Mackenzie, A.: Decred. <https://docs.decred.org/> (dcrdocs v003 Decred Project 2016–2025), memcoin2: A Hybrid Proof-of-Work, Proof-of-Stake Crypto-Currency
34. Micali, S., Rabin, M., Vadhan, S.P.: Verifiable random functions. In: *40th Annual Symposium on Foundations of Computer Science (FOCS '99)*. pp. 120–130 (1999)
35. Nakamoto, S.: Bitcoin: A peer-to-peer electronic cash system (2008), <https://bitcoin.org/bitcoin.pdf>
36. National Institute of Standards and Technology: Nist releases first 3 finalized post-quantum encryption standards. Press Release (August 2024), accessed: October 27, 2025. <https://www.nist.gov/news-events/news/2024/08/nist-releases-first-3-finalized-post-quantum-encryption-standards>
37. Nayak, K., Kumar, S., Miller, A., Shi, E.: Stubborn mining: Generalizing selfish mining and combining with an eclipse attack. In: *2016 IEEE European Symposium on Security and Privacy (EuroS&P)*. pp. 305–320 (2016)
38. Peikert, C.: A security analysis of the ecvrf. In: Unpublished manuscript (2022), available at <https://web.eecs.umich.edu/~cpeikert/pubs/ecvrf-security.pdf>
39. Proos, J., Zalka, C.: Shor's discrete logarithm quantum algorithm for elliptic curves. *Quantum Info. Comput.* **3**(4), 317–344 (2003), eprint = quant-ph/0301141

40. Saad, M., Sinha, A., Saxena, P.: Selfish mining re-examined. In: Financial Cryptography and Data Security. pp. 61–78. Springer (2020)
41. Schutza, A.M., Behrens, H.W., Duong, T., Aman, J.A.: Ouroboros taktikos: Regularizing proof-of-stake via dynamic difficulty. In: Blockchain and Trustworthy Systems. pp. 269–283 (2024)
42. Shor, P.W.: Algorithms for quantum computation: Discrete logarithms and factoring. In: Proceedings of the 35th Annual Symposium on Foundations of Computer Science. pp. 124–134. IEEE (1994). <https://doi.org/10.1109/SFCS.1994.365700>

## A Formal Specification of Protocol Functions

This appendix provides a formal specification for the core functions and procedures referenced throughout the Synergeia protocol. These definitions are intended to provide an unambiguous guide for implementers. These functions govern how a node selects the canonical chain and validates new blocks.

### Function: Adaptive\_Target\_Slope

This function calculates the target mean block time based on the consensus network load, ensuring it remains safely above the adaptive slot gap.

- 1: **Input:** Consensus network load  $L_{consensus} \in [0, 1]$ , base target time  $\mu_{max}$ , adaptive slot gap  $\psi_{adaptive}$ , safety margin  $M_{safety}$ .
- 2:  $\mu_{floor} \leftarrow \psi_{adaptive} + M_{safety}$ . ▷ Calculate minimum safe block time
- 3:  $\mu_{range} \leftarrow \mu_{max} - \mu_{floor}$ .
- 4:  $\mu_{target} \leftarrow \mu_{max} - (\mu_{range} \cdot L_{consensus})$ . ▷ Linearly interpolate based on load
- 5: **Return:**  $\max(\mu_{floor}, \mu_{target})$ . ▷ Ensure target never violates safety floor

### Function: Update\_Baseline\_Difficulty

Adaptively updates the baseline difficulty parameters ( $f_B$ ) to ensure a secure fallback rate and prevent inversion with the primary amplitudes ( $f_A$ ).

- 1: **Input:** New primary amplitudes  $f_{A,PoW}, f_{A,PoS}$ , fallback target time  $T_{fallback}$ .
- 2: **Step 1: Calculate Fallback-Targeted Baseline**
  - 3:  $b_{total} \leftarrow 1/T_{fallback}$ . ▷ Total hazard rate for fallback
  - 4:  $M_{total} \leftarrow f_{A,PoW} + f_{A,PoS}$ . ▷ Total primary amplitude
  - 5: **if**  $M_{total} > 0$  **then**
    - 6:  $f_{B,PoW}^* \leftarrow b_{total} \cdot (f_{A,PoW}/M_{total})$ . ▷ Distribute proportionally
    - 7:  $f_{B,PoS}^* \leftarrow b_{total} \cdot (f_{A,PoS}/M_{total})$ .
  - 8: **else** ▷ Handle edge case where both primary amplitudes are zero
  - 9:  $f_{B,PoW}^* \leftarrow b_{total}/2$ .
  - 10:  $f_{B,PoS}^* \leftarrow b_{total}/2$ .
- 11: **end if**
- 12: **Step 2: Apply Security Constraint (No Inversion)**
  - 13:  $f_{B,PoW,final} \leftarrow \min(f_{B,PoW}^*, f_{A,PoW})$ .
  - 14:  $f_{B,PoS,final} \leftarrow \min(f_{B,PoS}^*, f_{A,PoS})$ .
- 15: **Return:**  $(f_{B,PoW,final}, f_{B,PoS,final})$ .

### Function: Adaptive\_Target\_Slope

This function adjusts the target mean block time based on network load to manage congestion.

- 1: **Input:** Network load metric  $L(h)$ , parameters  $\mu_{min}, \mu_{max}, \eta$ .
- 2:  $\mu_{target} \leftarrow \max(\mu_{min}, \mu_{max} - \eta \cdot L(h))$ .
- 3: **Return:**  $\mu_{target}$ .

**Function: Select \_ Longest \_ Chain**

This function implements the fork-choice rule. Given a set of candidate chains, it returns the one with the highest Accumulated Synergistic Work (ASW).

```

1: Input: A set of candidate chains $\mathcal{C} = \{\mathcal{C}_1, \mathcal{C}_2, \dots, \mathcal{C}_n\}$.
2: Initialize: $\mathcal{C}_{\text{best}} \leftarrow \text{null}$, $\text{ASW}_{\text{max}} \leftarrow -1$.
3: for all $\mathcal{C}_i \in \mathcal{C}$ do
4: $\text{ASW}_i \leftarrow \text{Calc_ASW}(\mathcal{C}_i)$.
5: if $\text{ASW}_i > \text{ASW}_{\text{max}}$ then
6: $\text{ASW}_{\text{max}} \leftarrow \text{ASW}_i$.
7: $\mathcal{C}_{\text{best}} \leftarrow \mathcal{C}_i$.
8: end if
9: end for
10: Return: $\mathcal{C}_{\text{best}}$.
```

**Function: Calc \_ ASW**

This function calculates the total Accumulated Synergistic Work of a given chain.

```

1: Input: A chain $\mathcal{C} = (B_1, B_2, \dots, B_L)$.
2: Initialize: $\text{ASW}_{\text{total}} \leftarrow 0$.
3: for all block $B_k \in \mathcal{C}$ do
4: if B_k is a PoW block then
5: $\text{Work} \leftarrow 1/\text{Target}(B_k)$. ▷ Inverse of the numeric PoW target
6: $\text{ASW}_{\text{total}} \leftarrow \text{ASW}_{\text{total}} + \text{Work}$.
7: else if B_k is a PoS block then
8: $S_{\text{total}} \leftarrow B_k.\text{header.total_stake}$. ▷ Value committed in block header
9: $\alpha_{V_k} \leftarrow \text{Stake}(V_k)/S_{\text{total}}$. ▷ Validator's relative stake
10: $\text{Value} \leftarrow \text{Block_Reward} + \sum_{tx \in B_k} \text{Fee}(tx)$.
11: $\text{Commitment} \leftarrow \alpha_{V_k} \cdot \text{Value}$.
12: $\text{ASW}_{\text{total}} \leftarrow \text{ASW}_{\text{total}} + \text{Commitment}$.
13: end if
14: end for
15: Return: $\text{ASW}_{\text{total}}$.
```

**Procedure: Produce \_ Time \_ Beacon**

This procedure is run concurrently by a PoW miner during the main mining loop.

```

1: Input: Block header template H_{template} , beacon target $\mathcal{T}_{\text{beacon}}$.
2: In Mining Loop (for each nonce):
3: $h \leftarrow \text{Hash}(H_{\text{template}} \parallel \text{nonce})$.
4: if $h < \mathcal{T}_{\text{beacon}}$ then
5: $t_{\text{local}} \leftarrow \text{local_clock.time}()$.
6: $b_t \leftarrow (\text{beacon_type} = \text{TIME}, t_{\text{local}}, \text{miner_id})$.
7: $\text{sig} \leftarrow \text{Sign}(b_t, \text{miner_private_key})$.
8: Broadcast(beacon = b_t , signature = sig).
9: end if
```

**Procedure: Produce \_ Stake \_ Beacon**

This procedure is run by a PoS validator at the beginning of each stake synchronization interval.

```

1: Input: Current slot sl_{now} , stake interval R_{stake} , local UTXO set \mathcal{U} .
2: if $sl_{\text{now}} \pmod{R_{\text{stake}}} = 0$ then
3: $S_{\text{total}} \leftarrow \text{CalculateTotalStake}(\mathcal{U})$.
4: $b_s \leftarrow (\text{beacon_type} = \text{STAKE}, S_{\text{total}}, \text{validator_id})$.
5: $\text{sig} \leftarrow \text{Sign}(b_s, \text{validator_private_key})$.
6: Broadcast(beacon = b_s , signature = sig).
7: end if
```

**Function: Update\_Baseline\_Difficulty**

This function adaptively updates the baseline difficulty parameters ( $f_B$ ) to ensure a secure fallback rate and prevent inversion with the primary amplitudes ( $f_A$ ).

- 1: **Input:** New primary amplitudes  $f_{A,PoW}, f_{A,PoS}$ , fallback time  $T_{fallback}$ .
- 2: **Step 1: Calculate Fallback-Targeted Baseline**
- 3:  $\lambda_{fallback} \leftarrow 1/T_{fallback}$ .
- 4:  $f_{B,PoW}^* \leftarrow \lambda_{fallback} \cdot (f_{A,PoW}/(f_{A,PoW} + f_{A,PoS}))$ .
- 5:  $f_{B,PoS}^* \leftarrow \lambda_{fallback} \cdot (f_{A,PoS}/(f_{A,PoW} + f_{A,PoS}))$ .
- 6: **Step 2: Apply Security Constraint (No Inversion)**
- 7:  $f_{B,PoW,final} \leftarrow \min(f_{B,PoW}^*, f_{A,PoW})$ .
- 8:  $f_{B,PoS,final} \leftarrow \min(f_{B,PoS}^*, f_{A,PoS})$ .
- 9: **Return:**  $(f_{B,PoW,final}, f_{B,PoS,final})$ .

**Function: Validate\_Block**

This is a main validation function that checks if a received block is valid with respect to the local chain and consensus rules.

- 1: **Input:** A new block  $\mathcal{B}_{new}$ , local chain state  $\mathcal{S}_{local}$ .
- 2: **Parent Check:** Verify that  $\mathcal{B}_{new}.parent\_hash$  exists in  $\mathcal{S}_{local}$ . If not, **Return** Invalid.
- 3: **Slot Check:** Verify that  $\mathcal{B}_{new}.slot > parent(\mathcal{B}_{new}).slot$ . If not, **Return** Invalid.
- 4: **DCS Time Check:** Verify that  $\mathcal{B}_{new}.timestamp$  is consistent with the value from  $\mathcal{F}_{DCS}.GetTime(\mathcal{B}_{new}.slot)$ . If not, **Return** Invalid.
- 5: **if**  $\mathcal{B}_{new}$  is a PoW block **then**
- 6:   **PoW Validation:**
- 7:    $S_{consensus} \leftarrow \mathcal{F}_{DCS}.GetStake(\mathcal{B}_{new}.slot)$ .
- 8:   Verify that  $\mathcal{B}_{new}.header.total\_stake = S_{consensus}$ . If not, **Return** Invalid.
- 9:    $\delta \leftarrow \mathcal{B}_{new}.slot - parent(\mathcal{B}_{new}).slot$ .
- 10:    $\mathcal{T}_{target} \leftarrow Calc\_PoW\_Target(\delta, \mathcal{S}_{local}.difficulty\_params)$ .
- 11:   Verify that  $Hash(\mathcal{B}_{new}) < \mathcal{T}_{target}$ . If not, **Return** Invalid.
- 12: **else if**  $\mathcal{B}_{new}$  is a PoS block **then**
- 13:   **PoS Validation:**
- 14:    $\delta \leftarrow \mathcal{B}_{new}.slot - parent(\mathcal{B}_{new}).slot$ .
- 15:    $\alpha_i \leftarrow validator\_stake/\mathcal{B}_{new}.header.total\_stake$ .
- 16:    $\phi \leftarrow Calc\_LDD\_Threshold(\delta, \alpha_i, \mathcal{S}_{local}.difficulty\_params)$ .
- 17:   Verify that  $\mathcal{B}_{new}.vrf\_output < \phi$ . If not, **Return** Invalid.
- 18:   Verify VRF proof  $\mathcal{B}_{new}.vrf\_proof$  against the validator's public key. If not, **Return** Invalid.
- 19:   Verify block signature. If not, **Return** Invalid.
- 20: **end if**
- 21: **Transaction Validation:** Verify all transactions in  $\mathcal{B}_{new}.body$ . If any are invalid, **Return** Invalid.
- 22: **Beacon Validation:** For each beacon  $b$  in  $\mathcal{B}_{new}.body$ , run  $Validate\_Beacon(b)$ . If any are invalid, **Return** Invalid.
- 23: **Return:** Valid.

**Function: Get\_PoW\_Anchor\_Hash**

This function retrieves the hash of the appropriate PoW block to be used as a VRF seed, based on the anchor depth parameter  $k_{anchor}$ .

- 1: **Input:** Local chain  $\mathcal{C}_{local}$ , anchor depth  $k_{anchor}$ .
- 2: **Initialize:** cursor  $\leftarrow head(\mathcal{C}_{local})$ , depth  $\leftarrow 0$ .
- 3: **while** cursor is not Genesis Block **do**
- 4:   **if** depth  $\geq k_{anchor}$  and cursor is a PoW block **then**
- 5:     **Return** Hash(cursor).
- 6:   **end if**
- 7:   cursor  $\leftarrow parent(cursor)$ .
- 8:   depth  $\leftarrow depth + 1$ .
- 9: **end while**
- 10: **Return** Hash(Genesis Block). ▷ Fallback if no suitable PoW block is found

**Function: Calc\_LDD\_Threshold**

This function calculates the dynamic PoS eligibility threshold for a given slot interval  $\delta$  and a validator's relative stake  $\alpha_i$ .

```

1: Input: Slot interval δ , validator relative stake α_i , difficulty parameters $\mathcal{D} = \{f_{A,PoS}, f_{B,PoS}, \psi, \gamma\}$.
2: Calculate Hazard Rate $f_{PoS}(\delta)$:
3: if $\delta < \mathcal{D}.\psi$ then
4: $f_{PoS}(\delta) \leftarrow 0$.
5: else if $\mathcal{D}.\psi \leq \delta < \mathcal{D}.\gamma$ then
6: $f_{PoS}(\delta) \leftarrow \mathcal{D}.f_{A,PoS} \cdot \left(\frac{\delta - \mathcal{D}.\psi}{\mathcal{D}.\gamma - \mathcal{D}.\psi} \right)$.
7: else
8: $f_{PoS}(\delta) \leftarrow \mathcal{D}.f_{B,PoS}$.
9: end if
10: Calculate Threshold ϕ :
11: $\phi \leftarrow 1 - (1 - f_{PoS}(\delta))^{\alpha_i}$.
12: Return: $\phi \cdot 2^{l_{VRF}}$. ▷ Scale to VRF output space

```

**Function: Calc\_PoW\_Target**

This function calculates the dynamic PoW difficulty target for a given slot interval  $\delta$ .

```

1: Input: Slot interval δ , difficulty parameters $\mathcal{D} = \{f_{A,PoW}, f_{B,PoW}, \psi, \gamma\}$.
2: Calculate Hazard Rate $f_{PoW}(\delta)$:
3: if $\delta < \mathcal{D}.\psi$ then
4: $f_{PoW}(\delta) \leftarrow 0$.
5: else if $\mathcal{D}.\psi \leq \delta < \mathcal{D}.\gamma$ then
6: $f_{PoW}(\delta) \leftarrow \mathcal{D}.f_{A,PoW} \cdot \left(\frac{\delta - \mathcal{D}.\psi}{\mathcal{D}.\gamma - \mathcal{D}.\psi} \right)$.
7: else
8: $f_{PoW}(\delta) \leftarrow \mathcal{D}.f_{B,PoW}$.
9: end if
10: Calculate Target \mathcal{T} :
11: $\mathcal{T} \leftarrow f_{PoW}(\delta) \cdot 2^{256}$. ▷ Scale to 256-bit hash output space
12: Return: \mathcal{T} .

```

**Function: Validate\_Beacon**

This function is run by any node upon receiving a beacon before relaying it or including it in a block.

```

1: Input: Beacon b , signature sig.
2: Signature Check: Retrieve public key for $b.id$. Verify sig against b . If invalid, Return Invalid.
3: Duplicate Check: Check if beacon with same content from same ID is already in local cache. If yes, Return Invalid.
4: if $b.beacon_type = TIME$ then
5: Time Beacon Validation:
6: $I_t \leftarrow \lfloor \mathcal{F}_{DCS}.GetTime(current_slot)/R_{time} \rfloor$.
7: Verify beacon's timestamp is for interval I_t . If not, Return Invalid.
8: else if $b.beacon_type = STAKE$ then
9: Stake Beacon Validation:
10: $I_s \leftarrow \lfloor \mathcal{F}_{DCS}.GetTime(current_slot)/R_{stake} \rfloor$.
11: Verify beacon is for interval I_s . If not, Return Invalid.
12: end if
13: Return: Valid.

```

**Function: Dynamic\_Adjust**

This master function executes the two-step difficulty adjustment at the end of each adjustment window.

- 1: **Input:** Lookback window size  $N$ , local chain  $\mathcal{C}$ , responsiveness  $\kappa$ , current difficulty params  $\mathcal{D}$ .
- 2: **Step 0: Data Collection**
- 3: Let  $\mathcal{W} \leftarrow$  the last  $N$  blocks of  $\mathcal{C}$ .
- 4:  $N_{PoW} \leftarrow$  count of PoW blocks in  $\mathcal{W}$ .
- 5:  $T_{actual} \leftarrow (\text{head}(\mathcal{W}).\text{timestamp} - \text{tail}(\mathcal{W}).\text{timestamp})/N$ . ▷ Observed avg block time
- 6:  $L(h) \leftarrow$  measure of recent transaction load (e.g., avg block size in  $\mathcal{W}$ ).
- 7: **Step 1: Proportional Adjustment (Correct Balance)**
- 8:  $P_{PoW} \leftarrow N_{PoW}/N$ .
- 9:  $E \leftarrow P_{PoW} - 0.5$ .
- 10:  $f'_{A,PoW} \leftarrow \mathcal{D}.f_{A,PoW} \cdot (1 - \kappa \cdot E)$ .
- 11:  $f'_{A,PoS} \leftarrow \mathcal{D}.f_{A,PoS} \cdot (1 + \kappa \cdot E)$ .
- 12: **Step 2: Stability Scaling (Correct Speed)**
- 13:  $\mu_{target} \leftarrow \text{Adaptive\_Target\_Slope}(L(h))$ .
- 14:  $M_{req} \leftarrow \pi/(2 \cdot (\mu_{target} - \mathcal{D}.\psi)^2)$ . ▷ Target slope from simplified expectation
- 15:  $M'_{actual} \leftarrow f'_{A,PoW} + f'_{A,PoS}$ .
- 16:  $\beta \leftarrow M_{req}/M'_{actual}$ .
- 17:  $f''_{A,PoW} \leftarrow \beta \cdot f'_{A,PoW}$ .
- 18:  $f''_{A,PoS} \leftarrow \beta \cdot f'_{A,PoS}$ .
- 19: **Step 3: Update Baselines**
- 20:  $(f''_{B,PoW}, f''_{B,PoS}) \leftarrow \text{Update\_Baseline\_Difficulty}(f''_{A,PoW}, f''_{A,PoS})$ .
- 21: **Return:** New difficulty parameters  $(f''_{A,PoW}, f''_{A,PoS}, f''_{B,PoW}, f''_{B,PoS})$ .

## B Interactive Simulation Dashboard Guide

The dashboard is designed to provide a real-time, dynamic visualization of the protocol's performance and security under a wide range of network conditions and adversarial strategies. To run the model, please save the associated `Synergeia_Simulation.ipynb` file and run the following command in your terminal from the file's directory: `> voila Synergeia_Simulation.ipynb` This will launch a web server and open the interactive dashboard in your browser.

### B.1 Simulation Controls & Live Parameters

This panel contains the main controls for running the simulation and a display for key real-time metrics.

- **Start/Stop Button:** Toggles the main simulation loop.
- **Reset Button:** Stops the simulation and resets the blockchain and all parameters to their default state.
- **Live Parameters Display:** This text box provides a real-time view of the protocol's internal state:
  - **Difficulty Amplitudes ( $f_A$ ):** Shows the current peak amplitudes for the PoW and PoS snowplow curves. These values are constantly adjusted by the balancing mechanism.
  - **Responsiveness ( $\kappa$ ):** The dynamically calculated responsiveness factor. Smaller values correspond to a more stable (less oscillatory) resource-balancing adjustment.
  - **Baseline Difficulties ( $f_B$ ):** Displays the calculated fallback difficulty ( $f_{B,fallback}$ ) which targets a 10-minute block time, and the final, security-constrained value ( $f_{B,final}$ ) that is actually used.
  - **Network Effects:** Shows the calculated **Head Start** in seconds an adversary gains from strategic delay, and the **Honest Power Wastage** percentage due to natural network desynchronization.
  - **Chain Race:** Displays the total **Accumulated Synergistic Work (ASW)** of the public chain versus the adversary's private chain. The text turns red if the adversary is winning.
  - **Status Indicators:** Text flags appear to confirm when adversarial tactics like **Mempool Flooding** or **VRF Grinding** are active.

### B.2 Parameter Control Panels

The dashboard is divided into several control panels, allowing the user to manipulate every aspect of the simulation.

## Adversary & Network Resources

- **Adversary Resources:** Control the adversary’s percentage of the total **Hash Power** and **Stake** from 0% to 100%, allowing for the simulation of minority and majority attacks.
- **Global Network Model:** Define the physical characteristics of the P2P network.
  - **Num Nodes:** Sets the number of participants. A higher number of nodes increases the stability of the balancing mechanism (lower  $\kappa$ ).
  - $\mu$  **Delay (s):** The mean propagation delay for a block across the honest network. A higher value increases the honest power wastage.
  - $\sigma$  **Delay (s):** The standard deviation of the propagation delay, modeling the network’s geographic dispersion.

## Protocol & Economic Parameters

- **LDD Parameters:** Control the shape of the snowplow difficulty curve.
  - $\psi$  (**Slot Gap**): The initial period where block production is forbidden. This is the primary defense against the adversary’s strategic delay,  $\Delta$ .
  - $\gamma$  (**Recovery**): The time at which the difficulty ramp ends.
- **Economic Model:**
  - **Avg Tx/Block & Avg Fee/Tx:** These sliders control a Poisson-based random transaction generator, which creates realistic variance in the economic value (and thus the ASW) of PoS blocks.
- **Protocol Constants:**
  - Sliders to control the core protocol targets, including **Target Block Time**, **Target PoW Proportion**, the **Adjustment Window** for balancing, the base **Block Reward**, and the **Orphan Risk** during a mempool flood.

## Adversarial Tactics

- **Adversarial Delay Model:**
  - **Dropdown Menu:** Select different models for strategic delay, from ideal (no delay) to constant, uniform, or exponential distributions.
  - $\Delta$  (**Adv. Max Delay**): Sets the maximum delay an adversary can use to try to gain a head start on the next block. The simulation’s security degrades when  $\Delta > \psi$ .
- **Private Mining Toggle:** Switches the adversary’s behavior from broadcasting blocks publicly to building a secret chain to attempt a balance attack.
- **Mempool Flood Toggle:** Simulates a DoS attack, triggering the protocol’s ASL defense (slowing block times) and increasing the honest orphan risk.
- **VRF Grinding Toggle:** Simulates a PoS attack. This tactic is only effective if the PoW-anchored seed is stale (i.e., the last block was not PoW).

## C Node Implementation

This section provides a high-level architectural overview of the Synergeia full node implementation. The node is designed as a modular, concurrent application written in Rust, leveraging the Tokio asynchronous runtime for high-performance networking and consensus operations. The core design philosophy is to separate concerns into distinct modules that communicate via message-passing channels, ensuring thread safety and maintainability.

### C.1 Main Application ('main.rs')

- **'start-node' command:** Initializes the shared ‘Blockchain’ state within an ‘Arc<Mutex<>’, creates message-passing channels, and spawns the RPC, P2P, and Consensus tasks.
- **Client Commands:** ‘get-balance’, ‘send’, etc., function as clients making HTTP requests to the RPC server.

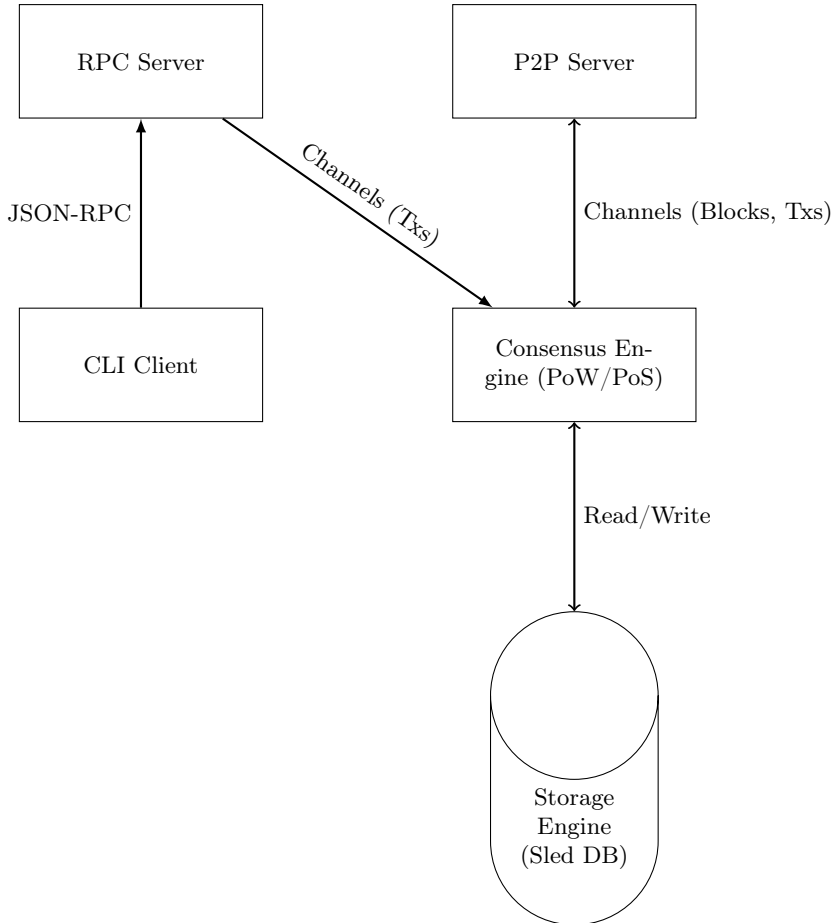


Fig. 9: High-level architectural diagram of the Synergeia node.

### C.2 P2P Server ('p2p.rs')

- **Concurrency:** Runs as a dedicated Tokio task, listening for incoming TCP connections and spawning a new task for each peer.
- **Synchronization:** Implements headers-first sync logic.
- **Message Passing:** Communicates with the Consensus Engine via a Tokio MPSC channel, sending verified blocks and transactions.

### C.3 RPC Server ('rpc.rs')

- **Interface:** Provides a JSON-RPC 2.0 compliant HTTP server.
- **Functionality:** Exposes methods like 'get\_balance', 'submit\_transaction'.
- **Interaction:** Forwards write requests to the Consensus Engine via the shared channel.

### C.4 Consensus Engine ('consensus.rs')

- **Main Loop:** Runs in a dedicated Tokio task, listening for messages and containing the block production logic.
- **Hybrid Consensus:** Based on the '--mode' flag, runs either the PoW mining loop or the PoS staking loop.
- **State Management:** The sole component with synchronous write access to the 'Blockchain' struct, validating new blocks, updating the UTXO set, and managing the mempool.

### C.5 Storage Engine ('blockchain.rs' & 'sled')

- **Database:** Uses 'sled', a high-performance embedded key-value store.
- **Data Structure:** Uses different "trees" for 'blocks' and the 'utxo' set.
- **Atomicity:** 'sled' provides transactional batches, ensuring atomic updates to the blockchain state.

## C.6 API Methods

The Synergeia node provides a JSON-RPC 2.0 interface for interacting with the blockchain. The server listens on ‘127.0.0.1:8332’ by default.

### **getbalance**

Returns the total balance of an address in satoshis.

- **Parameters:** ‘[String: address]’
- **Returns:** ‘"balance": u64’

### **sendtransaction**

Submits a raw, hex-encoded signed transaction to the mempool.

- **Parameters:** ‘[String: hex\_tx]’
- **Returns:** ‘"txid": String’

### **getblock**

Retrieves a full block by its hex-encoded hash.

- **Parameters:** ‘[String: block\_hash]’
- **Returns:** ‘"hash": String, "height": u32, ...’

### **gettip**

Returns the hash of the current best block in the chain.

- **Parameters:** None
- **Returns:** ‘"hash": String’